REPORT NO. FRA-OR&D-76-11

LONGITUDINAL FORCES IN RAILROAD TRACK

A. Ya Kogan

1967

(A Translation of the Original Report)

Document is available to the public
through the National Technical Information Service,
Springfield, Virginia 22161

Prepared for

U.S. DEPARTMENT OF TRANSPORTATION
Federal Railroad Administration
Office of Research and Development
Washington, D.C. 20590

01-Track & Structures

NOTICE

The translation and publication of this document does not constitute approval by the U.S. Department of Transportation of the inferences, findings, or conclusions contained therein. Publication is solely for the exchange and simulation of ideas.

Technical Report Documentation Page

1. Report No.	2. Government Accession No.	3. Recipient's Catalog No.
FRA-ORD 76-11		

4. Title and Subtitle	5. Report Date
LONGITUDINAL FORCES IN RAILROAD TRACK	1967
	6. Performing Organization Code
	8. Performing Organization Report No.
7. Author(s)	
A. Ya Kogan, M. Yanowitch	
9. Performing Organization Name and Address	10. Work Unit No. (TRAIS)
Centralny Nauchno-Isslodovatelski Institut Inzhenerov Zheleznodorozhogo Transporta (CHII) [Cent. Res. Inst. for R.R. Transport]	11. Contract or Grant No.
	13. Type of Report and Period Covered
12. Sponsoring Agency Name and Address Department of Transportation Federal Railroad Administration (OR&D) 2100 Second Street, SW Washington, D. C. 20590	14. Sponsoring Agency Code

15. Supplementary Notes

Translated by Professor M. Yanowitch, Aldelphi University, Long Island, New York.

16. Abstract

The work is devoted to the theory of design computations for track subjected to thermal and creep forces. The theory of longitudinal forces and displacements arising in continuous welded rail (CWR) track due to temperature changes is mathematically developed. A description of results of experimental investigations of the operation of CWR track is given, with the subsequent determination of parameters and functions which characterize the behavior of the track under the influence of temperature changes.

Results of investigations of longitudinal forces in CWR track resulting from moving trains are presented.

The work contains an investigation of railroad track stability. The problem is solved in a nonlinear formulation, under assumption that the rail is subjected to passive loads without any restrictions on the dependence of these quantities on the corresponding displacements.

The report is illustrated by the construction of longitudinal force-displacement diagrams, which facilitate practical application of the formulas presented for analysis of the operation of CWR track and of long rails.

17. Key Words	18. Distribution Statement
longitudinal forces, and displacements, continuous welded rail, track stability, force-displacement diagrams, track thermal forces.	Document is available to the public through the National technical Information Service, Springfield, Virginia 22161

19. Security Classif. (of this report)	20. Security Classif. (of this page)	21. No. of Pages	22. Price
UNCLASSIFIED	UNCLASSIFIED	225	

Form DOT F 1700.7 (8-72) Reproduction of completed page authorized

PREFACE

The growth in the speeds and loads intensities at which railroads are operated demand a further improvement in track facilities. This important problem can be solved by the installation of CWR track and long rails in stations and as part of open track. In evaluating the possibility of installing CWR track and long rails, and in solving the problem of anchoring the track against creep, the calculation of longitudinal forces and displacements is of great importance. In the present work an attempt is made to fill an existing gap in this very important area of railroad track analysis.

The basic results of this investigation are connected with the operation of CWR railroad track; however, whenever necessary they can also be applied to the calculation of longitudinal forces and displacements in long rails, and in conventional jointed track.

This work examines from a unified point of view questions connected with the influence on the track of all types of longitudinal forces, those produced by moving rolling stock (creep) as well as those due to temperature changes of rails. In so doing, the basic viewpoint of examining all longitudinal displacements simultaneously is adopted.

A. F. Zolotarskii, Assistant Director of the Institute

V. G. Al'brecht, Head of the Track and Track Operation Section

INDEX

SUMMARY

The work is devoted to the theory of design computations for track subjected to thermal and creep forces. The theory of longitudinal forces and displacements arising in continuous welded rail (CWR) track due to temperature changes is developed. (The problem is solved in a general formulation which takes into account the hereditary nature of tie displacement processes; A solution to the problem of finding the longitudinal forces and displacements as random functions of distance along the track, is given in the form of characteristic functionals.) A description of results of experimental investigations of the operation of CWR track is given, with the subsequent determination of parameters and functions which characterize the behaviour of the track under the influence of temperature changes.

An integro-differential equation, which describes the relaxation of the longitudinal forces in CWR track, is derived and solved for different forms of track deflection and for different tie resistance vs. displacement relations.

Results of investigations of longitudinal forces in CWR track in the zone of the moving train are presented. (The equation for longitudinal displacements in a moving train zone is derived, and its solution is given for the case of frictional and elastic interaction between the rail and the rail supporting foundation.)

The work contains an investigation of railroad track stability. The problem is solved in a nonlinear formulation, under the assumption that the rail is subjected to passive distributed tangential and normal loads and bending moments, without any restrictions on the dependence of these quantities on the corresponding displacements.

The work is illustrated by the construction of longitudinal force-displacement diagrams, which facilitate the practical application of the formulas presented for the analysis of the operation of CWR track and of long rails.

The book is intended for engineers, scientific investigators, and advanced students in institutes of transportation.

This is a translation from the Russian of "Prodol'nye Sily v Zheleznodorozhnom Puti" by A. Ya. Kogan, published in 1967 as the 332nd issue of the Trudy Vsesoyuznogo Naucho-Isseledovatel'skogo Instituta Zheleznodorozhnogo Transporta, by the Izdatel'stvo "Transport".

CHAPTER I

BRIEF SURVEY OF EXISTING METHODS FOR COMPUTING LONGITUDINAL FORCES IN CONTINUOUS WELDED RAIL TRACK AND ANALYSIS OF CONDITIONS FOR ITS STABILITY

Because of its technical and economic advantages, CWR track is at the present time gradually beginning to replace bolted track.

Bolted rail joints constitute the weakest part of the superstructure of the present day railroad track. This explains why since 1884 engineering thinking has been continuously aimed at perfecting rail joints and decreasing their number in the track.

The economic superiority of CWR track is determined by the following factors: decrease in the amount of labor required for track maintenance; diminished wear of rolling stock; improvement of electrical conductivity of rail lines; diminished resistance to train motion; improvement in passenger comfort; increased life of rails, ballast, and ties at or near welded joints, because of decreased impact at these joints.

The initial cost of CWR track is somewhat greater than the cost of conventional 12.5 and 25 meter rails, but it is amortized comparatively quickly. The economic problems pertaining to CWR track have been studied in the U.S.S.R. and abroad by many specialists. Of particular importance are the studies by Candidate of Technical Sciences V. Ya. Shul'ge.

Theoretical and experimental investigations of CWR track have been made and are continuing in the U.S.S.R.

The first experimental section of CWR track was laid in 1933 at Podmoskovnaya, on the Kalinin railroad, by scientists of the Moscow Institute of Railroad Engineers [38]. Operation of this experimental section has yielded data essential to theoretical planning and to the solution of practical problems in subsequent design of CWR track.

Several designs for CWR track were worked out in 1940 at the Scientific Research Institute of Ways and Construction, but the track was not laid because of the beginning of the war in 1941. Experimental investigations of stability of CWR track were conducted in West Germany and in Japan.

Experience in operating CWR track shows that the rail line is completely stable if specified conditions are observed in the installation and maintenance of the track. However, the stability problem has not been solved completely. Cases of track buckling indicate the existence of certain critical parameters which determine track stability. It is essential to determine these parameters as accurately as possible, to find how they are related to each other, and to construct in the parameter space the regions of stability and instability. Theoretical investigations have a great importance in connection with these problems.

A fairly complete account of the theory of thermal effects on rails was given by Candidate of Technical Sciences M. T. Chlenov in his book [38]. In 1948 Professor G. M. Shakhunyants proposed a more refined method for computing thermal stresses in rails, including the effects of the eccentricities of the forces [39]. Professor K. N. Mischenko [25] worked out a scheme for computing the stability of CWR track based on the energy method. In 1952 Cand. Tech. Sc. A. A. Krivobodryi [22] proposed somewhat different formulas for computing track stability. These were based on the method of integral equations, and differ but slightly from the formulas of Mischenko, since the only novelty consisted in the method of solution.

Some questions pertaining to longitudinal forces in CWR track with automatic stress relaxation were investigated by Cand. Tech. Sc. M. S. Bochenkov.

In West Germany I. Wattmann has conducted some investigations [8] devoted to longitudinal forces in railroad track.

In all the studies it was always assumed that all the parameters and characteristics were constant along the track, and

were obtained by averaging with respect to the stresses. In view of the spreading use of CWR track, such an approximate solution could not satisfy the demands of practice and called forth new theoretical developments which are continuing to this day.

Of the recent works devoted to methods of computing the stability of thermally stressed track one must single out the dissertation of Cand. Tech. Sc. C. P. Pershin. A number of proposals were made in this work to improve the accuracy of existing methods of computation. In the first place Pershin discarded the assumption of constant parameters (obtained by averaging with respect to the stresses) and instead solved the problem assuming functional relations between the resistance of the ties and their displacement, and of the rail fastenings and their twist. Although the relationships were assumed to be linear, the accuracy of the formulas was considerably improved and the formulas obtained have a structure fairly close to that of formulas obtained with nonlinear dependence between track characteristics and deformations

Of particular importance in Pershin's work is the inclusion of the effect of initial nonuniformities of the track on its stability. However, the work also contains some inaccuracies. Thus, for example, the slope of the curve defining the relation between the resistance of the tie and the displacement is assumed to be constant, in view of the assumption of linearity. On the other hand, this parameter, one of the most important in determining the zones of stability and instability of continuous track, decreases by a large factor when the ties are displaced by a few millimeters.

Furthermore, it is not so much the dependence of tie resistance on its displacement in the ballast that is of interest. Rather, it is the functional dependence between the force transmitted by the rail to the tie and the displacement of the rail which is important, since it includes the effect of the intermediate fasteners. It is quite evident that the displacements of the rail and of the ties are in general not the same

even with the strongest possible intermediate fasteners, and it is the deformations of the rails which must be taken into account in the computation, since they are the cause of the eccentricities of the longitudinal forces.

In solving the fundamental problem Pershin did not make a detailed study of the longitudinal forces in the track produced by its deformations, and therefore, the relaxation of the longitudinal forces connected with the curvature of the rails was not taken into account.

In solving the stability problem for CWR track it has been customary until now to consider the section of track which is subjected to thermal stresses only. However, the track is more likely to buckle laterally immediately in front or behind a moving train, where the track characteristics can be weakened by vibrations, which can partially eliminate the forces of dry friction. In addition, rail creepage in the moving train zone produces longitudinal forces due to the interaction of the elastic rail with the supporting foundation. The interaction between the track and rolling stock, connected with the production of rail creepage, is of great importance and has been studied by many specialists in the U.S.S.R. and abroad. The fundamental work devoted to rail creep is the monograph [1] of Dr. Tech. Sc. V. G. Al'brecht.

The author of the present work has attempted to solve the problem of longitudinal forces in the moving train zone assuming purely frictional and elastic interaction between rails and the supporting foundation.

Making use of the force-displacement diagrams constructed for the moving train zone, once can solve the track stability problem in this zone. Until now, the horizontal longitudinal forces acting on the railroad track have been divided into two categories. To the first category belong all the forces which arise from temperature changes which tend to alter the length of the rails. The second category includes horizontal longitudinal forces produced by the movement of the train, which

tends to shift the rails in the direction of motion. It appears to be worth while to attempt an examination of all longitudinal forces from a unified point of view, irrespective of how they are produced, based on the utilization of the continuity of the longitudinal track deformations.

In order to be able to solve problems of stability and strength of CWR track, it is essential to be able to determine the forces produced in the track. A great deal of work of Soviet and foreign scientists has been devoted to this extremely important question. Particularly important progress has been made recently in connection with the introduction of wider use of stochastic methods. The credit for the utilization of the powerful methods of moder probability theory in the design of railroad track belongs to Prof. M. F. Verigo [10].

A large contribution to the development of design methods for railroad track has been made by Professors N. T. Mityushin, A. M. Godytskii-T. Svirko, K. N. Mishchenko, P. G. Koziichuk, V. N. Danilov, K. P. Korolev, Candidates of Technical Sciences E. M. Bromberg, O. P. Ershkov, and many other Soviet scientists.

However, although methods for computing rail forces due to transverse loads are well developed, methods for computing longitudinal forces remain somewhat arbitrary until this day. Until most recently all the work devoted to longitudinal forces produced by increasing temperature was based on the assumption that a uniformly distributed tangential load, due to frictional forces between the rail and the foundation, acts on the rail.

In view of the increasing use of CWR track, the currently employed methods for computing longitudinal forces are becoming inadequate, since the thermally induced forces may reach a significant magnitude - up to 100 tons and more in each rail line.

In designing CWR track it is also important to know the magnitude of the oscillations of the ends of the lengths of continuously welded rail, the extent of the "transition"* zone,

---

* Also referred to as the "breathing" zone. (Trans.)

along which the rail cross-sections undergo longitudinal displacements, and the laws governing the variation of the longitudinal forces displacements, and the linear resistance* along the rail line.

In view of what has been said above, one can see the importance of determining correctly the longitudinal rail forces caused by temperature changes, or by the simultaneous action of temperature changes and forces due to rail creep which results from the rolling of the train wheels on flexible rails.

The laws of variation along the track length of the longitudinal forces and track displacements are determined by the interaction of the rails, fastenings, ties, and ballast. These characteristics change not only with time but also along the length of the track, in addition to which the character of the changes is, to a large extent, random.

The random nature of the dependence of the linear resistance on the point at which it is determined, is particularly evident. If it is assumed that the resistance does not depend on time, nor on the magnitude of the displacements of the rail cross-sections, it will be seen to vary from point to point since each individual rail tie has its own characteristics, while the reaction of the fasteners and of the ballast to the displacement of the rail also varies. Furthermore, the values of the linear resistance have a large scatter, and averaging them yields values of qualitative significance only. Thus, the parameter values used by different investigators in computations according to accepted formulas differ from each other by large amounts. Errors of 30 to 40% in the determinations of the parameters are considered acceptable.

In general, the linear resistance is a weakly correlated function which, for practical purposes, can be considered to be delta-correlated, since the characteristics of a tie in one cross-section are practically independent of the characteristics in

---

* The term linear resistance will be used to denote the resistance per unit length along the track. (Trans.)

another cross-section.

The present level of the theory of stochastic processes permits a complete solution of the problem posed above. The theory of stochastic processes is one of the most rapidly developing branches of probability theory.

Begun by Academician A. A. Markov, who examined discrete stochastic processes (Markov chains), this theory attained its definitive formulation after the appearance of the fundamental works of A. N. Kolmogorov and A. Ya. Khinchin.

The theory of stochastic processes finds its application in the most diverse areas of science and technology: medicine, biology, cybernetics, communication theory, theory of elementary particles, and many others. The application of the theory of stochastic processes to the design of CWR track may be of more general theoretical interest since time series are here replaced by series of random values along the length of the track, which, in the ideal case, can be considered to be infinitely long.

When the problem is formulated statistically, the construction of longitudinal force diagrams in CWR track can be related to the theories of random walks and Brownian motion, which have been treated quite extensively in modern physics (see Chapter II).

Finally, the investigation of hysteresis phenomena in the displacements of the rail ends is of great interest in the solution of problems connected with the design and operation of CWR track. Many specialists have concerned themselves with the construction of hysteresis loops when the ends of the rails undergo displacements, and with the investigation of questions connected with the existence of internal friction in the track. One of the early, but sufficiently detailed, works is the book of M. T. Chlenov [38].

Professors G. M. Shakhunyants and V. G. Al'brecht, Cand. Tech. Sc. M. S. Bochenkov, and many other specialists in the U.S.S.R. and abroad have studied the construction of diagrams of

displacement of rail ends with temperature. However, until the present time questions connected with track hysteresis have been solved under the assumption that the linear resistance acting on the rail is constant along it. Such solutions can be considered acceptable for short rails and simple* spike fastenings, in which case the resistance is close to being constant, and the small rail length guarantees a small absolute error in the computation of the displacements of the rail ends.

The fastenings coming into use at the present time ensure the application of 800 to 1000 kg to the clamps. Under these conditions the rail is displaced together with the tie, and the assumption of constant linear resistance is inaccurate.

The application of currently available formulas for the calculation of the displacements of the end points of thermally-stressed CWR track, taking into account the fairly large "transition" zone, is of doubtful validity and can be used to give only qualitatively correct results.

At the present time CWR track has become a reality, and to further expand its use it is essential to have more accurate methods of computation. Consequently, there arises the necessity of conducting a whole series of experiments, directed first of all towards the determination of the statistical parameters of the track. A portion of this task was accomplished by the author during the period 1957-1959. The problems examined in this book were first worked out by the author before 1962, and were described in a candidate's dissertation defended early in 1963.

It is important to conduct precise experiments to determine how the force transmitted by the rail to the tie depends on the displacement of the rail. Until the present time only the dependence of the tie resistance on the displacement has been investigated. However, this relation does not take into account the play and the elastic unloading in the intermediate fastenings, and consequently cannot be used in the stability computation. The longitudinal forces and bending moments are applied to the

---

* Fastenings which have no tie-plate and cannot be readily disassembled will be referred to as "simple fastenings", to distinguish them from "tie-plate fastening assemblies". (Trans.)

rail and, consequently, it is only the dependence of the forces resisting the track buckling on the deformation of the rails which is of interest, and not the dependence on the displacement of the ties and ballast.

CHAPTER II

THERMALLY INDUCED STRESSES AND DISPLACEMENTS IN CWR TRACK

1. Derivation of the differential equation for longitudinal railroad track displacement.

In recent years the investigation of the character of the distribution of longitudinal track forces, and of rail and tie displacements induced by these, has acquired more and more importance. This can be explained primarily by the expanding use of long rails and of CWR track in railroads in the Soviet Union and abroad.

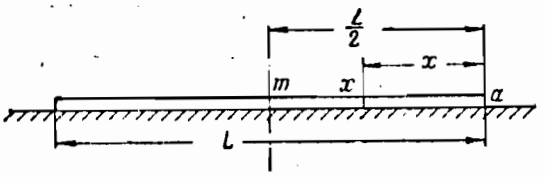

Fig. II.1. Temperature induced displacement of the ends of a string of welded rails

It is well known that in a string of welded rails it is only the end sections which suffer displacement, the middle portion remaining stationary, in a stressed state. Let us examine half of a rail string am (Fig. II.1). Since the mid point will not move when the temperature changes, it can be regarded as fixed.

Let $\rho(x)$ be the resistance of the rail due to the supporting foundation, and P_H - the resistance in the joint bars (or in the rail expansion joints). Let us suppose that the rail had been laid unstressed, and that its temperature has been raised by t°. If x is an arbitrary point sufficiently close to a free end of the rail, then the elongation of the middle section mx, produced by the temperature rise, will cause the end section of the rail ax to be displaced along the ties, or to displace the ties in the ballast. In each of these cases, the frictional force P_H at the end of the rail section a and the resistance from the foundation (i.e. the integrated effect of the linear

resistance to the displacement of the rail) $P_{\pi} = \int_{x}^{a} \rho(y)\,dy$ over the segment ax, produce a force $P_H + P_{\pi}$ which opposes the elongation of the middle section mx. Consequently, along the whole segment mx and at the point x there arises a compressive force P with magnitude $P_H + P_{\pi}$ if the length of the middle section can increase. As long as the compressive force at point x has not reached the value $P_H + P_{\pi}$ the elongation is impossible and, consequently, one can regard the rail over this section as a compressed rod, with the stress increasing in proportion to the rise in temperature.

When making computation for CWR track and for long rails it is important to establish the magnitude of the displacement of the ends of the rail strings, the size of the "transition" zone, and how the longitudinal forces vary within it. To make the computations it is essential to know the linear resistance of the rail to longitudinal displacements, which depends on the displacement of the tie along the direction of the track. On crushed stone of 25 to 70 mm one can observe an increase in the resistance when the displacement is 3 to 5 mm or greater. With a worn spike fastener, the coupling between the tie plate and the rail base is insignificant. As the rail increases in length, after the tie has been displaced by 2 to 4 mm, the rail base begins to slide along the tie plate. The magnitude of the linear resistance in this case is determined by the frictional forces and is constant. With heavy duty fastenings, for example, of type K, the displacement of the end of the CWR track leads to a continuous change in the linear resistance: the larger the displacement of a given section, the larger will be the linear resistance

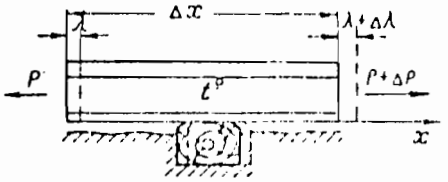

Fig. II.2. Equilibrium conditions of an element of a string of welded rails

Let us solve the problem of constructing the longitudinal force vs track displacement curve due to temperature changes of the rails, assuming the most general relation between the resistance of the ties to displacement and the magnitude of the displacement. It will be supposed that both rail lines are in the same state, so that the longitudinal forces and displacements of both rails are the same in every section.

Let us consider an element Δx of a string of welded rails, located between the center lines of two adjacent ties, and let us determine its deformation due to the action of the temperature and of the impressed forces (see Fig. II.2). As is well known, the elongation of the element Δx due to the temperature change is given by the formula

$$\Delta\lambda_t = \alpha t\ \Delta x,$$

where $\Delta\lambda_t$ is the elongation in cm due to a rise in temperature of 1°;

α is the coefficient of linear expansion of steel;

t is the rise in temperature of the rail string from the time it is installed in the track.

The elongation of the same element due to the action of a longitudinal force P is determined, according to Hooke's Law, from

$$\Delta\lambda_P = \frac{P}{EF}\ \Delta x,$$

where E is the modulus of elasticity of rail steel, kg/cm^2; and F is the cross-sectional area of rail, cm^2.

The total elongation of the element Δx produced by a temperature change of t° and a tensile force P is

$$\Delta\lambda = \Delta\lambda_t + \Delta\lambda_P = \alpha t + \frac{P}{EF}\ \Delta x. \qquad \text{(II.1)}$$

Since the track is subdivided into equal elements Δx, the length of each of which is considerably smaller than the "transition" zone, ratios of increments can be replaced by derivatives. Thus,

$$\frac{d\lambda}{dx} \approx \frac{\Delta\lambda}{\Delta x} = \alpha t + \frac{P}{EF}. \qquad \text{(II.2)}$$

Differentiation of expression (II.2) yields

$$\frac{d^2\lambda}{dx^2} = \frac{1}{EF} \cdot \frac{dP}{dx} \approx \frac{1}{EF} \cdot \frac{\Delta P}{\Delta x}, \qquad \text{(II.3)}$$

where ΔP is the longitudinal force transmitted by the rail to the tie.

The force $2\Delta P$, transmitted by the rails to the tie, depends in general on the displacement of the rails in the section where the tie is located, and on the initial displacement of the tie λ^*, produced by previous displacements of the rails and characterizing the state of contact between the tie and the ballast.

In earlier investigations [17], [18] it was always assumed that the force transmitted from the rails to the tie depends only on the displacement of the rails. Although this relation was an improvement over previous methods, which assumed a constant linear resistance, ρ (x) = const, at the surface of contact between the rail base and the underlying foundation, it constitutes only a particular case, appropriate to the first loading of the system. Averaging with respect to λ^* yields results of acceptable accuracy for longitudinal forces in CWR track, but make it impossible to explain such important phenomena as the appearance of residual stresses when the temperature is first raised and then decreased, and the residual displacements of the ends of the rail lengths produced by these stresses.

The quantity $2\Delta P$ depends on many factors: the degree of compression between the rail and the tie, the distance between adjacent ties, their weight, ballast grade, degree of packing of the ballast, etc.,; however, when the problem is formulated statistically, all these factors are taken into account indirectly. An analytical representation of the result can be put in the form

$$\Delta P = \frac{1}{2} \psi (\lambda, \lambda^*), \qquad \text{(II.4)}$$

Where $\psi(\lambda, \lambda^*)$ is, in general, a random function of two arguments,

determined statistically by analysing experimental results.

Substitution of (II.4) into expression (II.3) yields an equation for thermally induced longitudinal displacements,

$$\frac{d^2\lambda}{dx^2} = \frac{1}{2EF\Delta x}\psi(\lambda, \lambda^*) = \frac{1}{EF}\varphi(\lambda, \lambda^*). \tag{II.5}$$

The relation (II.5) characterizes a random process of track displacements produced by temperature changes. Since the derivative is the limit of the ratio of the increment of the function to the increment of the argument, and the mathematical expectation of the difference of two random quantities is equal to the difference of their expected values, the operations of differentiation and taking the expected value can be interchanged. Consequently, taking the expected value of equation (II.5) yields

$$M\frac{d^2\lambda}{dx^2} = \frac{d^2 M\lambda}{dx^2} = \frac{1}{EF} M\varphi(\lambda, \lambda^*), \tag{II.6}$$

where

$$M\varphi(\lambda, \lambda^*) = \int_{-\infty}^{\infty} \varphi(\lambda, \lambda^*) f[\varphi(\lambda, \lambda^*)]\, d\varphi(\lambda, \lambda^*), \tag{II.7}$$

where $f[\phi(\lambda_i, \lambda_j^*)]$ is the probability density of the random variable $\phi(\lambda_i, \lambda_j^*)$, which can be considered statistically prescribed.

Since formula (II.6) determines the mean value of the random variable $\phi[\lambda(x_k), \lambda^*(x_k)] = \phi(\lambda_i, \lambda_j^*)$ for every value of $x = x_k$, and the probability density $f[\phi(\lambda_i, \lambda_j^*)]$ is given, the process $\rho(x) = \phi[\lambda(x), \lambda^*(x)]$ is completely determined.

The process is completely described by the characteristic functional [30], defined by

$$g_\rho[\mu(x)] = M\left[e^{i\int_0^x \mu(x)\rho(x)\,dx}\right] = \int_{-\infty}^{\infty} e^{-\int_0^x \mu(x)\rho(x)\,dx} f\{\varphi[\lambda(x), \lambda^*(x)]\}\,d\rho(x), \tag{II.8}$$

where $i = \sqrt{-1}$, is the imaginary unit; $\mu(x)$ is an arbitrary function.

Let $\mu(x)$ be a linear combination of $n = [x/\Delta x]$ δ-functions; here $[x/\Delta x]$ denotes the largest integer less than or equal to $x/\Delta x$. Then

$$\mu(x) = \mu_n(x) = \sum_1^n \mu_n \delta(x - n\Delta x),$$

$$\delta(x - n\Delta x) = \frac{1}{2\pi}\int_{-\infty}^{\infty} e^{it(x-n\Delta x)}\,dt.$$

Taking into account the properties of the δ-function, we obtain

$$g_\rho[\mu(x)] = M\left[e^{i\int_0^x \mu_n(x)\rho(x)\,dx}\right] = M\left[e^{i\sum_1^n \mu_n \int_0^x \delta(x-n\Delta x)\rho(x)\,dx}\right] = M\left[e^{i\sum_1^n \mu_n \rho(n\Delta x)}\right] \tag{II.9}$$

The quantity $g_\rho[\mu(x)]$ is the characteristic function of an n-dimensional random vector ρ, with components $\rho_1(\Delta x)$, $\rho_2(2\Delta x)$, ..., $\rho_n(n\Delta x)$.

It is evident that except for the multiplying constant $1/\Delta x$, the random components of the vector are forces transmitted from the rail to the tie at the

discrete set of points $x = \Delta x$, $x = 2\Delta x$, ..., $x = n\Delta x$. Thus, in replacing the discrete process by a continuous one, its statistical properties are completely preserved.

If a random function $\psi(\lambda, \lambda^*)$ is considered prescribed, its variance is determined by a (nonrandom) function of the arguments λ and λ^*, so that $\partial\psi = \partial\psi(\lambda, \lambda^*)$, or, going over to the variable x, we obtain

$$D_{\Delta x\rho}(x) = \frac{1}{2}\partial\psi[\lambda(x), \lambda^*(x)].$$

From their nature, the quantities $\Delta x\rho(n\Delta k)$ and $\Delta x\rho(m\Delta x)$ are uncorrelated since the mean value of the random variable $\psi[\lambda(m\Delta x), \lambda^*(m\Delta x)]$ does not depend on the value taken on by the random function $\psi[\lambda(x), \lambda^*(x)]$ at the point $x = n\Delta x$.

In view of the above, the covariance matrix of the n-dimensional random vector $\overline{\Delta x\rho}$ takes the form

$$\|K_{\rho\Delta x}(i\Delta x, j\Delta x)\| = \begin{Vmatrix} D_{\rho\Delta x}(\Delta x) & 0 & 0 & \dots & 0 \\ 0 & D_{\rho\Delta x}(2\Delta x) & 0 & \dots & 0 \\ 0 & 0 & D_{\rho\Delta x}(3\Delta x) & \dots & 0 \\ \dots & \dots & \dots & \dots & \dots \\ 0 & 0 & 0 & \dots & D_{\rho\Delta x}(n\Delta x) \end{Vmatrix}.$$

Now, let us examine the random function P(x), which represents the longitudinal forces in the track. It is evident that the magnitude of the longitudinal forces in the section $x = n\Delta x$ can be computed from the formula

$$P(x) = P(0) + \sum_{1}^{n} \rho_k(k\Delta x)\Delta x. \qquad (11.10)$$

The process under examination splits up into two. The first one, P(0), is prescribed and represents a random variable with the characteristic function $g_{P(0)}(\nu) = M[\exp i\nu P(0)]$, where ν is an arbitrary parameter. Since the random variables $\rho_1(\Delta x)$, $\rho_2(2\Delta x)$, . . ., $\rho_q(q\Delta x)$ are independent and have the characteristic functions (II.9), letting $\mu_1=\mu_2=\cdots=\mu_q=\nu$, and taking into account the fact that when independent quantitites are added their characteristic functions are multiplied, one can compute the characteristic function of the random variable P(qΔx):

$$g_{P(q\Delta x)}(\nu) = g_{P(0)}(\nu)\prod_{i=1}^{q} g_{\Delta x\rho_i}(\nu). \tag{II.11}$$

If the characteristic function $g_{P(q\Delta x)}(\nu)$ is known, one can use the inversion formula to determine the distribution function of the random variable P(qΔx):

$$F[P(q\Delta x)] = \frac{1}{2\pi}\int_{-\infty}^{\infty} e^{i\nu P(q\Delta x)} g_{P(q\Delta x)}(\nu)\, d\nu, \tag{II.12}$$

The distribution function for P(qΔx) can be determined by taking the composition of the distributions of the quantities in (II.10).

Letting
$$F[P(0)] = F_0,\ f[\Delta x\rho_1(\Delta x)] = f_1,$$
$$f[\Delta x\rho_2(2\Delta x)] = f_2,\ \ldots,\ f[\Delta x\rho_q(q\Delta x)] = f_q,$$

we obtain
$$F[P(q\Delta x)] = F_0 * f_1 * f_2 * f_3 * \ldots * f_q, \tag{II.13}$$

with
$$f_i * f_j = \int_{-\infty}^{\infty} f_i(\Delta x\rho_k - \Delta x\rho_l)\, f_j(\Delta x\rho_j)\, d\Delta x\rho_j =$$
$$= \int_{-\infty}^{\infty} f_i(\Delta x\rho_l)\, f_j(\Delta x\rho_k - \Delta x\rho_l)\, d\Delta x\rho_l.$$

Formula (II.13) is cumbersome for computing purposes, and it is somewhat simpler to compose directly the distribution laws of $f[\Delta x_\rho(k\Delta x)]$; however, the moments of $P(q\Delta x)$ are easy to compute once the characteristic function of (II.11) is known.

Indeed, expanding $g_{P(q\Delta x)}(\nu)$ in a Maclaurin series, we obtain:

$$g_{P(q\Delta x)}(\nu) = g_{P_q}(0) + g'_{P_q}(0)\,\nu + g''_{P_q}(0)\frac{\nu^2}{2!} + \ldots + g^{(n)}_{P_q}(0)\frac{\nu^n}{n!} + \cdots$$

where

$$g_{P_q}(0) = \int_{-\infty}^{\infty} F[P(q\Delta x)]\,dF[P(q\Delta x)];$$

$$g'_{P_q}(0) = \int_{-\infty}^{\infty} iP(q\Delta x)\,F[P(q\Delta x)]\,dF[P(q\Delta x)];$$

$$g^{(n)}_{P_q}(0) = \int_{-\infty}^{\infty} \left(\frac{\partial^n}{\partial \nu^n} e^{i\nu P(q\Delta x)}\right)_{\nu=0} F[P(q\Delta x)]\,dF[P(q\Delta x)]..$$

Consequently,

$$g_{P(q\Delta x)}(\nu) = \sum_0^{\infty} \frac{(i\nu)^n \alpha_{nq}}{n!},$$

where α_{nq} is the n-th moment at $x = q\Delta x$.

Using the last equation, we can express the moments of the distribution by means of the coefficients of the expansion of $g_{P(q\Delta x)}(\nu)$:

$$\alpha_{nq} = i^{-n} g^{(n)}_{P(q\Delta x)}(\nu) \qquad \text{(II.14)}$$

Knowledge of the first three or four moments is sufficient for practical purposes, and the first two moments have the greatest significance.

The covariance matrix of the n-dimensional vector $\overline{P}_\rho$, with components $\Delta x \sum_0^n \rho_i(i\Delta x)$,..., $\Delta x \sum_0^n \rho_k(k\Delta x)$, can be computed directly, taking into account the fact that the covariance matrix of the n-dimensional random vector $\overline{\Delta x \rho}$ is known.

The formula for the covariance of a sum of random quantities has the form [30]:

$$K_{P_\rho}(m\Delta x, n\Delta x) = \sum_{i=1}^{m} \sum_{j=1}^{n} K(i\Delta x, j\Delta x). \tag{II.15}$$

Thus, the required covariance matrix has the form:

$$\|K_{P_\rho}(m\Delta x, n\Delta x)\| =$$

$$\begin{matrix}
D_{\Delta x\rho}(\Delta x) & D_{\Delta x\rho}(\Delta x) & D_{\Delta x\rho}(\Delta x) & D_{\Delta x\rho}(\Delta x) & \dots \\
D_{\Delta x\rho}(\Delta x) & \sum_1^2 D_{\Delta x\rho}(i\Delta x) & \sum_1^2 D_{\Delta x\rho}(i\Delta x) & \sum_1^2 D_{\Delta x\rho}(i\Delta x) & \dots \\
D_{\Delta x\rho}(\Delta x) & \sum_1^2 D_{\Delta x\rho}(i\Delta x) & \sum_1^3 D_{\Delta x\rho}(i\Delta x) & \sum_1^3 D_{\Delta x\rho}(i\Delta x) & \dots \\
D_{\Delta x\rho}(\Delta x) & \sum_1^2 D_{\Delta x\rho}(i\Delta x) & \sum_1^3 D_{\Delta x\rho}(i\Delta x) & \sum_1^4 D_{\Delta x\rho}(i\Delta x) & \dots \\
\dots & \dots & \dots & \dots & \dots \\
D_{\Delta x\rho}(\Delta x) & \sum_1^2 D_{\Delta x\rho}(i\Delta x) & \sum_1^3 D_{\Delta x\rho}(i\Delta x) & \dots & \sum_1^n D_{\Delta x\rho}(i\Delta x)
\end{matrix}$$

The variance of the random variable $P(q\Delta x)$ with $x = q\Delta x$, taking into account (II.10), is given by

$$D_P(x) = D_P(0) + \sum_{i=1}^{q} D_\rho(i\Delta x)\Delta x \approx D_P(0) + \int_0^x D_\rho(x)\,dx, \tag{II.16}$$

where $D_\rho(x) = (1/\Delta x) D_{\Delta x\rho}(x)$.

Instead of the covariance matrix, it is convenient to use the correlation function considering the process to be continuous. Making use of the commutativity of the correlation function, we can write

$$K_P(x_1, x_2) = \begin{cases} \int_0^{x_1} D_\rho(x)\,dx + D_P(0) & \text{при } x_2 > x_1 \\ \int_0^{x_2} D_\rho(x)\,dx + D_P(0) & \text{при } x_2 < x_1. \end{cases} \tag{II.17}$$

by analogy with (II.16).

The general form of this function is shown in Fig. II.3.

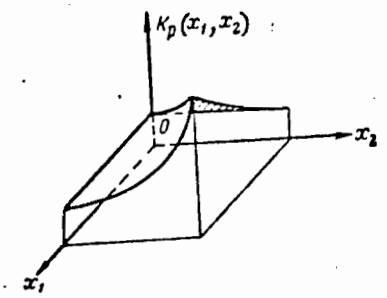

Fig. II.3. Correlation function $K_\rho(x_1, x_2)$ of the process of variation of the longitudinal forces along the length of the track.

Making use of the functional relation between the correlation functions of integral and differential random processes, one can show that the correlation function of the process $\rho(x)$ is given by:

$$K_\rho(x_1, x_2) = \frac{\partial^2 K_\rho(x_1, x_2)}{\partial x_1 \, \partial x_2}.$$

Taking into account the relation

$$\frac{\partial K_\rho(x_1, x_2)}{\partial x_2} = \begin{cases} 0 & \text{при } x_2 > x_1 \\ D_\rho(x_2) & \text{при } x_2 < x_1 \end{cases},$$

and making use of the integral representation of a step function,

$$\int_0^\infty D_\rho(x_1)\,\delta(x_2 - x_1)\,dx_1 = \begin{cases} 0 & \text{при } x_2 > x_1 \\ D_\rho(x_2) & \text{при } x_2 < x_1 \end{cases},$$

and of the symmetry of the correlation function, we obtain

$$K_\rho(x_1, x_2) = D_\rho(x_1)\,\delta(x_2 - x_1) = D_\rho(x_2)\,\delta(x_1 - x_2). \qquad \text{(II.18)}$$

Thus, if we consider the process $\rho(x)$ as continuous, the external influences must be regarded as a series of elementary impulses of infinitesimally short duration.

In the special case when $D_\rho(x) = D_0$, the correlation function $K_\rho(x_1, x_2)$ depends only on the difference $x_2 - x_1$, and not

on x_1 or x_2 separately. Processes for which the correlation function satisfies these conditions are stationary in the restricted sense. A special feature of stationary processes is the possibility of expanding them with respect to the spectrum of frequencies.

It is well known from the theory of stationary random processes that the spectral density can be expressed in terms of the correlation function by means of the relation.

$$S_\rho(\omega) = \frac{1}{2\pi}\int_{-\infty}^{\infty} K_\rho(x_2 - x_1)\, e^{-i\omega(x_2-x_1)}\, d(x_2 - x_1).$$

Substituting the relation $K_\rho(x_1,x_2) = D_o\delta(x_2-x_1)$ just obtained, results in

$$S_\rho(\omega) = \frac{D_0}{2\pi}\int_{-\infty}^{\infty} \delta(x_2-x_1)e^{-i\omega(x_2-x_1)}\, d(x_2-x_1) = \frac{D_0}{\pi}.$$

Thus, when $D^*(x) = D_o$, the random process $\rho(x)$ represents "white noise".

It should be noted that viewing the processes $\rho(x)$ as continuous has a significance beyond the mere fact that such processes preserve the statistical characteristics of discrete processes. For example, in examining a track on a continuous foundation, it is found that the approximate relations become considerably more accurate and permit a deeper understanding of the physical nature of the processes. A process, which has a correlation function of the form (II.18) is said to be delta-correlated, or uncorrelated.

For an uncorrelated disturbance, the mean square value is infinite, which is evident from (II.18) if we set $x_1 = x_2$. Consequently, such a disturbance has infinite energy. This result is a consequence of idealizing the properties of the actual disturbance.

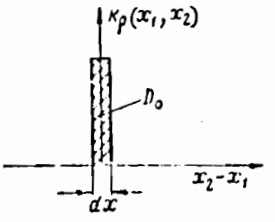

Fig. II.4. Correlation function $K(x_1x_2)$ of the process of variation along the length of logitudinal forces per unit length.

Let us note that an uncorrelated disturbance can create a finite response only if its mean square value is infinite. In order to understand this, let us introduce the notion of specific energy of the disturbance, by which we will mean the energy developed by the disturbance in a given section. If we now regard the disturbance as a succession of contiguous elementary impulses (with the amplitudes of the separate impulses uncorrelated), the graph of the correlation function for the case $D_\rho(x) = D_o = \text{const}$ will have the form illustrated in Fix. II.4. The area under the curve represents the mean specific energy of the elementary impulses.

Finally, let us examine the random function $\lambda(x)$, which represents the longitudinal displacement function along the track. In accordance with (II.1), one can write

$$\lambda(q\,\Delta x) = \lambda(0) + \alpha\, lq\,\Delta x + \frac{\Delta x}{EF}\sum_{1}^{q} P_k(k\,\Delta x). \qquad \text{(II.19)}$$

The above process splits up into three, the first of which, $\lambda(0)$, is given and represents a random quantity with the characteristic function $g_{\lambda(0)}(\nu) = M[\exp i\nu\lambda(0)]$, while the second is a nonrandom function of the argument $x = q\Delta x$. The covariance matrix of the third process $\lambda_p = (\Delta x/EF)\sum_{1}^{q} P_k(k\Delta x)$, which represents a sum of dependent random quantities,. can be determined, by analogy with (II.15), by means of the relations

$$K_{\lambda_p}(\alpha\,\Delta x, \beta\,\Delta x) = \frac{\Delta x^2}{(EF)^2}\sum_{m=1}^{\alpha}\sum_{n=1}^{\beta} K_{P_\rho}(m\,\Delta x, n\,\Delta x) = \qquad \text{(II.20)}$$

$$= \left(\frac{\Delta x}{EF}\right)^2 \sum_{m=1}^{\alpha}\sum_{n=1}^{\beta}\sum_{i=1}^{m}\sum_{j=1}^{n} K_\rho(i\,\Delta x, j\,\Delta x).$$

Instead of the covariance matrix, it is more convenient in practice to use the correlation function $K_\lambda(x_1 x_2)$, which can

be determined directly from the correlation function $K_p(x_1, x_2)$, recalling that the latter describes a differential process with respect to the process of displacements. Letting Q represent the domain of the values of the arguments x_1 and x_2, we obtain, in accordance with (II.17),

$$K_{\lambda_P}(x_1, x_2) = \frac{1}{(EF)^2}\int_Q\int_Q K_P(x_1, x_2)\,dx_1\,dx_2 = \tag{II.21}$$

$$= \begin{cases} \frac{x_2}{(EF)^2}\int_0^{x_1}\int_0^{x_2} D_p(x)\,dx\,dx + D_P(0)\frac{1}{(EF)^2}x_1x_2 + \\ + \frac{1}{EF}K_{P(0),\lambda_P(0)}x_1 + \frac{1}{EF}K_{\lambda_P(0),P(0)}x_2 + \\ + D_{\lambda_P}(0) \quad \text{при} \quad x_2 > x_1 \\ \frac{x_1}{(EF)^2}\int_0^{x_1}\int_0^{x_2} D_p(x)\,dx\,dx + D_P(0)\frac{1}{(EF)^2}x_1x_2 + \\ + \frac{1}{EF}K_{P(0),\lambda_P(0)}x_2 + \frac{1}{EF}K_{\lambda_P(0),P(0)}x_1 + \\ + D_{\lambda_P}(0) \quad \text{при} \quad x_2 < x_1. \end{cases}$$

It is easy to show that the quantity $K_{P(0),\lambda_P(0)} = K_{\lambda_P(0),P(0)}$ represents the covariance of the random variables $P(0)$ and $\lambda_P(0)$. Indeed, taking the partial derivative of (II.21) with respect to x_1, we obtain

$$\frac{\partial}{\partial x_1}K_{\lambda_P}(x_1, x_2) = \begin{cases} \frac{x_2}{(EF)^2}\int_0^{x_1} D_p(x)\,dx + \frac{D_P(0)}{(EF)^2}x_2 + K_{\frac{1}{EF}P(0),\lambda_P(0)} \\ \text{при} \quad x_2 > x_1 \\ \frac{x_1}{(EF)^2}\int_0^{x_2} D_p(x)\,dx + \frac{D_P(0)}{(EF)^2}x_1 + K_{\lambda(0),\frac{1}{EF}P(0)} \\ \text{при} \quad x_2 < x_1 \end{cases}$$

or, letting $x_1 = x_2 = 0$,

$$\frac{\partial}{\partial x_1}K_{\lambda_P}(0, 0) = K_{\frac{1}{EF}P(0),\lambda_P(0)} = K_{\lambda_P(0),\frac{1}{EF}P(0)}.$$

On the other hand,

$$\frac{\partial}{\partial x_1} K_{\lambda_P}(x_1, x_2) = \frac{\partial}{\partial x_1} M[\lambda_P(x_1)\lambda_P(x_2)] =$$
$$= \lim_{h \to 0} \left\{ \frac{M[\lambda_P(x_1+h)\lambda_P(x_2)]}{h} - \frac{M[\lambda_P(x_1)\lambda_P(x_2)]}{h} \right\} =$$
$$= M\left[\lim_{h \to 0} \frac{\lambda_P(x_1+h) - \lambda_P(x_1)}{h} \lambda_P(x_2) \right] =$$
$$= M\left[\frac{\partial}{\partial x_1} \{\lambda_P(x_1)\lambda_P(x_2)\} \right] = M\left[\frac{1}{EF} P(x_1)\lambda(x_2) \right] = K_{\frac{P}{EF}, \lambda}(x_1, x_2),$$

i.e. the partial derivative with respect to the x_1 of the correlation function of the process $\lambda_P(x)$ is the correlation function of two processes: $P(x)/EF$ and $\lambda(x)$. In the special case when $x_1 = x_2 = 0$, we obtain

$$K_{\frac{1}{EF} P, \lambda_P}(0, 0) = K_{\frac{1}{EF} P(0), \lambda_P(0)},$$

where $K_{P(0)/EF, \lambda_P(0)} = K_{\lambda_{P(0)}, P(0)/EF}$ is the covariance of the random quantities $\lambda_P(0)$ and $P(0)/EF$. It is completely evident that the same result can be obtained by differentiating the correlation function $K_{\lambda_P}(x_1, x_2)$ with respect to x_2. In particular the covariance is zero when the random variables $\lambda_P(0)$ and $P(0)$ are independent. Finally, it is easy to see that the quantity $D_{\lambda_P}(0)$ in (II.21) is the variance of the random variable $\lambda_P(0)$, which is easy to verify by setting $x_1 = x_2 = 0$ in this formula, and taking note of the fact that $D_{\lambda_P}(0) = K_{\lambda_P}(0,0)$.

In accordance with expression (II.21), the variance of the random function $\lambda(x)$ is equal to

$$D_\lambda(x) = \frac{x}{(EF)^2} \int_0^x \int_0^x D_\rho(x)\, dx\, dx + \frac{D_P(0)}{(EF)^2} x^2 + 2K_{\frac{1}{EF} P(0), \lambda(0)} x + D_\lambda(0). \quad \text{(II.22)}$$

In the above formula, the subscript P on λ is omitted since the total displacement process consists of two processes: the

random process λ_P with variance $D_{\lambda_P}(x)$, and the nonrandom one $\lambda_t(x)$, with variance $D_{\lambda_t}(x)$ identically equal to zero, so that $D_\lambda(x) = D_{\lambda_P}(x) + D_{\lambda_t}(x) = D_{\lambda_0}(x)$.

In the same way, one can omit the index P on λ in (II.21), since the correlation functions of the sum of two random processes are added and, at the same time, it is known that $K_{\lambda_t}(x_1,x_2) = 0$.

Sometimes it is more convenient to use normalized correlation functions of the form

$$R_\rho(x_1, x_2) = \frac{K_\rho(x_1, x_2)}{\sqrt{K_\rho(x_1, x_1) K_\rho(x_2, x_2)}};$$

$$R_P(x_1, x_2) = \frac{K_P(x_1, x_2)}{\sqrt{K_P(x_1, x_1) K_P(x_2, x_2)}};$$

$$R_\lambda(x_1, x_2) = \frac{K_\lambda(x_1, x_2)}{\sqrt{K_\lambda(x_1, x_1) K_\lambda(x_2, x_2)}}.$$

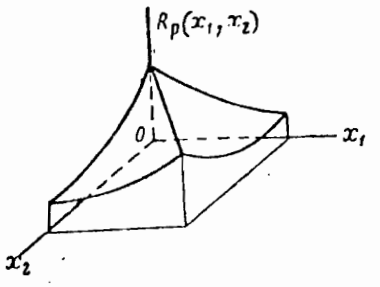

Fig. II.5. Normalized correlation function $R_P(x_1,x_2)$ of the process of variation of longitudinal forces along the length of the rail

The general form of the normalized correlation function of the process P(x) is shown in Fig. II.5. Since the random variable $\phi(\lambda_i,\lambda_j^*)$ depends on very many factors: the extent to which the rail is pressed into the tie, the weight, height, and width of the tie, the distance between the ties, the quality of the ballast and the degree of the packing, the dampness of the tie and of the ballast, the air temperature, the presence of clay particles in the ballast, and many other factors of approximately equal importance, there is every reason to suppose that this quantity has a normal distribution. This hypothesis is substantiated by a series of experiments conducted by the author.

If one assumes the random variable $\phi(\lambda_i, \lambda_j^*)$ to be normally distributed, it follows immediately that the centered process $\rho^o(x)$ is Gaussian, i.e. its n-dimensional probability density is normal with respect to the variables $\rho_1(\Delta x)$, $\rho_2(2\Delta x), \ldots, \rho_n(n\Delta x)$ and can be computed by the formula [30]

$$f_{1,2,\ldots,n}[\rho_1(\Delta x), \rho_2(2\Delta x), \ldots, \rho_n(n\Delta x)] = \frac{1}{(2\pi)^{\frac{n+1}{2}}\sqrt{|K_\rho|}} \exp\left(-\frac{1}{2}\sum_{i=1}^{n}\sum_{j=1}^{n} K^{-1}_{\rho ij}\rho_i(i\Delta x)\rho_j(j\Delta x)\right). \qquad \text{(II.23)}$$

The quantity $|K_q|$ is the determinant of the correlation matrix $\|K_{\rho\Delta x}(i\Delta x, j\Delta x)\|$. The quantities $K^{-1}_{\rho ij}$, which are elements of the matrix inverse to the covariance matrix is obtained by solving the n^2 equations

$$\sum_{j=1}^{n} K_{\rho ij} K^{-1}_{\rho ik} = \begin{cases} 0 & \text{при } i \neq k \\ 1 & \text{при } i = k. \end{cases}$$

Since the sums of normally distributed quantities are also normally distributed, we can conclude that the centered processes $P^o(x)$ and $\lambda^o(x)$ are also Gaussian. Its n-dimensional probability densities can be determined from expressions, analogous to formula (II.23), for the n-dimensional probability density of the process $\rho^o(x)$ replacing the covariance matrix $\|K_{\rho\Delta x}(i\Delta x, j\Delta x)\|$ and its elements by the matricies $\|K_{P_\rho}(m\Delta x, n\Delta x)\|$ and $\|K_{\lambda_o}(S\Delta x, r\Delta x)\|$ and their elements.

A random process is completely characterised by its characteristic functional. Since the processes are normally distributed, their characteristic functionals can be computed by means of the formulas [30]

$$\left.\begin{aligned} g_\rho[\mu(x)] &= e^{i\int \mu(x) M_\rho(x)\,dx - \frac{1}{2}\int\int \mu(x)\,\mu(x')\,K_\rho(x,x')\,dx\,dx'}; \\ g_P[\mu(x)] &= e^{i\int \mu(x) M_P(x)\,dx - \frac{1}{2}\int\int \mu(x)\,\mu(x')\,K_{P_\rho}(x,x')\,dx\,dx'}; \\ g_\lambda[\mu(x)] &= e^{i\int \mu(x) M_\lambda(x)\,dx - \frac{1}{2}\int\int \mu(x)\,\mu(x')\,K_{\lambda\rho}(x,x')\,dx\,dx'}. \end{aligned}\right\} \qquad \text{(II.24)}$$

Here $\phi(x)$ is an arbitrary function, particular forms of which determine all the distribution laws of the random function. In the special case when $\phi(x)$ is given to be a combination of $n = [x/\Delta x]$ δ-functions, the first equation of (II.24), after inverting by means of the Fourier integral, yields the n-dimensional probability density of the quantities $\rho_1(\Delta x),\ldots,\rho_n(n\Delta x)$, described by (II.23), the second equation yields the n-dimensional probability distribution of the quantities $P_1(\Delta x),\ldots,P_n(n\Delta x)$, and the third equation, the n-dimensional probability density of the quantities

$$\lambda_1(\Delta x),\ \lambda_2(2\Delta x),\ \ldots,\ \lambda_n(n\,\Delta x).$$

In conclusion, let us note that the random variables $\phi[\lambda(x_1),\lambda^*(x_1)]$ and $\phi\ [\lambda(x_2),\lambda^*(x_2)]$ may be statistically related. Indeed, the track may contain two types of ties, for example: old and new ties, each of which has its own random function of the tie resistance to displacement. Since the old and new ties occur randomly on the track section in use, in addition to the probability of occurrence of a new tie, determined by the fraction of the new ties in the section, we must consider the probability of transition from a new tie in section x to a new tie in section $x + \Delta x$, which we will denote by q. Corresponding to this, the probability of transition from a new tie in section x to an old tie in

section $x + \Delta x$ will be equal to $p = 1 - q$. Under these conditions, the probability of occurrence of resistance characteristics pertaining to new ties and to old ties are connected by a Markov chain. If the characteristics $\phi(\lambda,\lambda^*)$ are classified according to more than two criteria, the probability of transition from a tie with characteristic $\phi_i(\lambda,\lambda^*)$ in section x to a tie with characteristic $\phi_j(\lambda,\lambda^*)$ in section $x + \Delta x$ is determined by a Markov chain with transition matrix $\pi_1 = \| p_{ij} \|$ $(i,j = 1,2,3,\ldots,n)$, where n is the number of criteria used to classify $\phi(\lambda,\lambda^*)$.

Let π_m denote the matrix of transition across m ties. From the theory or homogeneous Markov chains [9], is is known that this matrix is related to the matrix of transition to the next tie by means of $\pi_n = \pi_1^n$. For practical purposes the probabilities of occurrence of any of the n functions $\phi_i(\lambda,\lambda^*)$ are equal after a passage across three ties. Consequently, in practice, the linear resistance can be considered to be an uncorrelated process, as noted earlier.

2. Solution of the equation of longitudinal track displacements for the case of the first temperature rise after the continuous welded rails are installed in the track

For the case of the first temperature rise of the rail strings after their installation in the track, it is evident that $\lambda^*(x) = 0$, which corresponds to the absence of previous tie displacements from their neutral positions. Consequently, (II.5) takes on the form

$$\frac{d^2\lambda}{dx^2} = \frac{1}{2EF\Delta x}\psi(\lambda, 0) \qquad \text{(II.25)}$$

To determine the function $\psi(\lambda,0)$ it is necessary to know two relations: the displacement resistance $\psi_1(\delta_1)$ of the tie (here δ_1 is the displacement of the tie in the ballast), and the resistance $\psi_2(\delta_2)$ of a pair of intermediate fastenings located on one tie to the displacement of the rail along that tie (δ_2 is the displacement of the rail with respect to the tie). It should be noted that $\delta_1 + \delta_2 = \lambda$.

Figure II.6a shows the form of $\psi_1(\delta_1)$ for the case of wooden ties of type IA, crushed stone ballast, and distance between ties $\Delta x = 55$ cm; Fig. II.6b shows the same function for wooden ties of type IIA, sand ballast, and distance between ties $\Delta x = 55$ cm.

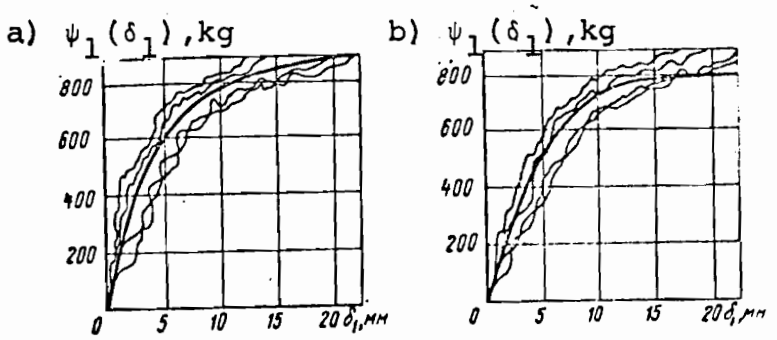

Fig. II.6. Realizations of the random process of tie resistance to displacement along the track in the form of functions of displacement (Δx = 55 cm): (a) ties IA, crushed stone ballast; (b) ties IIA, sand ballast.

The heavily drawn curves represent the expected value of the function $\psi_1(\delta_1)$. The graphs show that the rate of growth of the displacement resistance of the ties decreases with the growth of the displacement, and that the resistance reaches a maximum value for some displacement $\delta_1 = \delta_{1max}$, and stays approximately constant as the displacement is increased further. This critical state is characterized by the formation of a sliding surface in the ballast. The resistance to displacement of a single unloaded tie consists basically of the resistance due to the lower bed and of the resistance to displacement of the ballast in the tie crib. Consequently, the tie dimensions and the degree of packing of the ballast in the tie crib have a large influence on the resistance to displacement.

In addition to the factors indicated above, the dimensions of the tie crib play a decisive role. For a sufficiently large tie crib, a displacement of the tie results in a displacement of the ballast prism ABC (Fig. II.7), where the sliding surface is determined by the condition of least resistance to displacement. Usually, the angle α_o of the sliding surface is about 30-33°.

If all the ties are fastened to the rails in the same way (which is true, for example, for the case of a multiple component fastening of type K, or for a simple fastening if the rails are anchored to all the ties), a decrease in the distance between the ties leads to a decrease in the resistance. Indeed, Fig. II.8 shows that even with the same sliding angle α_o as before, the volume of the displaced prism and the sliding surface area decrease because of the preceding tie. Actually, the angle α_o decreases, which leads to a further decrease in the tie resistance.

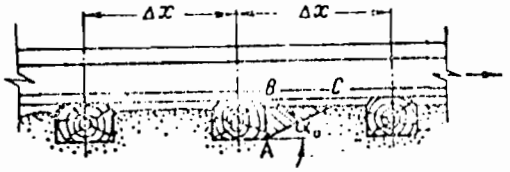

Fig. II.7. Formation of a sliding surface in the ballast if the displaced tie is sufficiently far from the preceding one

Fig. II.9 shows the relation between the magnitude of the tie displacement along the track and the expected value of its resistance to displacement in medium grain sand ballast for different sizes of tie crib. The curves are steeper for larger sizes of tie crib.

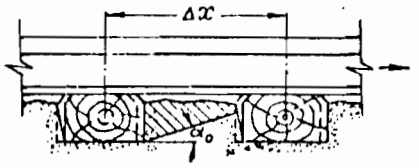

Fig. II.8. Formation of sliding surface in the ballast if the displaced tie is close to the preceding one

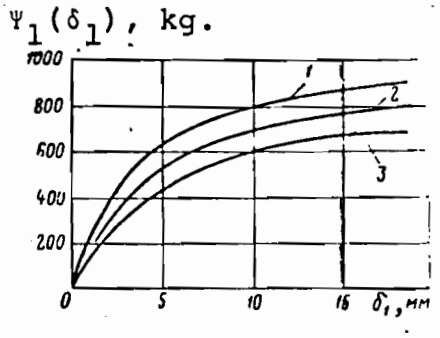

Fig. II.9. Mathematical expectation of the displacement resistance of the ties vs displacement. (1) $\Delta x \geq 75$ cm; (2) $\Delta x = 55$ cm; (3) $\Delta x = 50$ cm

When the distance Δx between the ties exceeds 70-75 cm, the ballast is pushed out according to the scheme indicated in Fig. II.7. Consequently, the function $\Psi_1(\delta_1)$ has the same form for all cases where the distance between the ties $\Delta x \geq 75$ cm.

If the track is anchored against the action of longitudinal forces in sections, these forces are not transmitted uniformly to the ties in each section, as a result of which the average utilization of the displacement resistance of each tie is decreased. Experiments conducted at the Moscow Institute of Railroad Engineers show that if the displacement resistance of a single tie is taken to be 100%, the resistance of an anticreep section consisting of two, three, four, or five ties will be considerably less (Table 1).

Table 1

Number of ties in section	Resistance of the section to displacement as a percentage of the resistance of a single tie	Average utilization of the resistance of each tie in the section,
1	100	100
2	156.6	78.3
3	202.2	78.3
4	244.8	61.2
5	298.5	59.7

The maximum resistance of a three tie section corresponds approximately to the resistance of two independently operating ties. The resistance of a five tie section is approximately equal to that of three ties, each equipped with an anticreeper.

These data are corroborated by practical experiences with track anchored against creep.

In computing the longitudinal forces and displacements in track fastened against creep in sections, we must take $\Psi_1(\delta_1)$ to be the resistance of the tie section divided by the number of ties in the section. Similarly, $\Psi_2(\delta_2)$ must be understood to represent the resistance against rail displacements along the track from the fastenings and anticreep devices in the tie section, divided by the number of ties in the section.

The resistance of the tie to displacement depends vitally on the degree of packing of the ballast. The importance of tamping the ballast in the tie cribs for track operation can be demonstrated by determining the resistance after tamping the ballast, and after packing it by tramping on it. The maximum resistance in the second case is only about 70-80% of the resistance after tamping.

Let us note that in the absence of vertical loads the tie resistance usually fluctuates in the following ranges: 800-1000 kg per tie in crushed stone ballast, 600-800 kg per tie in sand ballast.

Let us examine now in greater detail the function $\Psi_2(\delta_2)$, which represents the resistance to displacements of two rails over a tie. This function depends chiefly on the degree of compression

between the tie and the rail and on the quality of the anticreep devices, which is determined, in turn, by the type of intermediate fastening, the type of rail anchor, and also the quality of track maintenance. In a multiple component clamp fastening, which assures a pressure force on each clamp of 800-1000 kg, the force necessary to displace two rails over a tie exceeds 1000 kg. Under these conditions the tie will be practically displaced together with the rail, and the function $\Psi(\lambda,0)$ is determined with sufficient accuracy by the dependence of the resistance of the tie to displacement, $\Psi_1(\delta_1) \simeq \Psi_1(\lambda)$. With a worn spike fastener, the force needed for the displacement of two rails not fastened to the tie by rail anchors, does not exceed 200-300 kg. When δ_1 reaches the value δ_{1max}, there will occur a sudden displacement along the surface of contact between the rail and the tie (tie plate), and if the force is increased, the rail will be displaced with respect to the tie.

To construct the function $\Psi(\lambda,0)$ from the graphs of $\Psi_1(\delta_1)$ and $\Psi_2(\delta_2)$ one can use the following method. Assuming a certain value of the force $\Psi_i(\lambda_i,0)$ transmitted from the rail to the tie, let us compute the displacements δ_{1i} and δ_{2i} produced by this force.

The sum of these displacements yield the total rail displacement, $\lambda = \delta_{1i}+\delta_{2i}$. Thus, for every value of the function $\Psi(\lambda,0)$ one can determine a value of the argument λ, i.e. the graph of the force transmitted by the rail to the tie vs. the rail displacement is completely determined.

It should be noted that the function $\Psi_2(\delta_2)$ assumes not only the existence of dry friction between the rail and the tie plate, but also takes into account the play in the fastenings, the elastic unloading of the bolts and screw spikes, the compression of the wood under the rail anchors, and many other factors, so that $\Psi_2(\delta_2)$ is, in general, a random function with a nonlinear mathematical expectation. An especially large effect on the spread of the values of $\Psi_2(\delta_2)$ is produced by the nonuniform pressure of the clamps and the fastening spikes, and also of the rail anchors along the track. Consequently, the determination of the random function $\Psi(\lambda,0)$ from the random functions $\Psi_1(\delta_1)$ and $\Psi_2(\delta_2)$ presents certain technical difficulties.

The author has conducted a series of experiments to determine directly the graph of $\Psi(\lambda,0)$ for a track with wooden ties of type IA on crushed stone ballast, with fastenings of type K, and also for a track with wooden ties of type IIA on a sand ballast, with spike fastenings and with the track anchored in sections against longitudinal displacements (five ties to a section). The general form of these functions is shown in Fig. II.10, a and b.

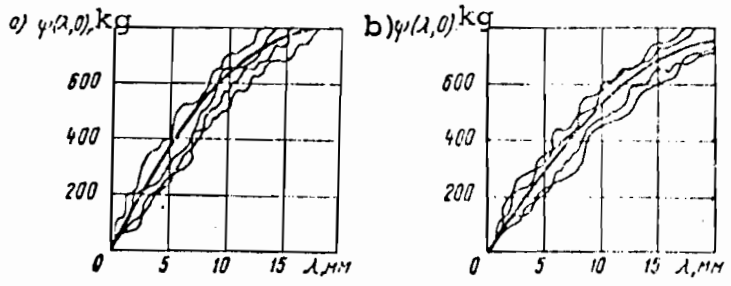

Fig. II.10. Realizations of the random process of force transmitted from rail to tie vs rail displacement (Δx = 55 cm): (a) ties IA, crushed stone ballast, fastenings of type K (b) ties IIA, sand ballast, simple fastenings

Comparing figures II.6b and II.10b, it is evident that for the track with spike fastenings, the graph of the function $\Psi(\lambda,0)$ is less steep than the corresponding graph for $\Psi_1(\delta_1)$. This can be explained by the fact that the same longitudinal force, transmitted from rail to tie, produces simultaneously a displacement of the rail with respect to the tie, and a displacement of the tie with respect to the ballast. For a track with fastenings of type K, the difference between the graphs of $\Psi(\lambda,0)$ and $\Psi_1(\delta_1)$ is less noticeable. This is explained by the circumstance that the tie is displaced together with the rail.

For a fixed value of the displacement λ_i, the random fuction $\Psi(\lambda,0)$ is transformed into the random variable $\Psi_i(\lambda_i,0)$, the distribution for which can be obtained from experiments in the usual way without any difficulty. The author's experiments show that the distribution of the centered random variable $\Psi_i^o(\lambda_i,0)$ is close to normal. The fact that the random variable $\Psi_i^o(\lambda_i,0)$ consists of a sum of at least ten different factors with comparable weights can serve as a basis for the adoption of the normal law for its distribution. Since the random variables $\Psi[\lambda(x_1)]$ and $\Psi[\lambda(x_2)]$ are uncorrelated, it is sufficient to know the variance $\partial\Psi(\lambda)$ for every value of λ in order to characterize the random process $\rho(x)$ completely.

Let us return now to the previously obtained equation (II.25) Taking the expected value of (II.25), we obtain

$$\frac{d^2 M_\lambda}{dx^2} = \frac{1}{2EF\sqrt{\Delta x}} M\psi(\lambda, 0). \qquad \text{(II.26)}$$

Equation (II.26) can be integrated by quadratures. Indeed, multiplying both sides of the equation by $2(dM_\lambda/dx)$, we obtain

$$2\frac{d^2M_\lambda}{dx}\cdot\frac{d^2M_\lambda}{dx^2}=\frac{1}{EF\Delta x}M\psi(\lambda,0)\frac{dM_\lambda}{dx},$$

or, in terms of differentials,

$$d\left(\frac{dM_\lambda}{dx}\right)^2=\frac{1}{EF\Delta x}M\psi(\lambda,0)\,dM_\lambda,$$

from which

$$\left(\frac{dM_\lambda}{dx}\right)^2=\frac{1}{EF\Delta x}\int_{M_{\lambda_0}}^{M_\lambda}M\psi(\lambda,0)\,dM_\lambda+c_1.$$

One can solve the last equation for the derivative

$$\frac{dM_\lambda}{dx}=\sqrt{\frac{1}{EF\Delta x}\int_{M_{\lambda_0}}^{M_\lambda}M\psi(\lambda,0)\,dM_\lambda+c_1}.$$

Separating the variables in this expression, we obtain

$$x+c_2=\int_{M_{\lambda_0}}^{M_\lambda}\frac{dM_\lambda}{\sqrt{\frac{1}{EF\Delta x}\int_{M_{\lambda_0}}^{M_\lambda}M\psi(\lambda,0)\,dM_\lambda+c_1}}.$$

For boundary values we must take the following:

$$M_\lambda\Big|_{x=x_0}=0;\quad\frac{dM_\lambda}{dx}\Big|_{x=x_0}=\alpha t+\frac{M_P}{EF}\Big|_{x=x_0}=0.$$

Physically, these conditions are a reflection of the fact that at a fixed point x_o the expected value of the longitudinal force is given by $M_P = -\alpha tEF$. The minus sign indicates that a positive temperature increase in the rail produces a compressive force. Finally, we obtain

$$M_P=\sqrt{\frac{1}{EF\Delta x}\int_0^{M_\lambda}M\psi(\lambda,0)\,dM_\lambda}-\alpha tEF; \tag{II.27}$$

$$x - x_0 = \int_0^{M_\lambda} \frac{dM_\lambda}{\sqrt{\frac{1}{EF\Delta x}\int_0^{M_\lambda} M\psi(\lambda, 0)\, dM_\lambda}}. \qquad \text{(II.28)}$$

Equation (II.27) relates the expected value of the longitudinal force to the magnitude of the longitudinal displacement at the same section.

Taking into account the fact that the longitudinal force at the end of a rail string is equal to the resistance against the displacement of the rails from the joint bars (rail expansion joints), $M_P = P_H$, one can easily obtain on the basis of (II.27) the relation between the temperature rise after the installation of the rail in the track and the expected value of the displacement λ_o of the end of the rail string produced by the temperature rise:

$$t = \frac{1}{\alpha}\sqrt{\frac{1}{EF\Delta x}\int_0^{M_\lambda} M\psi(\lambda, 0)\, dM_\lambda} + \frac{P_H}{\alpha EF}. \qquad \text{(II.29)}$$

The resistance against rail displacement in the joint bars fluctuates between 4000 and 1000 kg.

If in (II.28) we assume $M\Psi(\lambda O) = c = \text{const}$, which corresponds to the case of constant longitudinal resistance per unit length, and if we take as the origin of the coordinates the fixed point x_o of the rail string, integration of the expression yields

$$\int_0^{M_\lambda} \frac{dM_\lambda}{\sqrt{\frac{c}{EF\Delta x}\int_0^{M_\lambda} dM_\lambda}} = \sqrt{\frac{4EF\Delta x}{c}}\, M_\lambda = x;$$

solving the resulting equation for M_λ, we arrive at

$$M_\lambda = \frac{x^2}{2EF} \cdot \frac{c}{2\Delta x} = \frac{x^2}{2EF} M_\rho, \qquad \text{(II.30)}$$

where $M_\rho = (c/2\Delta x)$ is the expected value of the resistance to longitudinal rail displacement per unit length.

The equation of the expected value of the longitudinal forces can be obtained from (II.27):

$$M_P = \sqrt{\frac{EF}{\Delta x}\int_0^{M_\lambda} M\psi(\lambda, 0)\, dM} - \alpha t EF = \sqrt{\frac{EF}{\Delta x} c M_\lambda} - \alpha t EF; \qquad \text{(II.30)}$$

substituting from (II.30) for the value of M_λ, we finally obtain

$$M_P = \sqrt{\frac{EF}{\Delta x} c M_\lambda} - \alpha t EF = M_\rho x - \alpha t EF. \qquad \text{(II.31)}$$

Finally, the equation (II.29) for our case will take the form

$$t = \frac{1}{\alpha}\sqrt{\frac{2M_\lambda}{EF} M_\rho} + \frac{P_H}{\alpha EF}. \qquad \text{(II.32)}$$

The general form of the graph of the function $t(M_\lambda)$ is shown in fig. II.11.

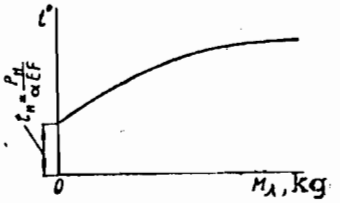

Fig. II.11. Dependence of the expected value of the displacement of the free end of a rail string on the rise in rail temperature.

For our case of constant resistance per unit length, the variance of the random quantity $\rho(x)\Delta x$ is constant, i.e.

$$D_{\rho\Delta x} = D_o \Delta x$$

Since the process $\rho(x)$ is delta-correlated, we find, in accordance with the results of the previous section, that the correlation function of the process is given by

$$K_\rho(x_1,x_2) = D_o\delta(x_2-x_1). \qquad \text{(II.33)}$$

Let us recall that a process which has a correlation function satisfying a relation of type (II.33) represents "white noise", since its spectral density is constant over the whole frequency range, from $-\infty$ to ∞.

Taking into account the boundary condition $D_P(0)$, the correlation function of the process $P(x)$ can be computed according to (II.17):

$$K_P(x_1, x_2) = D_0 \min(x_1, x_2) = \begin{cases} D_0 x_1 & \text{при } x_2 > x_1 \\ D_0 x_2 & \text{при } x_2 < x_1 \end{cases}. \qquad \text{(II.34)}$$

The surface described in (II.34) is shown in Fig. II.12.

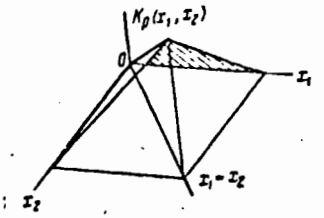

Fig. II.12. Correlation function $K_P(x_1,x_2)$ of the process of the variation of the longitudinal rail forces.

Finally, taking into account the boundary conditions $D_P(0) = 0$; $K_{P(0)/EF,\lambda_P(0)} = 0$; $D_{\lambda_P}(0) = 0$, we can determine the correlation function of the process $\lambda(x)$ according to (II.21):

$$K_{\lambda_P}(x_1, x_2) = \frac{D_0}{2(EF)^2} x_1 x_2 \min(x_1, x_2) = \begin{cases} \dfrac{D_0}{2(EF)^2} x_2 x_1^2 & \text{при } x_2 > x_1 \\ \dfrac{D_0}{2(EF)^2} x_1 x_2^2 & \text{при } x_2 < x_1 \end{cases}. \qquad \text{(II.35)}$$

The surface described by (II.35) is represented in Fig. II.13.

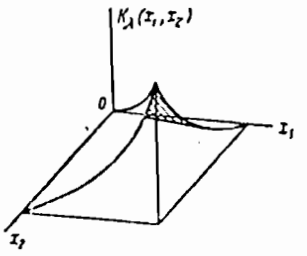

Fig. II.13. Correlation function $K_\lambda(x_1, x_2)$ of the process of displacements of rail sections

Finally, let us determine the correlation functions of the processes $P_\rho(x)$ and $\lambda_P(x)$. For the first of these we find, from the results of the previous section

$$R_P(x_1, x_2) = \frac{K_P(x_1, x_2)}{\sqrt{K_P(x_1, x_1) K_P(x_2, x_2)}} = \frac{D_{0\min}(x_1, x_2)}{\sqrt{D_0 x_1}\sqrt{D_0 x_2}} = \frac{\min(x_1, x_2)}{\sqrt{x_1, x_2}}. \qquad (II.36)$$

For the process $\lambda_P(x)$, the normalized correlation function has the form

$$R_\lambda(x_1, x_2) = \frac{K_\lambda(x_1, x_2)}{\sqrt{K_\lambda(x_1, x_1) K_\lambda(x_2, x_2)}} = \frac{\frac{D_0}{(EF)^2} x_1 x_2 \min(x_1, x_2)}{\sqrt{\frac{D_0}{(EF)^2} x_1^3}\sqrt{\frac{D_0}{(EF)^2} x_2^3}} = \frac{\min(x_1, x_2)}{\sqrt{x_1 x_2}}. \qquad (II.37)$$

Thus, the normalized correlation functions of the processes $P(x)$ and $\lambda(x)$ coincide.

Let us go over to cylindrical coordinates. Setting $x_1/x_2 = \tan\alpha$, and taking into account the equation

$$\frac{\min(x_1, x_2)}{\sqrt{x_1, x_2}} = \begin{cases} \sqrt{\frac{x_1}{x_2}} & \text{при } x_2 > x_1 \\ \sqrt{\frac{x_2}{x_1}} & \text{при } x_2 < x_1 \end{cases},$$

L3.

we obtain

$$R_P(x_1, x_2) = R_\lambda(x_1, x_2) = \begin{cases} \sqrt{\operatorname{tg}\alpha}, & \text{при} \quad 0 < \alpha < 45^\circ \\ \sqrt{\operatorname{ctg}\alpha} & \text{при} \quad 45^\circ < \alpha < 90^\circ; \end{cases}$$

$$\alpha = \operatorname{arctg}\frac{x_1}{x_2}.$$

Consequently, the surface consists of the intersection of two conoids. Fig. II.14 shows what such a surface looks like.

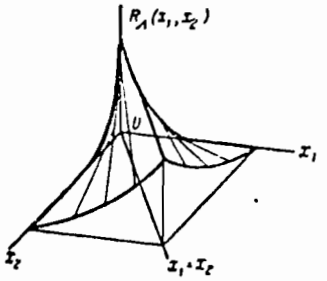

Fig. II.14. Normalized correlation function $R_\lambda(x_1, x_2)$ of the process of displacements of rail sections

For a track with worn spike fastenings, the expected value of the resistance per unit length, M_ρ, is 2 to 2.5 kg/cm, and the corresponding variance D_o varies from 40 to 60 kg^2/cm.

Figure II.15 shows the processes $P(x)+\alpha tEF$ and $\lambda(x)$ computed for the values M_ρ = 2 kg/cm, D_o = 50 kg^2/cm. The solid lines represent the mathematical expectation, the dotted ones - the mean square deviation.

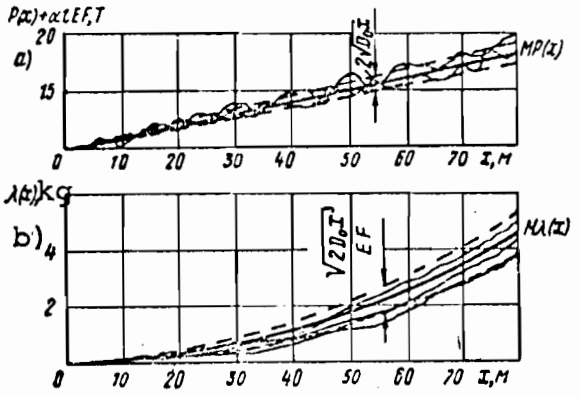

Fig. II.15. Realizations of the random processes $P(x)+\alpha tEF$ and $\lambda(x)$. (a) $D_p = D_o x$; (b) $D_\lambda = D_o x^3/2E^2F^2$.

Taking into account the Gaussian nature of the random process P(x) and the formulas (II.31) and (II.34), we obtain for the one-dimensional probability distribution [9]:

$$F(P, x) = \frac{1}{\sqrt{2\pi D_0 x}} e^{-\frac{(P+\alpha t EF - M_\rho x)^2}{2D_0 x}}. \qquad \text{(II.38)}$$

Let us recall that the coordinate origin is at x_o, the fixed point of the rail string. The quantity $F(P_1,x)\,dP_1$ gives the probability that the graph of the function passes through some "gap" in the P x plane, as shown in Fix. II.16.

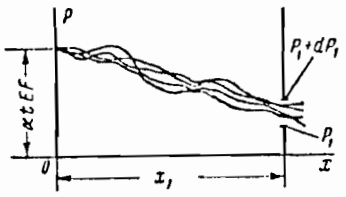

Fig. II.16. Passage of the random process P(x) through a "gap" in the P x plane

If ℓ represents the length of the "transition" zone of a rail string, and P_ℓ denotes the longitudinal force at the end, then, in view of

$$\left.\frac{dP}{dx}\right|_{x=l} \rho(l),$$

one can write

$$F(P_\ell, \ell)\,dP_\ell = F(P_\ell, \ell)\,\rho(\ell)\,d\ell = F^*(\ell, P_\ell)\,d\ell,$$

where $F^*(\ell, P_\ell)$ is the probability density of the random variable ℓ.

At the free end of the rail string, the value of the longitudinal force satisfies $P_\ell = -P_H$, where P_H is the resistance to rail displacements in the joint bars (rail expansion joints).

Consequently, in view of (II.38), the probability density of the random variable ℓ is given by the formula

$$F^*(l,\ P_н) = F(P_н,\ l)\rho(l) = \\ = \frac{\rho(l)}{\sqrt{2\pi D_0 l}} e^{-\frac{(M_\rho)^2}{2D_0} l + \frac{(\alpha l EF - P_н) M_\rho}{D_0} - \frac{(\alpha l EF - P_н)^2}{2D_0} \cdot \frac{1}{l}}. \qquad \text{(II.39)}$$

It should be added that formula (II.38) holds only when $t > P_H/\alpha EF$, since the free end of the rail string does not move if the temperature rise is smaller, i.e. $\ell = 0$.

Let us now compute the probability that ℓ lies between 0 and a:

$$P(0<l<a) = \int_0^a F(P_н,\ l)\rho(l)\,dl = \rho_{ср} \int_0^a F(P_н,\ l)\,dl,$$

where $\rho_{ср}$ is the mean value of the random function $\rho(\ell)$, in the domain $0<\ell<a$.

We can now determine the limit

$$\lim_{x\to\infty} \frac{1}{x^2} \int_0^x \int_0^x K_\rho(x_1,\ x_2)\,dx_1\,dx_2 = \lim_{x\to\infty} \frac{D_0 x}{x^2} = 0. \qquad \text{(II.40)}$$

The general ergodic theorem can be stated in the following way: if the expected value of a random function is constant, and the correlation function satisfies (II.40), then the mean value of the random function over the domain $0<x<\infty$ has as its mean square limit the expected value of the random function [30]. Thus,

$$P(0<l<a) = M_\rho \int_0^a F(P_н,\ l)\,dl,$$

and, differentiating this equation, we find

$$F^\circ(l;\ l) = \frac{M_\rho}{\sqrt{2\pi D_0 l}} e^{-\frac{(M_\rho)^2}{2D_0} l + \frac{(\alpha l EF - P_н) M_\rho}{D_0} - \frac{(\alpha l EF - P_н)^2}{2D_0} \cdot \frac{1}{l}}. \qquad \text{(II.41)}$$

Consequently, equations (II.39) and (II.41) are equivalent; however, the second one is more convenient since it involves a nonrandom function. It is easy to verify that the probability density of the random variable ℓ has the following properties: $F^{\circ}(\infty;t)=0$; $F^{\circ}(0;P_{H}/\alpha EF) = \infty$; and, in addition, $F^{\circ}(0;t>P_{H}/\alpha EF) = 0$. Indeed

$$F^{\circ}\left(0;\ t>\frac{P_{н}}{\alpha EF}\right)=A\lim_{l\to 0}\frac{e^{-\alpha l-\beta\frac{1}{l}}}{\sqrt{l}}=$$

$$=A\lim_{l\to 0}\frac{e^{-\beta\frac{1}{l}}}{\sqrt{l}}=A\lim_{\eta\to\infty}\frac{\eta}{e^{\beta\eta^{2}}},$$

где $A=\frac{M_{\rho}}{\sqrt{2\pi D_{0}}}e^{\frac{\alpha tEF-P_{н}}{D_{\bullet}}M_{\rho}}=\text{const};\quad \eta=\sqrt{\frac{1}{l}};$

$$\alpha=\frac{(M_{\rho})^{2}}{2D_{0}}>0;\quad \beta=\frac{(\alpha tEF-P_{н})^{2}}{2D_{0}}>0,$$

or, making use of L'Hospital's rule,

$$F^{\circ}\left(0;\ t>\frac{P_{н}}{\alpha EF}\right)=A\lim_{\eta\to\infty}\frac{\eta}{e^{\beta\eta^{2}}}=A\lim_{\eta\to\infty}\frac{1}{2\eta e^{\beta\eta^{2}}}=0.$$

Furthermore, one can show that

$$P(0<l<\infty)=\int_{0}^{\infty}F^{\circ}(l;\ t)\,dl=1,$$

which shows that the length of the "transition" zone satisfies $0<\ell<\infty$ with probability one. Integrating (II.41), we obtain

$$\int_{0}^{\infty}F^{\circ}(l;\ t)\,dl=$$

$$=e^{\frac{(\alpha tEF-P_{н})M_{\rho}}{D_{\bullet}}}\int_{0}^{\infty}\frac{M_{\rho}}{\sqrt{2\pi D_{0}l}}e^{-\frac{1+\left(l\frac{M_{\rho}}{\alpha tEF-P_{н}}\right)^{2}}{2l\frac{D_{0}}{(\alpha tEF-P_{н})^{2}}}dl},$$

or, making use of the notation

$$\xi=\frac{M_{\rho}}{\alpha tEF-P_{н}}l;$$

$$q=\frac{D_{0}}{(\alpha tEF-P_{н})M_{\rho}}>0,$$

we obtain

$$\int_0^\infty F^\circ(l;\ t)\,dl = e^{\frac{1}{q}} M_\rho \frac{1}{\sqrt{M_\rho}} \sqrt{\frac{\alpha t EF - P_н}{2\pi D_0}} \int_0^\infty e^{-\frac{1+\xi^2}{2q\xi}} \frac{d\xi}{\sqrt{\xi}}.$$

In view of the formula

$$\int_0^\infty e^{-\frac{1+\xi^2}{2q\xi}} \frac{d\xi}{\sqrt{\xi}} = \sqrt{2\pi q}\, e^{-\frac{1}{q}},$$

which can be found in the table of integrals [33], we finally arrive at

$$\int_0^\infty F^\circ(l;\ t)\,dl = e^{\frac{1}{q}} M_\rho \frac{1}{\sqrt{M_\rho}} \sqrt{\frac{\alpha t EF - P_н}{2\pi D_0}} \times$$

$$\times \sqrt{\frac{2\pi D_0}{\alpha t EF - P_н}} \cdot \frac{1}{\sqrt{M_\rho}} e^{\frac{1}{q}} = 1,$$

which is what had to be shown.

The general form of the distribution function of $F^\circ(\ell;t)$ is shown in Fig. (II.17).

From an analysis of (II.41) it follows that as the temperature rises after the rail has been installed in the track, the graph of the distribution function $F^\circ(\ell;t)$ appears to shift in the direction of increasing lengths of the "transition" zone , simultaneously becoming less steep; in other words, as the temperature of the rail string rises (falls), the expected value of the length of the "transition" zone and the variance both increase, which is quite evident from a physical point of view.

Finally, the determination of the displacement of the rail end λ_0 is of great importance in designing CWR track. Let us determine the conditional probability of the end of a rail string with a fixed value of "transition" zone length, taking into account the fact that the process $\lambda(x)$ has a normal distribution.

Making use of (II.30) and (II.35), we obtain

$$\Phi(\lambda_0/l) = \frac{1}{\sqrt{\frac{\pi D_0}{(EF)^2} l^3}} e^{-\frac{\left(\lambda_0 - \frac{M_\rho}{2EF} l^2\right)^2}{D_0 l^3} (EF)^2}. \qquad \text{(II.42)}$$

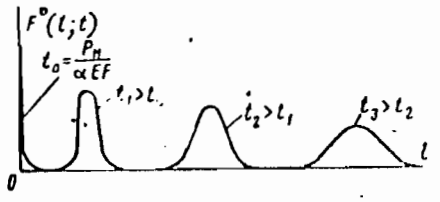

Fig. II.17. Distribution function of the length of the "transition" zone for different temperature rises of the rail string

However, the length of the "transition" zone ℓ is itself a random variable, with a probability distribution function $F^0(\ell;t)$.

At the same time, it is known from the theory of probability that a two dimensional probability distribution of the random variables ℓ, λ_0 is equal to the product of the probability density of one of them and the conditional probability of the other one with respect to the first one.

Thus,

$$\Phi^*(\lambda_0; l; t) = F^0(l; t)\Phi(\lambda_0/l) =$$

$$= \frac{M_\rho E^2 F^2}{EF\pi D_0 l^2 \sqrt{2}} e^{-\frac{(\alpha t EF - P_H - M_\rho l)^2}{2D_0 l} - EF\frac{\left(\lambda_0 - \frac{M_\rho}{2EF} l^2\right)^2}{D_0 l^3}} \qquad \text{(II.43)}$$

Formula (II.43), as well as formula (II.41) is valid if the condition $\lambda_0 < \delta$ is satisfied; here δ is the length of the joint gap (magnitude of the movement in the rail expansion joint), since we assume $P(\ell) = P_H$.

If after the gap is closed there is a further rise in temperature, the displacements remain the same as they were at

the time the gap closed.

The longitudinal force in cross-section x will then be

$$P(x) = P^{o}(x) + \alpha(t-t_{o})EF. \qquad \text{(II.44)}$$

Here the following designations are used:

$$P(x)|_{t=t_0} = P^{\circ}(x);\ t|_{x=3} = t_0.$$

It has been tacitly assumed that the averagedlongitudinal force-displacement relation remains the same, since, in fact, the track characteristics vary with changes in temperature and time.

Now, let us examine the case when the force transmitted from the rail to the tie grows according to

$$M\Psi(\lambda,O) = c + KM_{\lambda}.$$

Taking the fixed point x_o as the origin of the coordinates, as we have done in the previous case, we obtain

$$x = \int_0^{M_\lambda} \frac{dM_\lambda}{\sqrt{\frac{1}{EF\Delta x}\int_0^{M_\lambda}(c + KM_\lambda)\,dM_\lambda}} =$$
$$= \sqrt{\frac{2EF\Delta x}{K}}\,\operatorname{arch}\left(\frac{K}{c}M_\lambda + 1\right),$$

which yields

$$M_\lambda = \frac{c}{K}\left(\operatorname{ch}\sqrt{\frac{K}{2EF\Delta x}}\,x - 1\right). \qquad \text{(II.45)}$$

Differentiating (II.45) and substituting in (II.2) determines the magnitude of the longitudinal force in the track:

$$M_P = c\sqrt{\frac{EF}{2K\Delta x}}\operatorname{sh}\sqrt{\frac{K}{2EF\Delta x}}\,x - \alpha tEF. \qquad \text{(11.46)}$$

Relations (II.45) and (II.46) we obtained by the author in 1956 by a somewhat different method.

Equation (II.29) , which relates the displacement of the end of the rail to the temperature, assumes the form

$$t = \frac{1}{\alpha}\sqrt{\frac{1}{2EF\Delta x}[K M_\lambda^2 + cM_\lambda] + \frac{P_H}{\alpha EF}}. \qquad \text{(II.47)}$$

in our case.

If the experimentally determined function $M\Psi(\lambda)$ is approximated by a third degree polynomial without constant term,

$$M\psi(\lambda) = \alpha M_\lambda^3 + \beta M_\lambda^2 + \gamma M_\lambda,$$

or by the function

$$M\Psi(\lambda) = m_o M\lambda^n,$$

the right hand side of (II.28) can be reduced to a tabulated integral and can be expressed in terms of elementary functions. Finally, if $M\Psi(\lambda)$ is approximated by a third degree polynomial with a nonvanishing constant term, the right hand side of (II.28) will be an elliptic integral of the first kind. If the integral thus obtained is transformed to the Legendre form by means of an uncomplicated substitution [23] and then inverted, the expected value of the displacement of a track cross-section $\lambda(x)$ can be expressed by means of the elliptic sine function (of Jacobi), a function which has been studied in sufficient detail. Convenient graphs and tables for elliptic integrals and Jacobian elliptic functions are available in [33].

We will not explore these solutions further, except to note that for the case $M\Psi(\lambda) = \gamma\lambda$, the equation for longitudinal forces and displacements was studied by the author in 1956.

In the most general case, the integration of (II.28) can be accomplished by a graphical-analytical procedure, based on the experimentally determined graph of the function $M\Psi(\lambda)$ for the particular track under investigation. In performing the graphical integration it is not necessary to worry about the case when the function $\Psi(\lambda)$ vanishes for $\lambda = 0$. In this case it is sufficient to assume $\Psi(0) = \Psi(\lambda)$, where λ is the required accuracy in determining the displacements. With this assumption, the longitudinal force-displacement diagram does not change for all practical purposes; it is only the theoretically determined length of the zone in which the longitudinal forces decay which changes, and which become infinite for the case $\Psi(0) = 0$. But here anyway, we must for practical purposes take the length of the decay zone to be the distance to a point for which the displacement λ^0 is zero to within the required accuracy.

After the equation (II.28) has been integrated, one can associate with each value $\lambda(x)$ a value of $D_{\rho\Delta x}(x) = \partial\Psi[\lambda(x),0]$. Thus, one can consider the variance of the linear resistance to be known graphically. In view of (II.17) and the boundary condition $D_p(0) = 0$ (for the coordinate origin we take the fixed point x_o closest to the free end of the rail string), the correlation function of the process $P(x)$ takes the form

$$K_P(x_1, x_2) = \int_0^{\min(x_1, x_2)} D_\rho(x)\,dx. \qquad \text{(II.48)}$$

Since the graph of $D_\rho(x)$ is known, the surface described by (II.48) can also be constructed by using one of the approximating

schemes. Finally, taking into account the boundary conditions $D_P(0) = 0$; $K_{P(0),\lambda_{P(0)}}/EF = 0$; $D_{\lambda_P}(0) = 0$ the correlation function of $\lambda(x)$ for the general case being considered can be written, according to (II.21), in the form

$$K_{\lambda\rho}(x_1, x_2) = \begin{cases} \frac{x_2}{(EF)^2} \int_0^{x_1} \int_0^{x_1} D_\rho(x)\, dx\, dx \text{ при } x_2 > x_1 \\ \frac{x_1}{(EF)^2} \int_0^{x_2} \int_0^{x_1} D_\rho(x)\, dx\, dx \text{ при } x_2 < x_1. \end{cases} \tag{II.49}$$

If the graph of $D_\rho(x)$ is given, one can also construct the surface described by (II.49), If the function D (x) is determined at a sequence of points, $x = n\Delta x$, $x = 2n\Delta x$, ...,$x = qn\Delta x$, it suffices to compute the elements of the covariance matrices instead of constructing the correlation surfaces; here q is the number of points of division of the graphs $P(x)$ and $\lambda.(\bar{x})$.

Let us now compute the one dimensional probability density of the process $P(x)$. Taking into account the Gaussian nature of the process and (II.48), we obtain

$$F(P, x) = \frac{1}{\sqrt{2\pi D_P(x)}} e^{-\frac{[P - M_P(x)]^2}{2D_P(x)}}, \tag{II.50}$$

where $D_P(x) = (K_P x, x) = \int_0^x D_\rho(y)\, dy$ and $M_P(x)$ is given graphically or in tabular form

In view of the relation

$$\left.\frac{dP}{dx}\right|_{x=l} = \rho(l),$$

one can write

$$F(P_\ell, \ell)\, dP_\ell = F(P_\ell, \ell)\, \rho(\ell)\, d\ell = F^*(\ell, P_\ell)\, d\ell,$$

where $F^*(\ell, P_\ell)$ is the probability density of the random quantity ℓ.

Taking note of the condition at the end of the rail, $P_\ell = -P_H$, the probability density of ℓ is found to be

$$F^*(l,\ P_H) = \frac{\rho(l)}{\sqrt{2\pi D_P(l)}}\, e^{-\frac{[M_P(l)-P_H]^2}{2D_P(l)}}.$$

Here, as in the case of constant linear resistance, the relation $t > P_H/\alpha tEF$ must hold.

Let us now compute the probability

$$P(0<l<a) = \int_0^a F(P_H,\ l)\,\rho(l)\,dl = \qquad \text{(II.51)}$$

$$= \int_0^a F(P_H,\ l)\,M_\rho(l)\,dl + \int_0^a F(P_H,\ l)\,\rho^\circ(l)\,dl,$$

where $\rho^\circ(\ell)$ is centered random function.

Since $D_\rho(x)$ is bounded above, one can find an N such that $D_\rho(x) < N$; then

$$\lim_{x\to\infty} \frac{1}{x^2} \int_0^x \int_0^x K_\rho(x_1,\ x_2)\,dx_1\,dx_2 < \lim_{x\to\infty} \frac{Nx}{x^2} \to 0,$$

i.e. the random function $\rho^\circ(\ell)$ has the ergodic property.

The second integral in the right hand side of (II.51) can be reduced to zero in probability,

$$\int_0^a F(P_H,\ l)\,\rho^\circ(l)\,dl = M_{\rho^\circ} \int_0^a F(P_H,\ l)\,dl = 0.$$

Finally, the probability density of ℓ takes the form

$$F^\circ(l;\ t) = \frac{M_\rho(l)}{\sqrt{2\pi D_P(l)}}\, e^{-\frac{[M_P(l)-P_H]^2}{2D_P(l)}}. \qquad \text{(II.52)}$$

Let us prove that the function $F^\circ(\ell;t)$ satisfies the condition

$$P(0<l<\infty) = \int_0^\infty F^\circ(l;\ t)\,dl = 1.$$

Indeed, on the one hand we have

$$\int_{-\infty}^{\infty} F^{\circ}(l;\ t)\,dl = \int_{-\infty}^{\infty} F(P_{\text{н}},\ l)\,\rho(l)\,dl = \int_{-\infty}^{\infty} F(P_l,\ l)\,dP_l = 1;$$

on the other hand, for all negative x we have

$$P(-x) \equiv -\alpha t EF; \quad \rho(-x) \equiv 0.$$

Consequently,

$$\int_{-\infty}^{0} F^{\circ}(l;\ t)\,dl = \int_{-\infty}^{0} F(P_{\text{н}}, l)\,\rho(l)dl = 0,$$

i.e.

$$\int_{0}^{\infty} F^{\circ}(l;\ t)\,dl = \int_{-\infty}^{\infty} F^{\circ}(l;\ t)\,dl - \int_{-\infty}^{0} F^{\circ}(l;\ t)\,dl = 1,$$

which is what had to be proved.

Since the process $\lambda(x)$ has a normal distribution, the conditional probability of the displacement of the end of a rail for a given value of the random variable ℓ is determined by

$$\Phi(\lambda_0/l) = \frac{1}{\sqrt{2\pi D_\lambda(l)}}\, e^{-\frac{[\lambda_0 - M_\lambda(l)]^2}{2D_\lambda(l)}};$$

where

$$D_\lambda(l) = \frac{l}{EF}\int_0^l\int_0^l D_\rho(x)\,dx\,dx.$$

The quantity $M_\lambda(\ell)$, in view of (II.28) is determined by the integral

$$l = \int_0^{M_\lambda(l)} \frac{dM_\lambda}{\sqrt{\frac{1}{EF\Delta x}\int_0^{M_\lambda} M\psi(\lambda,\ 0)\,dM_\lambda}},$$

in which the expected value of the length of the "transition" zone is given implicitly.

Now let us determine the two dimensional probability density of the random quantities ℓ and λ_0.

$$\Phi^*(\lambda_0, l; t) = F^\circ(\dot{l}; t)\,\Phi(\lambda_0/l) =$$

$$= \frac{M_P(l)}{2\pi\sqrt{D_P(l)\,D_\lambda(l)}}\, e^{-\frac{[M_P(l)-P_H]^2}{2D_P(l)} - \frac{[\lambda_0 - M_\lambda(l)]^2}{2D_\lambda(l)}}, \qquad \text{(II.53)}$$

where, in accordance with (II.27), $M_p(\ell)$ is determined by

$$M_P(l) = \sqrt{\frac{1}{EF\Delta x}\int_0^{M_\lambda(l)} M\psi(\lambda, 0)\,dM_\lambda - \alpha l EF}.$$

Finally, knowing the joint probability density of λ_o and ℓ, let us determine the probability density of λ_o. It is known from probability theory [30] that to obtain the probability density of one of the variables in a system, one must integrate the probability density of the system from $-\infty$ to $+\infty$ with respect to the other random variable.

Thus,

$$\Phi_0(\lambda_0; t) = \int_{-\infty}^{\infty} \Phi^*(\lambda_0, l; t)\,dl = \int_0^{\infty} \Phi^*(\lambda_0, l; t)\,dl =$$

$$= \int_0^{\infty} \frac{M_p(l)}{2\pi\sqrt{D_P(l)\,D_\lambda(l)}}\, e^{-\frac{[M_P(l)-P_H]^2}{2D_P(l)} - \frac{[\lambda_0 - M_\lambda(l)]^2}{2D_\lambda(l)}}\, dl. \qquad \text{(II.54)}$$

Let us look at a practical case of computing longitudinal track forces and displacements.

Computation of longitudinal forces and displacements in continuous track

Rail characteristics: rails of type P50; $E = 2.1 \times 10^6$ kg/cm^2; $F = 64$ cm^2, wooden ties of type 1A, 1840 per km; fastenings of type K; crushed stone ballast. The graph of $M\Psi(\lambda)$ is given in Fig. II.18; the graph of the variance $\partial\Psi(\lambda)$ - in Fig. II.19.

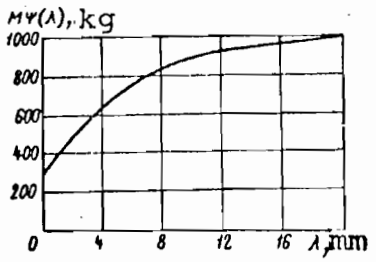

Fig II.18. Graph of the expected value of the force transmitted from the rail to the tie vs displacement of the cross-section

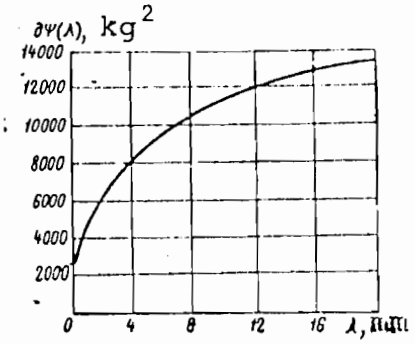

Fig. II.19. Graph of the variance of the force transmitted from the rail to the tie vs displacement of the cross-section

Suppose the temperature rise after the rails are installed in the track is $t = 15^{\circ}$. Resistance in the joint bars, P_H = 3000 kg.

First, let us determine the mathematical expectation of the random functions $\rho(x)$, $P(x)$, and $\lambda(x)$, making use of (II.27) and (II.28). Let us take the fixed point x_o for the coordinate origin. Fig. II.20 shows the graphical integration of $\Psi(\lambda)$ by the method of tangents. In performing the integration, the polar distance is taken to be $EF\Delta x$, so that the integral curve defines, according to (II.28), the square of the derivative of the displacement.

Fig. (II.21) shows the graph of the function $M_{\lambda},(\lambda)$, constructed from the graph of $(M_{\lambda},)^2$ with the aid of a table of square roots. It follows from (II.29) that, except for the scale factor $1/\alpha$, the graph represents the expected value of the displacement of the free end of the rail and of the temperature rise causing the displacement, translated by $t_H = P_H/\alpha tEF$.

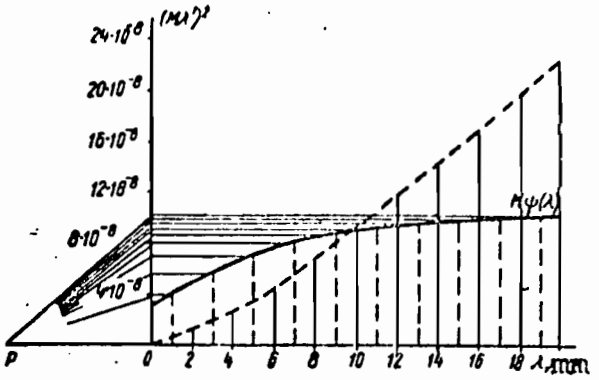

Fig. II.20. Graphical integration $M\Psi(\lambda)$

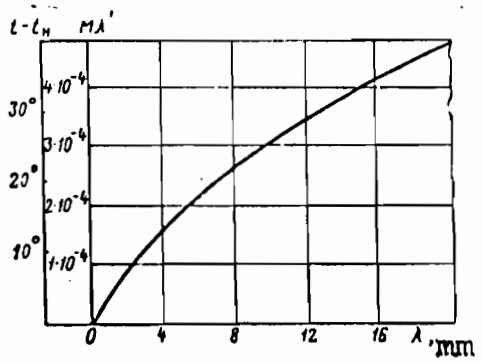

Fig. II.21. Graph of $M_{\lambda},(\lambda)$

Fig. II.22 show the graphical integration of the function $1/M_{\lambda},(\lambda)$, constructed from the graph of $M_{\lambda},(\lambda)$ and a table of reciprocals.

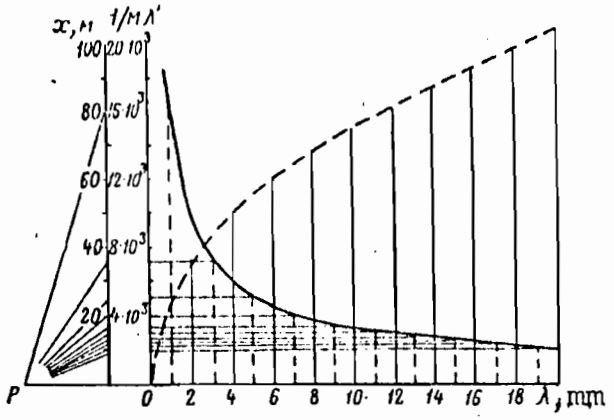

Fig. II.22. Graphical integration of $1/M_{\lambda}, (\lambda)$

Let us now construct the graph of $EFM_{\lambda}, (x)$. As a starting point we will use the graph of $M_{\lambda}(x)$, which is represented by a solid curve on Fig. II.23, and which constitutes the graph of $x(M_{\lambda})$ turned by 180° with respect to the diagonal of the quadrant. The differentiation is also performed by the method of tangents, taking EF for the polar distance.

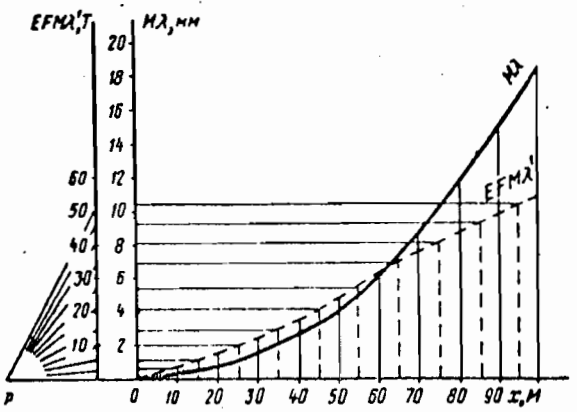

Fig. II.23. Graphical differentiation of the function $EFM_{\lambda}, (x)$

By making use of (II.2) solved for P, we construct the diagram of the expected value of the longitudinal force along the track (Fig. II.24). Taking the mathematical expectation of (II.2), we

obtain

$$D_P(x) = K_P(x, x) = \int_0^x D_\rho(x)\,dx.$$

Figure II.24 also shows the graph of longitudinal displacements of the track. At the point A the longitudinal force is $P = P_H$, i.e. this point is a free end of the rail string. The displacement is maximum at this point.

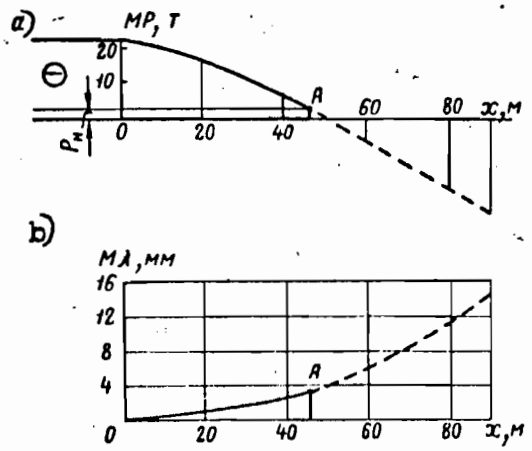

Fig. II.24. Longitudinal force and displacement diagrams in a string of welded rails: (a) longitudinal force; (b) longitudinal displacement

Finally, differentiating the graph of the expected value of the longitudinal force, we obtain the graph of the expected value of the linear resistance $M_\rho(x)$. Figure II.25 shows the graphical differentiation of the function EFM_λ,.

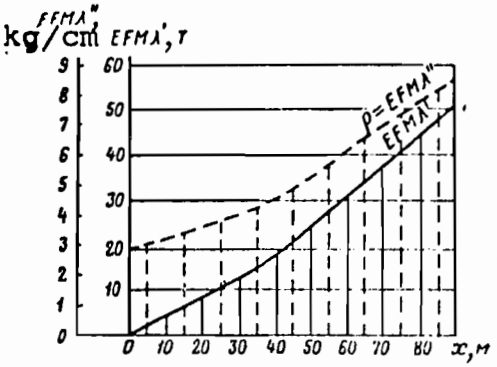

Fig. II.25. Graphical differentiation of EFM_λ,

Let us note that in constructing the diagrams of the expected value of the longitudinal force and of the longitudinal displacement according to the simplified formulas, the values of the parameters entering these formulas should be determined from the condition of minimal deviation of the approximating function $M\psi(\lambda)$ from the real one on the interval $0 \leq \lambda \leq \lambda_0$, where λ_0 is the displacement of the end of the rail string.

In general, the values of the optimal parameters of the approximate curve $M\psi(\lambda)$ change with the variation of the displacement of the free end of the rail connected with changes in the domain of values of λ. However, the displacement of the free end depends on the rail temperature. Thus, the values of the optimal parameters depend continuously on the temperature. This is confirmed in practice: It is known, for example, that the mean value of the linear resistance along the length of the "transition" zone of the rail varies with the increase and decrease in the temperature.

Now that the diagrams of the expected values of the functions $\rho(x)$, $P(x)$, and $\lambda(x)$ have been constructed, let us begin to compute the variances of the processes. Assigning to each value of $M_\lambda(x)$ the quantity $\partial\psi(M_\lambda)/2\Delta x = \partial\phi(M_\lambda)$*, we can construct the graph of the variance $D_\rho(x)$ of the random function $\rho(x)$. Figure II.26 shows this graph, computed with the use of the graphs of $\partial\psi(M_\lambda)$ and $M_\lambda(x)$ shown in Figures II.19 and II.24.

---

* The factor 1/2 is introduced since only one rail line is considered in the computation.

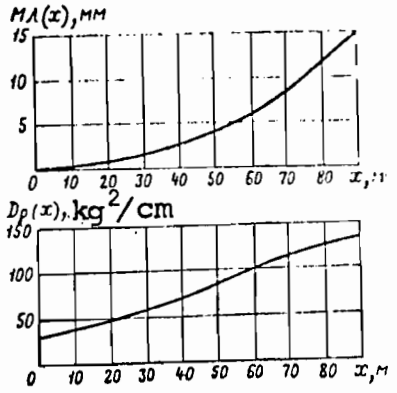

Fig. II.26. Graphs of $M_\lambda(x)$ and $D_\rho(x)$

Making use of (II.48), let us determine the variance $D_p(x)$ of the process $P(x)$:

$$M_p = EF\frac{dM_\lambda}{dx} - \alpha t EF.$$

Figure II.27 shows the graphical integration of the function $D_\rho(x)$.

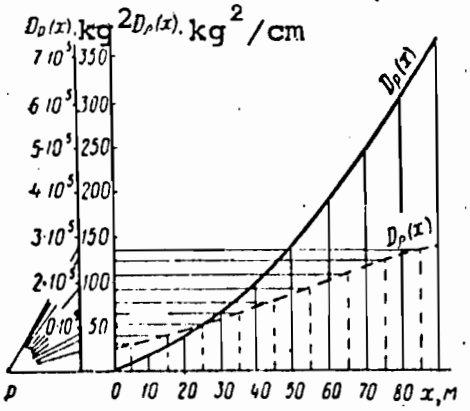

Fig. II.27. Graphical integration of $D_\rho(x)$

The graph of $D_p(x)$ determines completely the correlation function of the process, as is evident in Figure II.28.

Since the process P(x) is Gaussian, the mathematical expectation and the correlation function characterize this process completely.

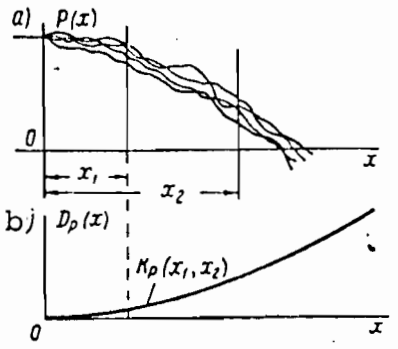

Fig. II.28. (a) The random process P(x) and (b) its correlation function $K_P(x_1, x_2)$

Let us compute the joint probability density of the quantities $P(10) = P_1$; $P(15) = P_2$; and $P(20) = P_3$. By analogy with (II.23), we will have

$$F_{1,2,3}(P_1 x_1;\ P_2 x_2;\ P_3 x_3) = \frac{1}{(2\pi)^{3/2}\sqrt{|K_{P_{ij}}|}} \exp\left(-\frac{1}{2}\sum_{1}^{3}\sum_{1}^{3} K^{-1}_{P_{ij}} P_i P_j\right).$$

The quantity $|K_{P_{ij}}|$ is the determinant of the covariance matrix

$$\|K_{P_{ij}}\| = \begin{Vmatrix} 30\,000 & 30\,000 & 30\,000 \\ 30\,000 & 50\,000 & 50\,000 \\ 30\,000 & 50\,000 & 73\,000 \end{Vmatrix}.$$

The quantities $K^{-1}_{P_{ij}}$ are the elements of the matrix $|K^{-1}_{P_{ij}}|$,

the inverse matrix of $\|K_{P_{ij}}\|$. Let us compute the determinant of $\|K_{P_{ij}}\|$:

$$|K_{P_{ij}}| = \begin{vmatrix} 30\,000 & 30\,000 & 30\,000 \\ 30\,000 & 50\,000 & 50\,000 \\ 30\,000 & 50\,000 & 73\,000 \end{vmatrix} = 10\,000^3 (3 \cdot 5 \cdot 7{,}3 + 3 \cdot 3 \cdot 5 \cdot 2 - 3 \cdot 5 \cdot 3 - 3 \cdot 3 \cdot 7{,}3 - 5 \cdot 5 \cdot 3) = 13{,}8 \cdot 10^{12}\ \kappa\Gamma^6.$$

To find the matrix $\| K_{P_{ij}}^{-1} \|$, we first go to a new matrix $\|A\|$ by means of the transformation

where

$$A = \sigma \|K_{P_{ij}}\| \sigma,$$

$$\sigma = \begin{Vmatrix} \frac{1}{\sqrt{K_{P_{11}}}} & 0 & 0 \\ 0 & \frac{1}{\sqrt{K_{P_{22}}}} & 0 \\ 0 & 0 & \frac{1}{\sqrt{K_{P_{33}}}} \end{Vmatrix}.$$

It is well known [35] that $D_1 = A_1 B_1 C_1$ implies $D^{-1} = C_1^{-1} B_1^{-1} A_1^{-1}$; consequently, $A_1^{-1} = \sigma^{-1} \|K_{P_{ij}}^{-1}\| \sigma^{-1}$, which yields

$$\| K_{P_{ij}} \| = \sigma A^{-1} \sigma,$$

Let us note that the matrix $\| A \|$ has the elements

$$(A)_{ij} = \frac{K_{P_{ij}}}{\sqrt{K_{P_{ii}} K_{P_{jj}}}},$$

i.e. it represents the normalized covariance matrix

$$A = \| R_{P_{ij}} \|$$

After some simple calculations, we obtain

$$A = \|R_{P_{ij}}\| = \begin{Vmatrix} 1 & 0,258 & 0,214 \\ 0,258 & 1 & 0,166 \\ 0,214 & 0,166 & 1 \end{Vmatrix}.$$

Let us denote the elements of the given matrix **A** by a_{ij}, and those of the inverse matrix B by b_{ij}.

Let us compute the inverse matrix by using Guassian elimination (the entries in Table 2 are successively obtained following the scheme given in Table 1 of Smirnov's monograph [36]).

TABLE 2

Equations	x_1	x_2	x_3	a_{K_2}	a_{K_3}	y_1	y_2	y_3	S
1	1	0,258	0,214	−0,258	−0,214	1	0	0	$S_1(x) = 1,472$
2	—	1	0,166	—	—	0	1	0	$S_2(x) = 1,424$
$a_{12}\times$I	—	−0,0666	−0,0552	—	—	−0,258	—	—	$a_{12}\times S_1(x) = -0,379$
II	—	0,9334	0,1108	—	−0,119	−0,258	1	0	$S_{II}(x) = 1,045$
3	—	—	1	—	—	0	0	1	$S_3(x) = 1,380$
$a_{13}\times$I	—	—	−0,0458	—	—	−0,214	0	0	$a_{13}\times S_1(x) = -0,315$
$a_{23}\times$II	—	—	−0,0198	—	—	0,307	−0,119	0	$a_{23}\times S_{II}(x) = -0,124$
III	—	—	0,9344	—	—	−0,183	−0,119	1	$S_{III}(x) = 0,941$ $S_{III}(y) = 0,677$
x_3	—	—	—	—	—	−0,196	−0,127	1,072	$S_3(y) = 0,749$
II	—	—	—	—	—	−0,258	1	0	$S_{II}(y) = 0,742$
$-a_{23}\times x_3$	—	—	—	—	—	+0,0218	0,0141	−0,119	$-a^*_{23}S_3(y) = 0,083$
II*	—	—	—	—	—	−0,236	1,0141	−0,119	$S^*_{II}(y) = 0,659$
x_2	—	—	—	—	—	−0,251	1,090	−0,127	$S_2(y) = 0,712$
I	—	—	—	—	—	1	0	0	1
$-a_{13}\times x_3$	—	—	—	—	—	+0,0419	+0,0272	−0,2290	$-a_{13}S_3(y) = -0,160$
$-a_{12}\times x_2$	—	—	—	—	—	+0,0776	−0,2810	+0,0327	$-a_{12}S_2(y) = -0,270$
I*	—	—	—	—	—	1,1195	−0,251	−0,196	$S^*_1(y) = 0,673$
x_1	—	—	—	—	—	1,1195	−0,251	−0,196	$S_1(y) = 0,673$

The matrix B has the form

$$A^{-1} = B = \|R^{-1}_{P_{ij}}\| = \begin{Vmatrix} 1,12 & -0,251 & -0,196 \\ -0,251 & 1,090 & -0,127 \\ -0,196 & -0,127 & 1,072 \end{Vmatrix}.$$

Now let us compute the matrix σ:

$$\sigma = \begin{Vmatrix} 5{,}77\cdot10^{-3} & 0 & 0 \\ 0 & 4{,}47\cdot10^{-3} & 0 \\ 0 & 0 & 3{,}70\cdot10^{-3} \end{Vmatrix}.$$

Let us form the product $C = \sigma A^{-1}$:

$$C = \begin{Vmatrix} 5{,}77\cdot10^{-3} & 0 & 0 \\ 0 & 4{,}47\cdot10^{-3} & 0 \\ 0 & 0 & 3{,}70\cdot10^{-3} \end{Vmatrix} \cdot \begin{Vmatrix} 1{,}12 & -2{,}51 & -0{,}196 \\ -0{,}251 & 1{,}090 & -0{,}127 \\ -0{,}196 & -0{,}127 & 1{,}072 \end{Vmatrix} =$$

$$= \begin{Vmatrix} 6{,}45\cdot10^{-3} & -1{,}45\cdot10^{-3} & -1{,}13\cdot10^{-3} \\ -1{,}12\cdot10^{-3} & 4{,}87\cdot10^{-3} & -5{,}67\cdot10^{-4} \\ -7{,}24\cdot10^{-4} & -4{,}70\cdot10^{-4} & 3{,}96\cdot10^{-3} \end{Vmatrix}.$$

Finally, let us compute $C\sigma = cA^{-1}\sigma = \left\| K_{P_{ij}}^{-1} \right\|$

$$\left\| K_{P_{ij}} \right\| = \begin{Vmatrix} 6{,}45\cdot10^{-3} & -1{,}45\cdot10^{-3} & -1{,}13\cdot10^{-3} \\ -1{,}12\cdot10^{-3} & 4{,}87\cdot10^{-3} & 5{,}67\cdot10^{-4} \\ -7{,}24\cdot10^{-4} & -4{,}70\cdot10^{-4} & 3{,}96\cdot10^{-3} \end{Vmatrix} \times$$

$$\times \begin{Vmatrix} 5{,}77\cdot10^{-3} & 0 & 0 \\ 0 & 4{,}47\cdot10^{-3} & 0 \\ 0 & 0 & 3{,}70\cdot10^{-3} \end{Vmatrix} =$$

$$= \begin{Vmatrix} 3{,}72\cdot10^{-5} & -6{,}47\cdot10^{-6} & -4{,}17\cdot10^{-6} \\ -6{,}47\cdot10^{-6} & 2{,}18\cdot10^{-5} & -2{,}10\cdot10^{-6} \\ -4{,}17\cdot10^{-6} & -2{,}10\cdot10^{-6} & 1{,}46\cdot10^{-5} \end{Vmatrix}.$$

Thus, the expression for the joint probability density of the random variables P_1, P_2, P_3 will have the form

$$F_{1,2,3}(P_1 x_1;\ P_2 x_2;\ P_3 x_3) =$$

$$= \frac{1}{(2\pi)^{3/2}\sqrt{|K_{P_{ij}}|}} \exp\left(-\frac{1}{2}\sum_{1}^{3}\sum_{1}^{3} K_{P_{ij}}^{-1} P_i P_j\right) =$$

$$= 5{,}4\cdot10^{-9}\, e^{-\left(18{,}67P_1^2 - 10{,}90P_2^2 - 7{,}3P_3^2 + 6{,}47P_1P_2 + 4{,}17P_1P_3 + 2{,}10P_2P_3\right)10^{-6}}.$$

Assuming given values of the longitudinal forces at $x_1 = 10$, $x_2 = 15$, and $x_3 = 20$ m, we can easily compute by means of the above formula the probability that the process passes through three fixed points in the P, x plane.

In a similar way one can compute the joint probability density of the n random variables $P_1, P_2, \ldots, P_n$. In the process, the computation of the inverse matrix $\| K_{P_{ij}}^{-1} \|$ is most conveniently done on an electronic computer.

Let us now construct the graph of the function $u_1(x) = \int_0^x D_P(s)$. The graphical integration of $D_P(x)$ is shown in Figure II.29.

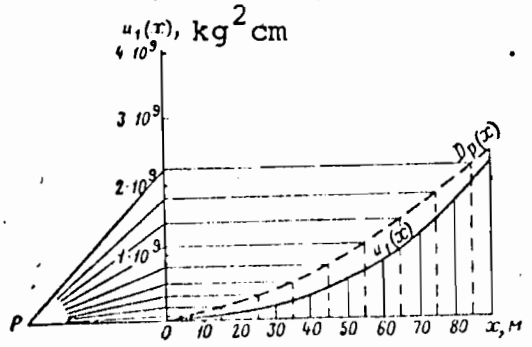

Fig. II.29. Graphical integration of $D_P(x)$

The function $u_1(x)$ together with $u_2(x) = x/(EF)^2$ determine completely the correlation function of the process $\lambda(x)$; this is made evident in Figure II.30.

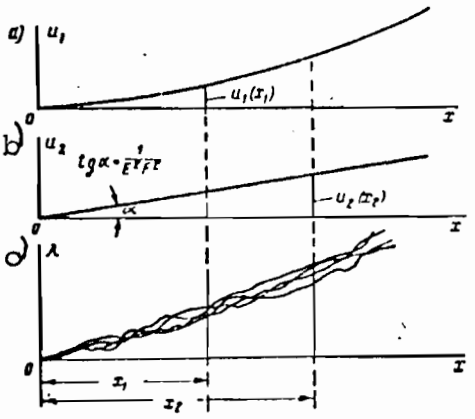

Fig. II.30. Graphs of u_1 and u_2, and of the correlation function of $\lambda(x)$

In accordance with (II.49), we have

$$K_\lambda = \begin{cases} u_2(x_2)\,u_1(x_1) & \text{при} \quad x_2 > x_1 \\ u_2(x_1)\,u_1(x_2) & \text{при} \quad x_2 < x_1 \end{cases}.$$

Thus, in order to obtain the covariance of $\lambda(x_1)$ and $\lambda(x_2)$, it is sufficient to multiply $u_1[\min(x_1,x_2)]$ and $u_2[\max(x_1,x_2)]$.

The process $\lambda(x)$ has a normal distribution and is, therefore, completely determined if the mathematical expectation and the correlation function are prescribed.

For practical purposes, it is the expected value and the dispersion of the random processes P_x and λ_x which are of interest.

In the example being investigated here, the graph of $D_\rho(x)$ obtained is close to being a straight line, hence we will replace it by one. Let us use the method of least squares to approximate $D_\rho(x)$ in the form

$$D_\rho(x) = a_o x + a_1.$$

The coefficients a_o and a_1 can be determined from two equations [13]:

$$\begin{cases} \dfrac{\partial \sum_i [a_0 x_i + a_1 - D_\rho(x_i)]^2}{\partial a_0} = 0; \\ \dfrac{\partial \sum_i [a_0 x_i + a_1 - D_\rho(x_i)]^2}{\partial a_1} = 0. \end{cases}$$

Differentiation yields

$$\begin{cases} 2\sum_i [a_0 x_i + a_1 - D_\rho(x_i)]\, x_i = 0; \\ 2\sum_i [a_0 x_i + a_1 - D_\rho(x_i)] = 0. \end{cases}$$

These equations can be put in the form

$$\begin{cases} a_0 \sum_i x_i^2 + a_1 \sum_i x_i - \sum_i D_\rho(x_i)\, x_i = 0; \\ a_0 \sum_i x_i + a_1 l - \sum_i D_\rho(x_i) = 0, \end{cases}$$

Table 3 shows the values of the quantities x_i, $D_\rho(x_i)$, x_i^2, and $D_\rho(x_i)x_i$ and the corresponding summations.

TABLE 3

i	x_i	$D_\rho(x_i)$	x_i^2	$D_\rho(x_i)x_i$
1	0	27	0	0
2	10	40	100	400
3	20	48	400	960
4	30	57	900	1 710
5	40	72	1 600	2 880
6	50	87	2 500	4 350
7	60	102	3 600	6 120
8	70	116	4 900	8 120
9	80	129	6 400	10 320
10	90	138	8 100	12 510
Σ	450	816	28 500	47 370

Substituting the values obtained in Table 3 into the equation, we obtain

$$28\ 500\ a_o + 450\ a_1 - 47\ 370 = 0$$

$$450\ a_o + 10\ a_1 - 816 = 0$$

Solving this system of equations, we obtain

$a_o = 1.29\ kg^2/cm.m = 0.0129\ kg^2/cm^2$; $a_1 = 23.5\ kg^2/cm$.

Thus,

$$D_\rho(x) = 23.5 + 0.0129\ x$$

The variance of the longitudinal force, according to (II.48), is given by

$$D_P(x) = \int_o^x D(s)\,ds = 23.5 + 0.00645\ x^2.$$

Finally, the variance of the function $\lambda(x)$, according to (II.49), will have the form

$$D_\lambda(x) = (x/EF) \int_o^x D_P(s)\,ds = x^3(EF)^{-2}(11.75 + 0.0043\ x).$$

Let us now use (II.52) to compute the probability density of the random variable ℓ. The computations are shown in Table 4.

The quantities $M_\rho(\ell)$, $D_P(\ell)$, and $M_P(\ell) - P_H$, shown in columns 2, 3, and 5 were taken from graphs in Figures II.25, 27, and 24 respectively. Figure II.31 shows the graph of the probability density of the random variable ℓ , constructed from the values given in Table 4.

TABLE 4

l, м	$M_\rho(l)$, kg/cm	$D_P(l)$, kg^2	$\sqrt{2\pi D_P(l)}$, kg	$M_P(l) - P_H$, kg	$\frac{[M_P(l)-P_H]^2}{2DP(l)}$	$\exp\frac{[M_P(l)-P_H]^2}{2\,D\,p(l)}$	$\frac{M_\rho(l)}{\sqrt{2\pi D_P(l)}}$, $см^{-1}$	$F^\circ(l;\,15)$, $см^{-1}$
1	2	3	4	5	6	7	8	9
40	4,60	$197\cdot10^3$	$1,11\cdot10^3$	$4,0\cdot10^3$	40,60	0	—	—
41	4,67	$205,1\cdot10^3$	$1,13\cdot10^3$	$3,3\cdot10^3$	26,60	0	—	—
42	4,74	$213,2\cdot10^3$	$1,16\cdot10^3$	$2,6\cdot10^3$	15,90	0	—	—
43	4,81	$221,3\cdot10^3$	$1,18\cdot10^3$	$1,9\cdot10^3$	7,20	0,001	$4,08\cdot10^{-3}$	$4,08\cdot10^{-6}$
44	4,88	$229,4\cdot10^3$	$1,20\cdot10^3$	$1,2\cdot10^3$	3,14	0,043	$4,07\cdot10^{-3}$	$1,75\cdot10^{-4}$
45	4,95	$237,5\cdot10^3$	$1,22\cdot10^3$	$0,5\cdot10^3$	0,53	0,589	$4,07\cdot10^{-3}$	$2,40\cdot10^{-3}$
45,7	5,00	$243,2\cdot10^3$	$1,23\cdot10^3$	0	0	1	$4,06\cdot10^{-3}$	$4,06\cdot10^{-3}$
46	5,02	$245,6\cdot10^3$	$1,24\cdot10^3$	$-0,2\cdot10^3$	0,81	0,923	$4,05\cdot10^{-3}$	$3,74\cdot10^{-3}$
47	5,09	$253,7\cdot10^3$	$1,26\cdot10^3$	$-0,9\cdot10^3$	1,60	0,202	$4,04\cdot10^{-3}$	$8,15\cdot10^{-4}$
48	5,16	$261,8\cdot10^3$	$1,28\cdot10^3$	$-1,6\cdot10^3$	4,90	0,007	$4,03\cdot10^{-3}$	$2,53\cdot10^{-5}$
49	5,23	$268,9\cdot10^3$	$1,30\cdot10^3$	$-2,3\cdot10^3$	8,60	0,001	$4,02\cdot10^{-3}$	$4,02\cdot10^{-6}$
50	5,30	$278\cdot10^3$	$1,32\cdot10^3$	$-3,0\cdot10^3$	16,20	0	—	—

Remark. In the interval $40 < \ell < 50$, the values of $M_\rho(\ell)$, $D_P(\ell)$, and $M_P(\ell) - P_H$ were obtained by linear interpolation.

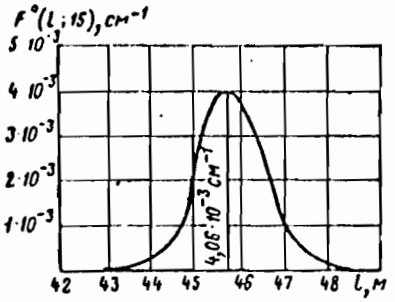

Fig. II.31. Probability distribution of the length of the "transition" zone with t = 15° C

For our problem we can write with sufficient accuracy

$$\frac{D_P(l)}{[M_\rho(l)]^2} \approx \frac{D_P(l_0)}{[M_\rho(l_0)]^2} = D_l(l_0) = \text{const},$$

in the interval $43<\ell<49$; here ℓ_0 is the abcissa of the point of intersection of the graphs $P = M_P(x)$ and $P = P_H$. In general, ℓ_0 is not the expected value of the random variable ℓ.

In this interval, therefore, we can take

$$\left|\frac{M_p(l) - P_H}{M_p(l)}\right| \approx |l - l_0|.$$

Consequently, one can write

$$F^\circ(l; t) = \frac{1}{\sqrt{2\pi D_l(l_0)}} e^{-\frac{(l-l_0)^2}{2D_l(l_0)}},$$

which represents the normal distribution of ℓ. The relation obtained holds for a sufficiently narrow interval of values of ℓ, which are of practical significance. Furthermore, it permits, albeit with a very small probability, the existence of negative values of ℓ. However, because of its simplicity, this equation is convenient to use to obtain rough estimates.

Let us note that for the case M_ρ = const, D_ρ = const, the characteristics of the expression just obtained for the approximate calculation of the probability density will be:

$$l_0 = \frac{\alpha t E F - P_H}{M_\rho};$$

$$D_l = \frac{D_\rho(\alpha t E F - P_H)}{(M_\rho)^3}.$$

To put it another way, although D_ℓ is not the variance of the random variable ℓ, the variance is close to D_ℓ for a sufficiently narrow range of ℓ-values which are of practical significance.

Let us compute the conditional distribution function for the displacement λ_0 of the end of the rail with respect to the length of the "transition" zone:

$$\Phi(\lambda_0/l) = \frac{1}{\sqrt{2\pi D_\lambda(l)}} e^{-\frac{[\lambda_0 - M_\lambda(l)]^2}{2D_\lambda(l)}}.$$

All the calculations are shown in Table 5. Columns 2 and 3 of the table show values of $D_\lambda(\ell)$ and $M_\lambda(\ell)$ taken from graphs in Figure II.30 and II.23.

TABLE 5

l, м	$D_\lambda(l)$, см²	$M_\lambda(l)$ см	$\sqrt{D_\lambda(l)}$, м	$\Phi(\lambda_0/l)$			
				$\lambda_0 - M_\lambda(l)$, см$^{-1}$	$\lambda_0 - M_\lambda(l) \pm \sqrt{D_\lambda(l)}$, см$^{-1}$	$\lambda_0 - M_\lambda(l) \pm 2\sqrt{D_\lambda(l)}$, см$^{-1}$	$\lambda_0 - M_\lambda(l) \pm 3\sqrt{D_\lambda(l)}$, см$^{-1}$
1	2	3	4	5	6	7	8
43,0	$1,32\cdot10^{-4}$	0,300	$1,15\cdot10^{-2}$	34,8	21,1	4,7	0,3
43,5	$1,38\cdot10^{-4}$	0,306	$1,17\cdot10^{-2}$	34,2	20,8	4,6	0,3
44,0	$1,42\cdot10^{-4}$	0,312	$1,19\cdot10^{-2}$	33,6	20,4	4,5	0,3
44,5	$1,49\cdot10^{-4}$	0,318	$1,22\cdot10^{-2}$	32,8	19,9	4,4	0,3
45,0	$1,55\cdot10^{-4}$	0,324	$1,25\cdot10^{-2}$	32,0	19,4	4,3	0,3
45,5	$1,63\cdot10^{-4}$	0,330	$1,28\cdot10^{-2}$	31,3	19,0	4,2	0,3
46,0	$1,69\cdot10^{-4}$	0,336	$1,30\cdot10^{-2}$	30,7	18,6	4,1	0,3
46,5	$1,76\cdot10^{-4}$	0,342	$1,32\cdot10^{-2}$	30,3	18,3	4,1	0,3
47,0	$1,85\cdot10^{-4}$	0,348	$1,36\cdot10^{-2}$	29,4	17,8	4,0	0,3
47,5	$1,90\cdot10^{-4}$	0,354	$1,38\cdot10^{-2}$	29,0	17,6	3,9	0,3
48,0	$1,97\cdot10^{-4}$	0,360	$1,40\cdot10^{-2}$	28,6	17,3	3,9	0,3
48,5	$2,06\cdot10^{-4}$	0,366	$1,43\cdot10^{-2}$	28,0	17,0	3,8	0,3
49,0	$2,13\cdot10^{-4}$	0,370	$1,46\cdot10^{-2}$	27,4	26,6	3,7	0,3

Remark. In the interval $43 < \ell < 49$, the values of $D_\lambda(\ell)$ and $M_\lambda(\ell)$ were obtained by linear interpolation.

Using the calculated results we construct graphs of $\Phi(\lambda_o/\ell)$ for different values of ℓ, as shown in Figure II.32,a - m. An examination of the graphs shows that the probability density of the random variable λ_o varies smoothly with changes in the length of the "transition" zone ℓ. This indicates that the random variables λ_o and ℓ are correlated. Tables 4 and 5 and Figures II.31 and 32 determine the two dimensional probability density of these quantities.

Results of the calculations of the joint probability density of λ_o and ℓ are shown in Table 6. Column 2 of this table is obtained from the graph of $F^o(\ell;15)$, given in Figure II.31. The entries in the remaining columns are computed according to the

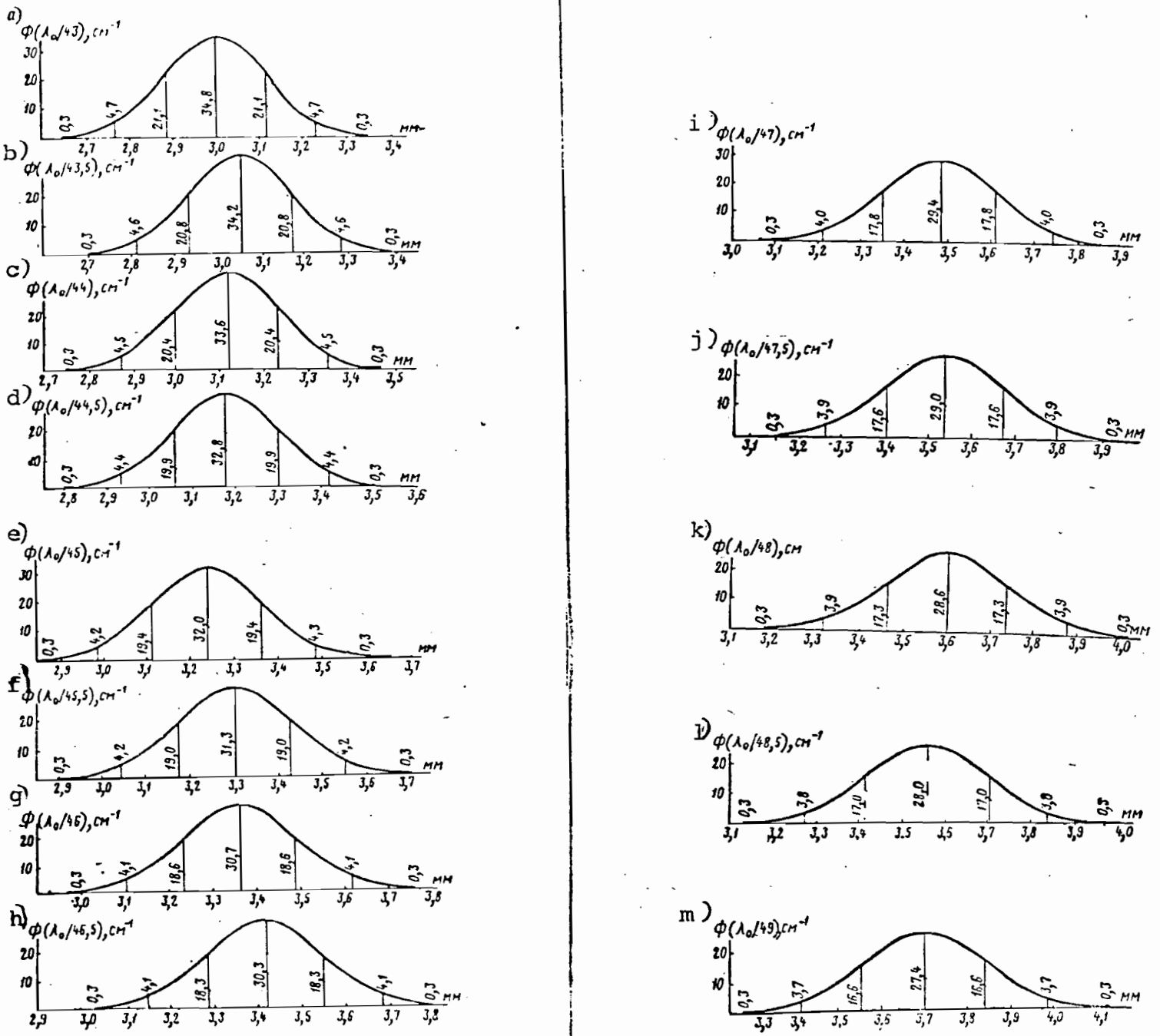

Fig. II.32. Probability density of the displacement of a free end of a rail for different values of "transition" zone length

l, м	i
43,0	
43,5	
44,0	
44,5	
45,0	
45,5	
46,0	
46,5	
47,0	
47,5	
48,0	
48,5	

rule $\Phi^*(\lambda_{oi};\ell_j;15) = F^o(\ell_j;15)\Phi(\lambda_i/\ell_j)$. The sum of each column is given at the end of Table 6. It is not difficult to see that, except for the multiplying constant 20, the quantity $10^3 \sum_j \Phi^*(\lambda_{oi};\ell_j;15)$ is equal to the probability density of the random variable λ_{oi}.

Indeed, according to (II.54), we have

$$\Phi_o(\lambda_{oi};15) = \int_0^\infty \Phi^*(\lambda_{oi};\ell;15)d\ell \approx \Delta\ell \sum_j \Phi^*(\lambda_{oi};\ell_j;15);$$

however, $\Delta\ell$ = 50 cm, which proves the assertion. Figure II.33 shows the probability density of the random variable λ_o.

TABLE 6

l, m	$F^o(l;15)$, cm^{-1}	$\Phi^*(\lambda_o, l; 15) = F^o(l;15)\,\Phi(\lambda_o/l)\,10^3$, cm^{-2} for λ_o, mm													
		λ_o=2,7	λ_o = 2,8	λ_o = 2,9	λ_o = 3,0	λ_o = 3,1	λ_o = 3,2	λ_o = 3,3	λ_o = 3,4	λ_o = 3,5	λ_o = 3,6	λ_o = 3,7	λ_o = 3,8	λ_o = 3,9	λ_o = 4,0
1	2	3	4	5	6	7	8	9	10	11	12	13	14	15	16
43,0	0	0	0	0	0	0	0	0	0	0	0	0	0	0	0
43,5	$0{,}03\cdot10^{-3}$	0	0,09	0,43	0,89	0,96	0,48	0,12	0,01	0	0	0	0	0	0
44,0	$0{,}2\cdot10^{-3}$	0	0,08	1,44	4,08	6,56	5,13	2,08	0,32	0,02	0	0	0	0	0
44,5	$0{,}7\cdot10^{-3}$	0	0,14	1,96	8,40	17,90	22,10	13,90	5,03	1,00	0,01	0	0	0	0
45,0	$2{,}4\cdot10^{-3}$	0	0	0,77	11,50	42,20	70,90	65,20	34,50	9,60	0,57	0	0	0	0
45,5	$3{,}9\cdot10^{-3}$	0	0	0,75	7,50	39,00	93,50	122,00	77,20	32,00	7,80	0,75	0	0	0
46,0	$3{,}7\cdot10^{-3}$	0	0	0	3,00	14,80	51,80	98,00	105,00	61,20	19,60	4,45	0,30	0	0
46,5	$2{,}3\cdot10^{-3}$	0	0	0	0,30	4,60	20,70	48,30	69,10	56,40	27,70	6,90	0,92	0	0
47,0	$0{,}8\cdot10^{-3}$	0	0	0	0	0,03	3,00	10,40	19,70	22,80	16,00	6,40	1,60	0,20	0
47,5	$0{,}2\cdot10^{-3}$	0	0	0	0	0	0,15	1,20	3,60	5,60	5,20	2,80	0,90	0,08	0
48,0	$0{,}02\cdot10^{-3}$	0	0	0	0	0	0	0,06	0,20	0,44	0,57	0,45	0,20	0,06	0
48,5	0	0	0	0	0	0	0	0	0	0	0	0	0	0	0

In conclusion, let us note that the formulas derived here can be applied not only to the case of the first loading. For this it is sufficient to make use of the function $\Psi(\lambda^*)$, averaged

Fig. II.32. Probability density of the displacement of a free end of a [illegible] of [illegible] some length

with respect to λ^*, which will certainly lead to a change in the statistical parameters and, in particular, to the increase in the variance of the random functions $\rho(x)$, $P(x)$, $\lambda(x)$.

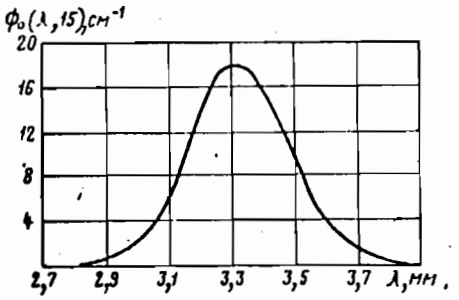

Fig. II.33. Probability density of the displacement of a free end of a rail string

3. Solution of the equation for longitudinal track displacements for the case of the second and subsequent loadings. Hysteresis phenomenon in CWR track.

In the following presentation we will examine problems and their solutions in the classical (not statistical) setting; therefore, it will not be necessary to take the mean value in equation (II.6). The general solution of (II.5) in a statistical formulation was given in the first section of the present chapter, and there is no further need for refinements relating to boundary conditions on the correlation functions of $\rho(x)$, $P(x)$, and $\lambda(x)$, similar to the ones presented in the second section of this chapter, since this would amount to a repetition with changes which have no practical interest in view of the paucity of statistical data. The general form of the function $\phi(\lambda,\lambda^*)$ (more precisely, the expected value) is shown in Figure II.34.

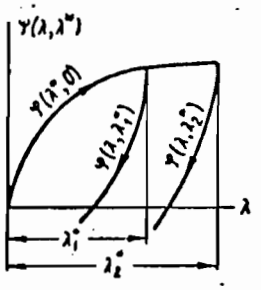

Fig. II.34. Graphs of the force transmitted from rail to tie when the tie is loaded for the second time

If a tie (more precisely, rail cross-section) is displaced by λ^* while the temperature varies in one direction, it does not return to its original position when the direction of the temperature change is reversed and the temperature returns to its initial value, i.e. a residual deformation is created. For the second loading, it is evident that the function $\phi(\lambda,\lambda^*)$ can be put in the form

$$\varphi(\lambda, \lambda^*) = \varphi(\lambda^*, 0) - f[(\lambda^* - \lambda), \lambda^*]. \qquad \text{(II.55)}$$

Here $f[(\lambda^*-\lambda),\lambda^*] = f(\theta,\lambda^*)$ is an increasing function, which can be considered given on the basis of processed experimental data.

For the experimental determination of the function $f(\theta,\lambda^*)$ it is sufficient to first displace the tie by the amount λ^* along the track and then to construct the graph of the decrease in the force transmitted to the tie, against the magnitude of the displacement of the tie (rail cross-section) from the initially displaced state in the direction of the initial position of the tie. Except for the multiplying factor $2\Delta x$, this graph determines the required function $f(\theta,\lambda^*)$. The relations between the quantities λ^*,λ, and θ are shown in Figure II.35.

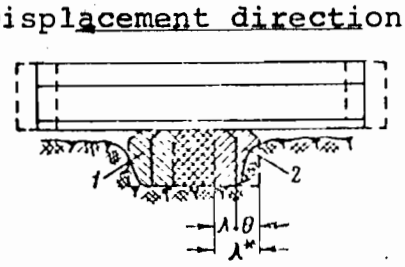

Fig. II.35. Tie displacement under repeated loading:
1 - tie position at the initial moment of the first loading;
2 - tie position at the initial moment of the second loading.

Substituting (II.6) into formula (II.55) yields

$$EF\frac{d^2\lambda}{dx^2} = -\varphi(\lambda^*, 0) - f[0, \lambda^*]. \qquad \text{(II.56)}$$

However, since the preliminary displacement takes place during the first loading, it must satisfy

$$EF\frac{d^2\lambda^*}{dx^2} = -\varphi(\lambda^*, 0). \qquad \text{(II.56a)}$$

Subtracting (II.56) from (II.56a), we obtain

$$\frac{d^2\lambda^*}{dx^2} - \frac{d^2\lambda}{dx^2} = \frac{1}{EF} f(\theta, \lambda^*),$$

or, making use of $\lambda^* - \lambda = \theta$, we finally arrive at

$$\frac{d^2\theta}{dx^2} = \frac{1}{EF} f(\theta, \lambda^*). \qquad \text{(II.57)}$$

It is easier to solve (II.57) than (II.6) because the boundary conditions are simpler, as will be shown below. In accordance with (II.2) we can write:

$$\frac{d\lambda}{dx} = \alpha t + \frac{P}{EF};$$
$$\frac{d\lambda^*}{dx} = \alpha t^* + \frac{P^*}{EF},$$

where t^* is the temperature rise from the time the rail is installed in the track to the time when the direction of the temperature change reverses, and P^* is the longitudinal force in the rail length at the moment the temperature change reverses direction.

Subtracting the second equation from the first one, we obtain

$$\frac{d\theta}{dx} = \alpha\tau + \frac{G}{EF}, \qquad \text{(II.58)}$$

where $\tau = t^* - t$ is the decrease in the temperature from the time of the reversal of the direction of the change, and $G = P^* - P$ is the decrease in the longitudinal force in the track produced by the decrease in temperature by τ.

It is quite obvious that if in the first stage (during first loading) the temperature of the rail string is lowered, it will rise during the second stage, during which, of course, it can cross the temperature at which the rail string was installed in the track, so that the quantities τ and G can be

either positive or negative.

At the cross-section x = s, where the first loading zone borders on the second loading zone, the conditions

$$\lambda^*(s) = \lambda(s);$$
$$G(s) = -\alpha\tau EF,$$

must be satisfied, from which it follows that

$$\theta|_{x=s} = 0 \quad \theta'|_{x=s} = 0.$$

Let us examine the solutions of (II.56) for several special cases. When the interaction between the rail and the foundation under the rail is due solely to friction, the graph of $\phi(\lambda,\lambda^*)$ has the form shown in Figure II.36.

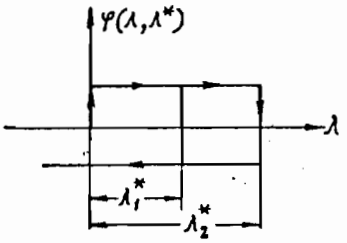

Fig. II.36. Graph of the distributed force transmitted by the rail as a function of displacement for the case of repeated loading, assuming frictional interaction between rail and the foundation under the rail.

For the case the following conditions hold:

$$\phi(\lambda^*,0) = c; \quad f(\theta,\lambda^*) = 2c,$$

where c is the linear resistance to rail displacement.

Let the origin of the coordinate system be located at the left hand end-point of the rail string. The boundary conditions on the function $P^*(x)$ will be:

$$P^*(0) = P_H; \quad P^*(x_o) = -\alpha t^* EF,$$

from which, taking into account $(P^*)' = c$, we obtain

$$x_0 = \begin{cases} 0 & \text{при } t^* < \dfrac{P_н}{\alpha EF}, \\ \dfrac{\alpha t^* EF - P_н}{c} & \text{при } t^* > \dfrac{P_н}{\alpha EF}, \end{cases}$$

and the expressions for P^* take the form

$$P^* = \begin{cases} -P_н - cx & \text{при } x < x_0 = \dfrac{\alpha t^* EF - P_н}{c}. \\ -\alpha t^* EF & \text{при } x > x_0. \end{cases}$$

The boundary conditions on G(x) will be:

$$G(0) = P^*(0) - P(0) = -2P_н; \quad G(s) = -\alpha\tau EF,$$

which, since $G' = 2c$, implies

$$s = \begin{cases} 0 & \text{при } \tau < \dfrac{2P_н}{\alpha EF}. \\ \dfrac{\alpha\tau EF - 2P_н}{2c} & \text{при } \tau > \dfrac{2P_н}{\alpha EF}. \end{cases}$$

Solving (II.57), we obtain

$$G = \begin{cases} -2P_н - 2cx & \text{при } x < s. \\ -\alpha\tau EF & \text{при } x > s. \end{cases}$$

Figure II.37 shows the graphs of P^* and G, and their difference, which represents the longitudinal force P(x) in the track.

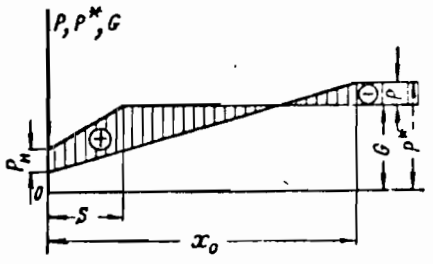

Fig. II.37. Longitudinal forces in the rail for repeated loading and purely frictional interaction between the rail and the foundation

The case examined above was treated quite extensively by Wattmann [8] using a method which cannot be generalized to apply

to cases more complicated than the one for which the interaction between the rail and the supporting foundation is purely frictional.

When the rail-foundation interaction is elastic and frictional, the function $\phi(\lambda,\lambda^*)$ has a form shown in Figure II.38.

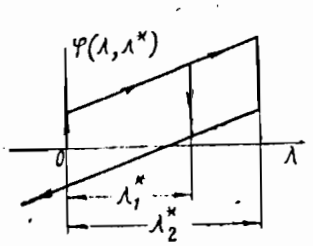

Fig. II.38. Graph of the distributed force transmitted by the rail as a function of displacement, for the case of repeated loading and frictional-elastic interaction between the rail and the supporting foundation

If the interaction law is linear, $\phi(\lambda^*,0)$ and $f(\theta,\lambda)$ have the form

$$\phi(\lambda^*,0) = c + K\lambda^*;\ f(\theta,\lambda^*) = 2c + K\theta.$$

The case of frictional-elastic interaction differs from the purely frictional one in the existence of constraints which oppose elastically the sliding of the rail on the supporting foundation. Consequently, in addition to the frictional forces, there arise between the rail and the foundation tangential interaction forces of an elastic nature, which we assume to be distributed along the whole length of the rail. As in the case previously considered, we will take the coordinate origin to coincide with the left hand end-point of the rail string. The boundary conditions on $P^*(z)$ will now be

$$P^*(0) = -P_H;\quad P^*(\ell) = -\alpha t^* EF.$$

Here ℓ is the "transition" zone of the rail string, which, in

view of (II.46), has the form

$$l=\begin{cases}\sqrt{\frac{EF}{K}}\,\mathrm{arsh}\,\frac{\alpha t^{*}EF-P_{н}}{c}\sqrt{\frac{K}{EF}} & \text{при } t^{*}>\frac{P_{н}}{\alpha EF}\\ 0 & \text{при } t^{*}<\frac{P_{н}}{\alpha EF}\end{cases}, \qquad \text{(II.59)}$$

where we have taken into account

$$P^{*}|_{x=\ell}=-P_{H}.$$

The arguments z and x are related through $x = \ell - z$. In the new coordinates, the longitudinal force equation has the form

$$P^{*}(z)=\begin{cases}c\sqrt{\frac{EF}{K}}\,\mathrm{sh}\sqrt{\frac{K}{EF}}(l-z)-\alpha t^{*}EF & \text{при } z<l\\ -\alpha t^{*}EF & \text{при } z>l\end{cases}, \qquad \text{(II.60)}$$

The boundary values for G(z) will be

$$G\ (0)=-2P_{H};\quad G(s)=-\alpha\tau EF,$$

where, by analogy with (II.69), s is determined by

$$s=\begin{cases}\sqrt{\frac{EF}{K}}\,\mathrm{arsh}\,\frac{\alpha\tau EF-2P_{н}}{2c}\sqrt{\frac{K}{EF}} & \text{при } \tau>\frac{2P_{н}}{\alpha EF}\\ 0 & \text{при } \tau<\frac{2P_{н}}{\alpha EF}\end{cases}.$$

Similarly, by analogy with (II.60), we can write

$$G(z)=\begin{cases}2c\sqrt{\frac{EF}{K}}\,\mathrm{sh}\sqrt{\frac{K}{EF}}(s-z)-\alpha\tau EF & \text{при } z<s\\ -\alpha\tau EF & \text{при } z>s\end{cases}.$$

Figure II.39 shows the graphs of $P^{*}(z)$, G(z), P(z) and $\lambda(z)$ for the particular case $\tau = t^{*}$, i.e. for the case when the rail temperature goes down to the level at which it was installed in the track. It is evident that when this happens, residual stresses and accompanying longitudinal displacements will be produced. All the results obtained above are valid only if $s \leq \ell$, for, if $s > \ell$, the ties which were in the neutral position before

(i.e. those, for which $\lambda^* = 0$), begin to move. The force transmitted to these ties, as a function of displacement, has the form $\phi(\lambda,\lambda^*) = \phi(\lambda,0)$, along the length of the rail the function $\phi(\lambda,\lambda^*)$ becomes piecewise continous:

$$\varphi(\lambda, \lambda^*) = \begin{cases} \varphi(\lambda^*, 0) - f(0, \lambda^*) & \text{при } x < l; \\ \varphi(\lambda, 0) & \text{при } x > l. \end{cases}$$

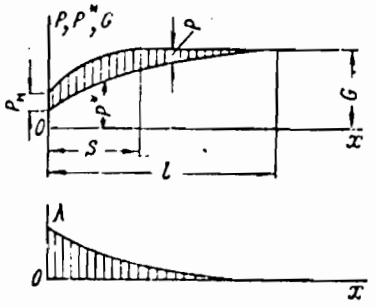

Fig. II.39. Diagram for the longitudinal forces in rails loaded for the second time, with combined frictional-elastic interaction between the rails and the rail supporting foundation

To construct longitudinal rail force diagrams for the case $s > \ell$, and also for the case $s < \ell$, with $f(\theta,\lambda^*) = f_1(\theta)$ specified graphically, it is convenient first to construct special templates. (This case is clearly a generalization of the previously investigated cases of purely frictional and elastic interaction between the rail and the foundation.) These templates are formed from the curves which correspond to solutions of (II.56a) and (II.57) with boundary conditions:

$$\lambda^*(0) = 0; \quad \lambda^{*\prime}(0) = 0; \quad \theta(0) = 0; \quad \theta'(0) = 0;$$

the general shape of these templates is shown in Figure II.40.

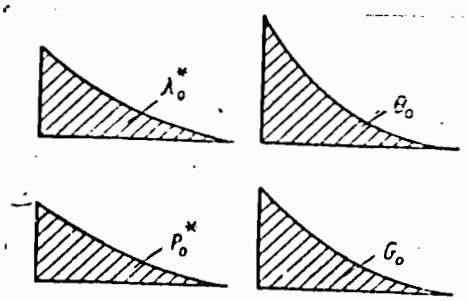

Fig. II.40. Templates for constructing longitudinal force-rail displacement diagrams when the rails are loaded for the second time

The construction of longitudinal force diagrams for the case of second loading when $s < \ell$ is very simple if the P_o^* and G_o templates are available, as is evident from Figure II.41.

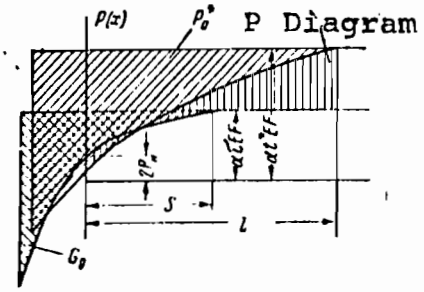

Fig. II.41. Longitudinal rail force diagram for the case of second loading, with arbitrary resistance-rail displacement relation, assuming the second loading induces displacements in the zone displaced during the first loading

For example, to construct the $P^*(x)$ diagram it is sufficient to place the P_o^* template on the graph of the straight line $P^* = \alpha t^* EF$ in such a way that the curve passes through the point (O, P_H) and, drawing the curve along the template from the origin to the point $x = \ell$, where $P^* = \alpha t^* EF$, to continue it as a horizontal line. In the same way, letting the curve G_o of the template applied to the straight line $G = \alpha_\tau EF$ pass through the point $(0, 2P_H)$, one constructs the $G(x)$ diagram. The difference between the $P^*(x)$ and $G(x)$ curves then yields the longitudinal force diagram for the second loading, as shown earlier.

If in the process of constructing the G(x) diagram by the above method it turns out that $s > \ell$, the diagram must be constructed in a somewhat different way, as shown in Figure II.42.

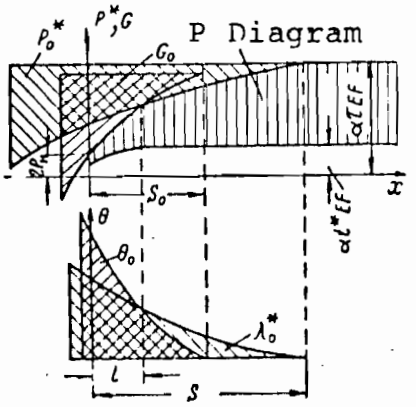

Fig. II.42. Longitudinal rail force diagram for the case of second loading, with arbitrary linear resistance-rail displacement relation, assuming the second loading induces displacements in the zone displaced during the first loading and outside of it

Assuming a value for the length of the "transition" zone under second loading with $s > \ell$, we construct the displacement diagram on the interval $\ell < x < s$ by applying the λ_o^* template to the abcissa in such a way that the template origin coincides with the point $x = s$. At the point $x = \ell$ we must have $\theta(\ell - 0) = \theta(\ell + 0)$. Consequently, applying the θ_o template to the abscissa in such a way that the curve passes through the point $\theta(\ell)$ of the curve constructed with the λ_o^* template, and, fixing the position of the curve on $0 < x < \ell$, one can construct the complete longitudinal displacement diagram. (Let us recall that the origin of the coordinates is at the end of the rail string.) Now, positioning the end-point of the G_o template at a point with abscissa s_o, corresponding to the end-point of the θ_o template, let us draw the longitudinal

force curve G on $0<x<\ell$ in such a way that it passes through the point $(0,2P_H)$.

Finally, taking into account the condition $G(\ell - 0) = G(\ell + 0)$, let us construct the force diagram G on $\ell<x<s$. To do this, it is sufficient to locate the end-point of the template P_o at a point with abscissa $x = s$ and, move the template vertically until the curve passes through a point on the curve constructed with the G_o template. Taking into account the fact that at the point $x = s$ the longitudinal force is equal to $\alpha\tau EF$, one can find for every value of s a corresponding value of the temperature decrease τ after the direction of the temperature change is reversed. The general form of $s = s(\tau)$ is shown in Figure II.43.

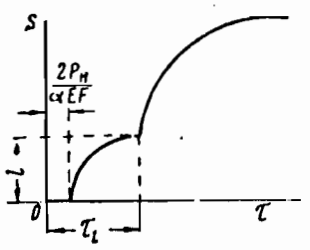

Fig. II.43. Graph of transition zone length vs temperature rise τ in the second loading process

If the temperature is lowered by an amount τ_1 after the direction of its change has been reversed, the length of the "transition" zone is the same during the second loading as during the first one; as the temperature τ is decreased further, the ties, which had been in a neutral position, are displaced. Since the linear resistance has a jump discontinuity at the point $x = \ell$, the curve $s = s(\tau)$ will have a corner at that point. From the graph of $s = s(\tau)$ one can quickly find the length of the "transition" zone as well as the discontinuity conditions

at $s = \ell$.

Having the graph $s = s(\tau)$, one can construct the longitudinal force diagram for the rail string without first constructing the displacement diagram. The displacement diagram for the second loading can be constructed very simply with the aid of the λ^*, and θ_o templates. Figure II.44 shows the construction of the diagram for the cases $\ell > s$ and $\ell < s$.

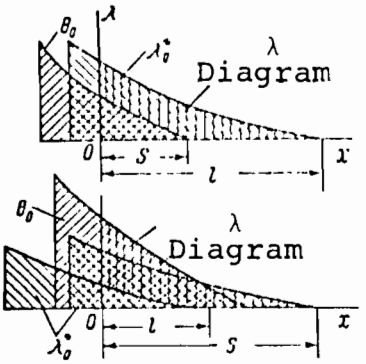

Fig. II.44. Longitudinal displacement diagrams in rails during the second loading of the rail string, with linear resistance being an arbitrary function of rail displacements.

If the functions $P(x)$ and $\lambda(x)$ are represented in the form $P(x) = P^*(x) - G(x)$, $\lambda(x) = \lambda^*(x) - \phi(x)$, as had been done for all the solutions previously presented, then in solving the corresponding statistical problems it should be recalled that in adding random functions their expected values and correlation functions must be added. In this case, the distribution of the random variable $\lambda(0)$ is determined by the composition of the distributions of the random variables $\lambda^*(0)$ and $\theta(0)$.

Equation (II.6) can be solved by some approximate method (for example, the method of finite differences) for the most general form of $\phi(\lambda, \lambda^*)$. It is evident that this solution applies not

only to the case of the second loading, but also the cases which pertain to all subsequent loadings.

In general, equation (II.57) can be integrated graphically in the following manner. The displacement diagram for the case of the first loading will have a form shown in Figure II.45a. The free end of the length of rail is denoted by a. Let us pick a value for the "transition" zone length for the second loading, and let us take for the coordinate origin the point whose distance to the end is s. The initial conditions will be

$$\theta|_{x=0} = 0; \quad \theta'|_{x=0} = 0.$$

The second of these is equivalent to

$$P(0) = P^*(0) - \alpha\tau EF.$$

Let us mark off interval $\overline{0_1 P}$ of unit length to the left of the origin on the horizontal axis (Fig. II. 45, b and c).

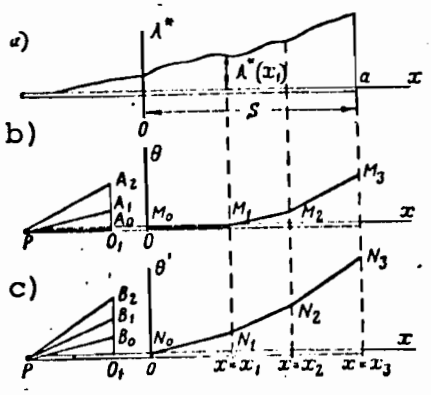

Fig. II.45. Graphical construction of the $\theta(x)$ and $\theta'(x)$ diagrams.

Let us rewrite (II.57) as a system of two first order differential equations for y and θ :

$$\frac{d\theta}{dx} = y; \quad \frac{dy}{dx} = \frac{1}{EF} f[\theta, \lambda^*(x)].$$

The length of the segment $\overline{0_1P}$ will serve as the scale unit for y and $(EF)^{-1}f(\theta,\lambda^*(x))$.

Let us construct the straight lines $x = x_1$, $x = x_2$, $x = x_3$,... parallel to the λ-axis.

Let us mark off the points M_o and N_o with coordinates $(0,\theta(0))$ and $(0,\theta'(0))$, which, evidently, coincide with the origins of the coordinate systems θox and $\theta' ox$. Let us lay off along $x = 0_1$ the segments 0_1A_o and 0_1B_o, equal to $\theta(0)$ and $(EF)^{-1}f(\theta(0), \lambda^*(0))$. The second of these quantities can always be assumed to be different from zero, for even if there were no dry friction during the displacement of the rail, one can always take $\theta(0) = \varepsilon$, where ε is any value smaller than the accuracy of the measurements (Figure II.46).

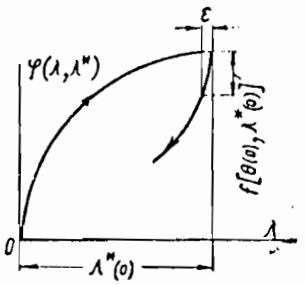

Fig. II.46. Graph of the force per unit length transmitted by the rail to the foundation, as the direction of the displacement of the rail cross-section is reversed

Friction forces are present in any real system, and consequently the power series, for the function $f(\theta,\lambda^*)$ contains a constant term. The directions of the segments PA_o and PB_o yield the tangent directions $\theta'(0)$ and $(EF)^{-1}f(\theta(0),\lambda^*(0))$ and, consequently, the directions of the integral curves at the initial points M_o and N_o. From these points, let us construct segments $\overline{M_oM_1}$ and $\overline{N_oN_1}$ parallel to PA_o and $\overline{PB_o}$, until they intersect the line $x = x_1$. Let (x_1,y_1) be the coordinates of the points M_1 and N_1. On the 0_1 axis, we lay off

segments 0_1A_1 and 0_1B_1, equal to y_1 and $(EF)^{-1}f(\theta_1,\lambda^*(x_1))$.

Starting at M_1 and N_1, let us draw segments $\overline{M_1M_2}$ and $\overline{N_1N_2}$, parallel to $\overline{PA_1}$ and $\overline{PB_1}$, until they intersect the straight line $x = x_2$, etc. In this way we obtain two polygonal curves, $M_oM_1M_2\ldots$ and $N_1N_2N_3\ldots$, which provide an approximate representation for the desired integral curves.

According to (II.58) the quantity G(x) is determined from the expression

$$G(x) = \theta'EF - \alpha\tau EF,$$

from which, taking into account the end condition $G(s) = -2P_H$, we obtain

$$\tau = \frac{1}{\alpha}\,\theta'(s) + 2\frac{P_H}{EF}.$$

Assuming different values s for the length of the "transition" zone and, for each of these, a value for the temperature decrease, we can construct the graph $s = s(\tau)$ which, in general, will resemble the graph in Figure II.43.

For the case of the n-th loading, the function $\phi_n(\lambda,\lambda^*)$ can be represented in the form

$$\phi_n(\lambda,\lambda^*) = \phi_{n-1}(\lambda,\lambda^*) - (-1)^n f_n(\theta,\lambda^*), \quad (n = 2, 3, 4, \ldots). \tag{II.61}$$

Here $\theta = |\lambda-\lambda^*|$.

For n = 2 this formula coincides with (II.55). If the longitudinal force and logitudinal displacement diagrams are available, this representation allows one to construct such diagrams for the next loading, the problem bring reduced to that of finding functions which satisfy (II.57). Thus, starting

with the first loading and making use of the recursion formula (II.61), one can construct the P(x) and $\lambda(x)$ diagrams for a system successively loaded and unloaded n times. It should be noted that the influence of previous loadings is erased to such and extent that after the fourth loading one can assume $\phi_n(\lambda,\lambda^*) = \phi_o(\lambda)$ for $n > 4$, where $\phi_o(\lambda)$ is the function obtained by averaging with respect to λ^*.

Thus, all the developments of this section are applicable only to the investigation of the effects of diurnal temperature oscillations on the longitudinal rail forces and displacements; to study processes which affect the track over more extended periods of time, one should assume the relations derived for the first loading, replacing the function $\phi(\lambda,0)$ with $\phi_o(\lambda)$. This is also justified by the fact that in the course of time atmospheric influences, the movement of rolling stock, and improvements due to track maintenance all affect the nature of the contact between the ties and the ballast, and between the ties and rail.

In studying hysteresis phenomena in CWR track, we will confine ourselves to examining the case of a special assignment of the function $\phi(\lambda,\lambda^*)$, which, however, is general enough to include the cases of purely frictional and frictional-elastic interaction between the rail and the supporting foundation.

Let us assume that

$$\phi_n(\lambda,\lambda^*) = \phi_{n-1}(\lambda,\lambda^*) - (-1)^n f_o(\theta), \quad (n = 2,3,4, \ldots). \tag{II.62}$$

For a purely frictional interaction this formula has the form

$$\phi_n(\lambda,\lambda^*) = c - (-1)^n 2c.$$

For elastic-frictional interaction,

$$\phi_n(\lambda,\lambda^*) = c + K\lambda - (-1)^n[2c + K\theta].$$

Here θ is the tie displacement from a previously displaced position (due to previous loads).

For practical purposes $f_o(\theta)$ can be obtained by averaging $f(\theta,\lambda^*)$ with respect to positive values of λ^*. It should be recalled that the function $\phi_o(\lambda)$ is obtained by averaging $\phi(\lambda,\lambda^*)$ with respect to both positive and negative values of λ^*.

It is quite obvious that the variance of $f_o(\theta)$ is smaller than the variance of $\phi_o(\lambda)$; however, after several successive loadings the variance of $\phi_n(\lambda,\lambda^*)$ will become greater than the variance of $\phi_o(\lambda)$ (for some n).

Let us examine successively three stages of temperature change (loading): 1) increase in temperature t from zero to its maximum value t^*; 2) decrease from the maximum value t* to its minimum value t_{min}; 3) increase from the minimum value t_{min} to the maximum value t^*.

With repeated cyclical changes in temperature in the interval $[t_{min},t^*]$, the last two stages will be alternately repeated.

It follows from (II.29) that during the first loading the displacement of the end of a length of rail and the temperature rise are related by the following formula:

$$t_1 = \frac{1}{\alpha}\sqrt{\frac{2}{EF}\int_0^{\lambda}\varphi(\lambda, 0)\,d\lambda + \frac{P_н}{\alpha EF}}.$$

Solving (II.57) and substituting the boundary conditions, we obtain

$$\tau = \frac{1}{\alpha}\sqrt{\frac{2}{EF}\int_0^{\theta} f(0)\,d0} + \frac{2P_{\text{н}}}{\alpha EF},$$

during the second loading, which yields

$$t_2 = t^* - \tau = \frac{1}{\alpha}\sqrt{\frac{2}{EF}\int_0^{\lambda_o^*} \varphi(\lambda, 0)\,d\lambda} - \frac{1}{\alpha}\sqrt{\frac{2}{EF}\int_0^{\lambda_o^* - \lambda_o} f(0)\,d0} - \frac{P_{\text{н}}}{\alpha EF},$$

where λ_o^* is the maximal displacement of the rail end at the end of the first stage of temperature change, and λ_o is the displacement of the end during the second stage.

Making use of (II.62), one can obtain the relation between the temperature t and the rail end displacement λ_o during the third stage. Obviously,

$$t_3 = \frac{1}{\alpha}\sqrt{\frac{2}{EF}\int_0^{\lambda_o^*} \varphi(\lambda, 0)\,d\lambda} - \frac{1}{\alpha}\sqrt{\frac{2}{EF}\int_0^{\lambda_o^* - \lambda_{o\min}} f(0)\,d0} + \frac{1}{\alpha}\sqrt{\frac{2}{EF}\int_0^{\lambda_o - \lambda_{o\min}} f(0)\,d0} + \frac{P_{\text{н}}}{\alpha EF},$$

where $\lambda_{o\min}$ is the minimal displacement of the rail end at the end of the second stage.

The graphs of $t(\lambda_{o1})$, $t(\lambda_{o2})$, and $t(\lambda_{o3})$ are plotted in Figure II.47, which clearly shows the hysteresis loop.

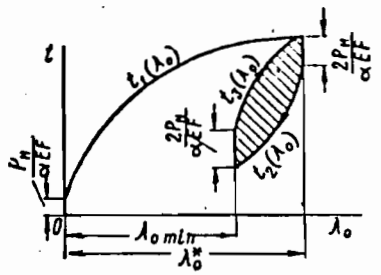

Fig. II.47. Displacement of a free rail end due to cyclical temperature variations

Except for the multiplying constant (1/αEF), the area of the loop represents the irreversible part of the work done by the sun in destroying the ballast, ties, and fastenings in the "transition" zone region. To prove this it is sufficient to note that the work done by the sun in the "transition" zone region is equal to the work done by the external force P = αtEF applied to the end of the rail.

To compute the work done by the sun, we can use the formula

$$A = \alpha EF \int_{\lambda_{0\,min}}^{\lambda_0^*} [t_3(\lambda_0) - t_2(\lambda_0)]\, d\lambda_0 = \sqrt{2EF} \int_{\lambda_{0\,min}}^{\lambda_0^*} \left(\sqrt{\int_0^{\lambda_0^* - \lambda_0} f(0)\, d0} + \right.$$
$$\left. + \sqrt{\int_0^{\lambda_0 - \lambda_{0\,min}} f(\theta)\, d0} - \sqrt{\int_0^{\lambda_0^* - \lambda_{0\,min}} f(0)\, d0} + \frac{2P_n}{\sqrt{2EF}} \right) d\lambda_0. \qquad \text{(II.63)}$$

To construct the hysteresis loop it is convenient to use templates bounded by the curves

$$\frac{1}{\alpha} \sqrt{\frac{2}{EF} \int_0^{\lambda} \varphi(\lambda, 0)\, d\lambda} \quad \text{и} \quad \frac{1}{\alpha} \sqrt{\frac{2}{EF} \int_0^{0} f(0)\, d0}.$$

For the case of frictional interaction these curves become parabolas:

$$\lambda = \frac{\alpha^2 EF}{2c} t^2; \quad 0 = \frac{\alpha^2 EF}{4c} t^2.$$

For this case the area of the hysteresis loop can be computed quite simply (Fig. II.48).

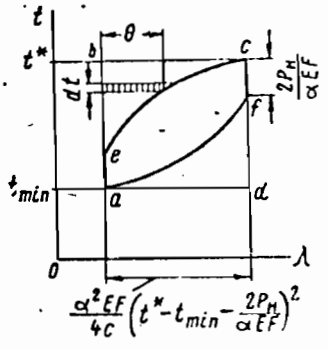

Fig. II.48. Construction of the hysteresis loop in the motion of a free end of a rail

It is clear that the area s of the figure aecf is given by

$$S_{aecf} = S_{abcd} - 2S_{ebc},$$

where

$$S_{abcd} = \frac{\alpha^2 EF}{4c}\left(t^* - t_{min} - \frac{2P_н}{\alpha EF}\right)^2 (t^* - t_{min});$$

the second term can be computed from the integral

$$S_{ebc} = \int_0^{t^* - t_{min} - \frac{2P_н}{\alpha EF}} f(\theta)\, d\theta = \frac{\alpha^2 EF}{12c}\left(t^* - t_{min} - \frac{2P_н}{\alpha EF}\right)^3.$$

Thus, the energy dissipated is given by

$$A = \alpha EF S_{aecf} = \frac{\alpha^3 E^2 F^2}{12c}\left(t^* - t_{min} - \frac{2P_н}{\alpha EF}\right)^2\left(t^* - t_{min} - \frac{4P_н}{\alpha EF}\right). \quad \text{(II.64)}$$

If $P_H = 0$, the equation (II.64) takes the form

$$A = \frac{\alpha^3 E^2 F^2}{12c}(t^* - t_{min})^3. \quad \text{(II.65)}$$

Let

$$\alpha EF(t^* - t_{min}) = 2P_\phi,$$

where P_ϕ is the amplitude of the fictitious force applied to the end of the rail.

Then formula (II.65) takes the form

$$A = \frac{2P_\phi^3}{3cEF} \qquad \text{(II.66)}$$

The cubic dependence is consistent with the relation between the area of a hysteresis loop for steel and the stress amplitude. For the case of elastic-frictional interaction between the rail and the supporting structure, the integral in (II.63) can be found in integral tables and is expressible in terms of elementary functions. In the more general case when the function $f(\theta)$ is approximated by a polynomial of third degree, the expression (II.63) can be reduced to a system of elliptic integrals of the second kind.

It was already noted that in examining forces and displacements in CWR track, produced as a result of temperature changes over a period of several days, the function $\phi(\lambda,\lambda^*)$ should be replaced by $\phi_o(\lambda)$. When even longer periods - a month, or several months - are examined, even the dependence on the rail displacement is erased; this can be explained by the existence of creep at a steady temperature, the relaxation of forces transmitted from the ballast to the ties, and even by atmospheric effects. Important effects which tend to smooth out the function $\phi_o(\lambda)$ are produced by the movement of trains, and even by work done to maintain the track. In general, the smaller the rate of temperature increase, the more weakly correlated will the function $\phi(\lambda,\lambda^*)$ be, and the

formulas previously derived are most accurate for the ideal case of a sudden temperature rise, $dt/dT = \infty$. Here T is the time. In what follows, dt/dT will denote the average rate of temperature change for the period of time being considered.

When $dt/dT = 0$, when constructing force and displacement diagrams produced by a temperature rise over an infinite time period, the dependence of the linear resistance on the displacement of the rails disappears completely.

Let us examine this phenomenon in somewhat greater detail. Suppose the temperature of a rail string increases by an amount t_1 during a time interval $\Delta T_1 = T_{21} - T_{11}$, so that $dt/dT = t_1/\Delta T_1$. Let us measure the magnitude of the displacement of the rail cross-section at several points, and let us compute the magnitude of the linear resistance at these points using, for example, the approximate formula $\rho \simeq EF(\Delta^2\lambda/\Delta x^2)$. Repeating this experiment under the same conditions many times, one can construct the ρ,λ correlation net, and compute the correlation function $K_{\rho(t),\lambda(t)}(\Delta T_1)$ of the random variables $\rho(t_1)$ and $\lambda(t_1)$.

Now, taking a different time interval $\Delta T_2 = T_{22} - T_{21}$, during which the temperature is raised by the same amount t_1 as during the previous series of experiments, one can compute the correlation coefficient $K_{\rho(t),\lambda(t)}(\Delta T_2)$.

In exactly the same way, given a time interval ΔT_n, one can compute $K_{\rho(t),\lambda(t)}(\Delta T_n)$ (Figure II.49). The graph obtained can be regarded as the correlation function between the processes $\rho_t(T)$ and $\lambda_t(T)$; furthermore, if the correlation coefficients

were determined by a regression of ρ over λ , the correlation function $K_{\rho(t),\lambda(t)}(\Delta T)$ characterizes the closeness of the dependence of the linear resistance $\rho_t(T_2)$ at time T_2 on the displacement of the rail cross-section $\lambda_t(T_1)$ at time T_1.

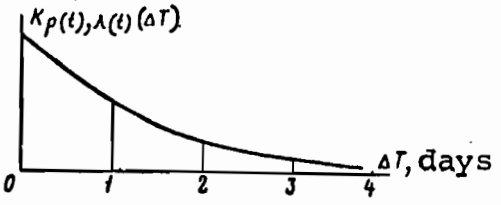

Fig. II.49. Graph of the correlation function of the linear resistance and rail cross-section displacement as a function of the time interval during which the displacement takes place

Having the information about the order of the system [we have in mind the graph of $\phi(\lambda,\lambda^*)$] at time T_1 when the temperature begins to rise, we must construct the force and displacement diagrams for time T_2 at which the temperature stops rising. If during the period $\Delta T = T_2 - T_1$ no further information is received concerning changes in the state of the system, its order must decrease according to the second law of thermodynamics simultaneously with an increase in the entropy - a measure of the system indeterminancy.

Since ρ grows together with the growth of the displacement λ, we can assert that the correlation function $K_{\rho(t),\lambda(t)}(\Delta T)$ is positive. It is convenient to approximate this function by the formula

$$K_{\rho(t),\lambda(t)}(\Delta T) = A_t e^{-\frac{|\Delta T|}{\beta_t}}, \qquad \text{(II.67)}$$

where βt is the correlation time, i.e. a period during which the correlation is, for all practical purposes, erased. This quantity varies between 3 and 7 days. It is easy to see that

$A_t = K_{\rho(t),\lambda(t)}(0)$. In the first approximation, the quantities A_t and β_t can be considered independent of the temperature.

Consequently, in examining yearly temperature changes we must look for the linear resistance as a function of the temperature and time, and not of cross-section displacement.

At the present time the following relation between the linear resistance and the temperature is accepted:

$$\rho = \begin{cases} \rho s, \text{ for } t_C > 0, \\ \rho w, \text{ for } t_C < 0, \end{cases} \qquad \text{(II.68)}$$

where ρ_s is the averaged linear resistance to displacement for summer temperatures, ρ_w is the same quantity for winter temperatures, and t_C is the temperature in degrees Celcius.

It is unnecessary to examine the construction of temperature diagrams based on the use of equation (II.68), since these can be found in any textbook devoted to railroad track construction.

CHAPTER III

INVESTIGATION OF THE OPERATION OF CONTINOUS WELDED RAILROAD TRACK AND EXPERIMENTAL DETERMINATION OF PARAMETERS AND FUNCTIONS WHICH DETERMINE ITS BEHAVIOUR UNDER TEMPERATURE CHANGES

1. Determination of the statistical parameters of the function $\psi(\lambda,0)$. Experimental goals and methods, and results obtained.

The basic statistical characteristics of the dependence of the rail displacement on the force transmitted by the rail to the tie were determined in experiments conducted by the author at the Tsaritsin station on the Moscow line.

Two 550 cm lengths of P50 rails, isolated from the rest of the track by 50 mm gaps, were laid in the experimental section. Ten wooden ties, attached to the rail by intermediate fastenings of type K, were installed along the length of these rails. The distance between the ties was taken to be $\Delta x = 55$ cm, which corresponds to 1840 ties per kilometer. Crushed stone of medium hardness was used for the ballast. Joint bars were omitted.

The displacement of the rails was fixed by means of dial gauges installed at both ends of each rail.

Figure III.1 shows the arrangement for displacing the 5.50 m section. The actual displacement was effected by means of a two-cylinder hydraulic jack equipped with a manometer.

Before each experiment the ballast was packed by an electric tie tamper. The clamp bolts were tightened once every ten experiments

To eliminate the influence of displacements of one rail on displacements of the other rail, the ties were cut in half, and to prevent misalignment, the rails were fastened to the center of the half-ties, as shown on Figure III.2.

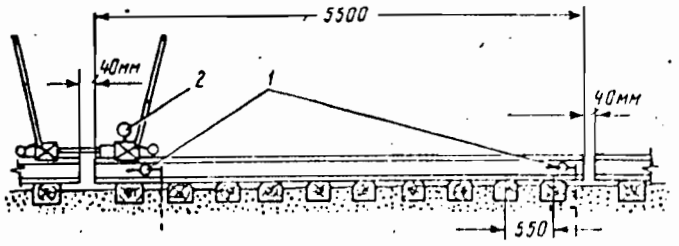

Fig. III.1. Arrangement for moving the rails by means of a hydraulic jack; (1) dial gauge; (2) manometer.

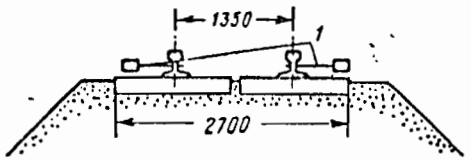

Fig. III.2. Track-stand cross section; (1) pin for attaching dial gauge.

Because of the narrowing of the track gauge in the experimental section, the gauge was also made smaller in the adjoining sections of the track to permit the use of the hydraulic jacks. The longitudinal forces were computed from the manometer readings to within m_o = 160 kg. The arrangement of the dial gauges is shown in Figure III.3. The forces transmitted to the rail were fixed after every 2 mm of longitudinal displacement.

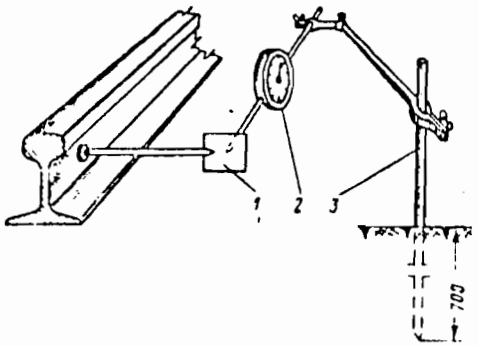

Fig. III.3. Arrangement for fixing the displacement of a rail cross-section; (1) plate; (2) dial gauge; (3) stand.

The simultaneous displacement of five ties (ten half-ties) was dictated by the following considerations: (1) In moving a single tie the ballast in the tie crib (if the tie crib is not too large) is subjected to a higher pressure because the preceding tie remains stationary, which does not correspond to actual operating conditions in a track. (2) When a large number of ties is moved simultaneously one must take into account the differences in the displacements of the individual ties, since these differences can be appreciable. (3) The accuracy of the experiment is improved when several ties are moved simultaneously by the hydraulic jack, since the accuracy m of determining the force transmitted to one tie is equal to $m = 2m_o/n_o$, where n_o is the number of ties in the displaced section of the track. In particular, when $n_o = 10$, $m = 2(160)/10 = 32$ kg.

Thus, an optimal number of ties to be moved simultaneously must be selected, on the one hand, to create conditions which are similar to actual operating conditions for ties in a track, and, on the other hand, to achieve conditions of equal displacement (within certain limits of accuracy) of all the ties (more precisely, of rail cross-sections opposite the ties). In addition to this, it is desirable that the force needed to effect the displacement should be in the range 9 - 10 tons, since larger pressures may cause oil leakage through the cylinder seals, which will result in erroneous manometer readings (the cylinder pressure drops quite precipitously with time).

The experiments were perfomed during dry summer weather. The results are shown in Table 7. On the basis of these results

Table 7

N	$\delta\phi(\lambda, \overline{0})$ (Divisions)										
	$\lambda = 0$ MM	$\lambda = 2$ MM	$\lambda = 4$ MM	$\lambda = 6$ MM	$\lambda = 8$ MM	$\lambda = 10$ MM	$\lambda = 12$ MM	$\lambda = 14$ MM	$\lambda = 16$ MM	$\lambda = 18$ MM	$\lambda = 20$ MM
1	$\frac{10}{11}$	$\frac{16}{16}$	$\frac{21}{21}$	$\frac{25}{25}$	$\frac{28}{27}$	$\frac{29}{29}$	$\frac{30}{30}$	$\frac{30}{31}$	$\frac{30}{31}$	$\frac{30}{30}$	$\frac{30}{32}$
2	$\frac{10}{11}$	$\frac{16}{15}$	$\frac{21}{20}$	$\frac{25}{23}$	$\frac{28}{26}$	$\frac{29}{27}$	$\frac{30}{28}$	$\frac{31}{29}$	$\frac{31}{31}$	$\frac{31}{33}$	$\frac{33}{35}$
3	$\frac{10}{10}$	$\frac{17}{17}$	$\frac{22}{23}$	$\frac{25}{26}$	$\frac{27}{29}$	$\frac{29}{31}$	$\frac{30}{32}$	$\frac{30}{33}$	$\frac{33}{32}$	$\frac{33}{32}$	$\frac{29}{33}$
4	$\frac{12}{10}$	$\frac{16}{17}$	$\frac{21}{22}$	$\frac{24}{25}$	$\frac{27}{27}$	$\frac{29}{29}$	$\frac{31}{30}$	$\frac{32}{30}$	$\frac{30}{31}$	$\frac{32}{31}$	$\frac{33}{33}$
5	$\frac{9}{10}$	$\frac{14}{16}$	$\frac{18}{22}$	$\frac{21}{25}$	$\frac{24}{27}$	$\frac{25}{29}$	$\frac{26}{30}$	$\frac{27}{31}$	$\frac{29}{35}$	$\frac{29}{31}$	$\frac{30}{31}$
6	$\frac{10}{10}$	$\frac{16}{17}$	$\frac{20}{23}$	$\frac{23}{25}$	$\frac{26}{28}$	$\frac{28}{30}$	$\frac{29}{31}$	$\frac{30}{32}$	$\frac{30}{32}$	$\frac{29}{32}$	$\frac{29}{33}$
7	$\frac{10}{10}$	$\frac{16}{16}$	$\frac{21}{21}$	$\frac{25}{25}$	$\frac{28}{27}$	$\frac{30}{28}$	$\frac{31}{29}$	$\frac{32}{29}$	$\frac{35}{31}$	$\frac{33}{35}$	$\frac{36}{32}$
8	$\frac{10}{10}$	$\frac{15}{15}$	$\frac{20}{20}$	$\frac{22}{23}$	$\frac{24}{25}$	$\frac{26}{26}$	$\frac{26}{27}$	$\frac{28}{28}$	$\frac{29}{29}$	$\frac{29}{29}$	$\frac{30}{30}$
9	$\frac{10}{11}$	$\frac{16}{18}$	$\frac{21}{23}$	$\frac{23}{26}$	$\frac{26}{29}$	$\frac{28}{31}$	$\frac{30}{32}$	$\frac{31}{33}$	$\frac{34}{32}$	$\frac{36}{33}$	$\frac{36}{33}$
10	$\frac{10}{8}$	$\frac{15}{15}$	$\frac{20}{20}$	$\frac{23}{23}$	$\frac{26}{26}$	$\frac{27}{27}$	$\frac{28}{29}$	$\frac{29}{31}$	$\frac{30}{31}$	$\frac{31}{32}$	$\frac{31}{33}$
11	$\frac{9}{9}$	$\frac{16}{16}$	$\frac{20}{20}$	$\frac{23}{23}$	$\frac{26}{26}$	$\frac{27}{28}$	$\frac{28}{30}$	$\frac{29}{31}$	$\frac{31}{33}$	$\frac{32}{33}$	$\frac{31}{31}$
12	$\frac{10}{11}$	$\frac{15}{19}$	$\frac{20}{24}$	$\frac{23}{27}$	$\frac{25}{30}$	$\frac{26}{31}$	$\frac{26}{33}$	$\frac{28}{31}$	$\frac{30}{33}$	$\frac{31}{33}$	$\frac{29}{32}$
13	$\frac{10}{10}$	$\frac{16}{16}$	$\frac{21}{21}$	$\frac{24}{24}$	$\frac{27}{27}$	$\frac{29}{29}$	$\frac{30}{30}$	$\frac{31}{31}$	$\frac{30}{31}$	$\frac{31}{31}$	$\frac{31}{33}$
14	$\frac{10}{10}$	$\frac{16}{17}$	$\frac{21}{23}$	$\frac{24}{27}$	$\frac{26}{30}$	$\frac{28}{31}$	$\frac{29}{33}$	$\frac{29}{31}$	$\frac{31}{33}$	$\frac{33}{33}$	$\frac{32}{33}$
15	$\frac{10}{10}$	$\frac{15}{15}$	$\frac{20}{20}$	$\frac{23}{23}$	$\frac{26}{26}$	$\frac{28}{28}$	$\frac{30}{30}$	$\frac{30}{30}$	$\frac{29}{32}$	$\frac{31}{31}$	$\frac{30}{31}$
16	$\frac{10}{10}$	$\frac{16}{16}$	$\frac{21}{21}$	$\frac{25}{25}$	$\frac{28}{27}$	$\frac{30}{29}$	$\frac{31}{30}$	$\frac{32}{31}$	$\frac{31}{29}$	$\frac{32}{30}$	$\frac{32}{32}$

Table 7 (continued).

N	$5\psi(\lambda, 0)$ (Divisions)										
	$\lambda = 0$ mm	$\lambda = 2$ mm	$\lambda = 4$ mm	$\lambda = 6$ mm	$\lambda = 8$ mm	$\lambda = 10$ mm	$\lambda = 12$ mm	$\lambda = 14$ mm	$\lambda = 16$ mm	$\lambda = 18$ mm	$\lambda = 20$ mm
17	10/10	16/15	21/20	25/24	27/26	29/28	30/29	31/29	33/32	33/32	33/32
18	10/9	16/16	22/22	25/25	27/27	29/28	30/29	31/30	31/34	32/32	34/32
19	10/11	17/17	22/22	25/25	28/27	30/28	31/30	31/32	33/31	33/33	32/34
20	9/10	16/17	20/22	23/25	26/27	28/28	29/29	30/30	31/33	30/33	32/32
21	10/10	16/17	20/22	23/25	26/27	28/28	30/30	32/30	34/31	34/32	34/31
22	11/10	18/16	24/22	27/23	30/26	31/27	32/28	32/29	31/33	31/32	31/32
23	9/9	15/14	20/18	24/22	27/25	29/28	30/29	30/30	31/33	31/34	29/32
24	10/11	17/19	20/24	23/27	26/29	28/31	30/33	31/34	32/34	31/35	31/33
25	9/11	16/16	21/21	24/24	27/27	30/29	31/30	32/31	34/32	35/33	33/32
26	10/10	16/17	20/23	22/26	24/29	26/30	27/31	28/30	31/32	32/33	33/33
27	10/10	16/17	20/22	22/25	25/27	27/28	29/30	30/30	32/32	32/33	32/34
28	10/10	16/16	21/20	24/24	27/27	30/28	31/29	33/30	33/33	34/34	33/32
29	10/10	17/17	23/23	26/26	29/29	30/30	32/31	33/30	35/32	36/32	32/35
30	10/9	17/14	22/19	25/22	27/25	29/27	30/29	31/29	35/32	35/34	36/32

Remarks. 1. The numerator and denominator shows the manometer readings when moving the east and west rails respectively.
2. The zero of the manometer is displaced by half a division, so that a manometer reading of n divisions corresponds to an interval $m_o(n-1) - m_o n$ of the values of the longitudinal force transmitted from the hydraulick jack to the rail, where $m_o = 160$ kg, corresponding to one division on the manometer. Consequently, the interval of values of the longitudinal force transmitted to one tie (two half-ties) is $m_o(n-1)/5 - m_o n/5$. Here $m = m_o/5$ is the limit of accuracy for computing the longitudinal force, m = 32 kg.
3. N denotes the experiment number.

the mathematical expectation and the variance were computed for the longitudinal force transmitted to one rail when it is displaced by a fixed amount.

For rail displacements $\lambda > 20$ mm, the force transmitted to the rail did not go up as a rule, and instead oscillated as the rate of oil movement was varied. This can be explained by the appearance, for large displacements, of sliding surfaces within the ballast and the existence of sizable plastic deformations; in addition, the appearance of creep is very obvious for large displacements.

Let us turn our attention now to the analysis of the experimental data. The columns of Table 7 represent the statistical series of distributions of the random variables $5\psi(\lambda_i,0)$.

Let us compute the statistical characteristics of the random variables $5\psi(\lambda_i,0)$, and verify the agreement between the empirical and the theoretical Gaussian distribution by means of the Pearson "χ^2 test". Special tables for the χ^2 distribution are available [30].

Making use of the tables, one can determine for every value of χ^2 and the number of degrees of freedom r, the probability P that the value of the random variable distributed according to the χ^2 law will exceed that value. The number of degrees of freedom r of the χ^2 distribution is the difference between the number of interval ranges k of the statistical series and the number s of constraints imposed on the empirically determined frequencies P_{ji}. The sume of the frequencies must be equal to one, i.e.

$$\sum_{j=1}^{k} P^*_{ji} = 1,$$

and we will choose the theoretical distribution so that the theoretical and the statistically determined mean values and variances coincide, i.e.

$$\sum_{j=1}^{k} 5\tilde{\psi}_j(\lambda_i, 0)\, P^*_{ji} = M5\psi(\lambda_i, 0);$$
$$\sum_{j=1}^{k} [5\tilde{\psi}_j(\lambda_i, 0) - M5\psi(\lambda_i, 0)]^2 P^*_{ji} = \partial 5\psi(\lambda_i, 0),$$

where $\tilde{\psi}_j(\lambda_i,0)$ is the "representative" of the j-th interval range of the random variable $\psi(\lambda_i,0)$; P^*_{ji} is the frequency of the j-th interval range (for $\lambda = \lambda_i$); and k_i is the number of interval ranges.

The number of constraints s_i imposed on the frequencies in this case is equal to 3.

Let us note that the χ^2 distribution with r degrees of freedom is the distribution of the sum of squares of r independent random variables, each one of which obeys the normal law with the expected value equal to zero, and the variance equal to one. This distribution is completely characterized by the density

$$R_r(u) = \begin{cases} \dfrac{1}{2^{\frac{r}{2}}\,\Gamma\left(\dfrac{r}{2}\right)} u^{\frac{r}{2}-1} e^{-\frac{u}{2}} & \text{при } u > 0 \\ 0 & \text{при } u < 0 \end{cases},$$

where $\Gamma(\alpha) = \int_0^\infty t^{\alpha-1}e^t dt$ is the well known gamma function.

Thus, let us compute the statistical parameters of the distributions of the random variables $\psi(\lambda_i,0)$.

1. $\lambda_i = 0$

For this case the forces for which the rails begin to move were fixed. Using the second column of Table 7, we construct

the statistical series of the random variable $5\psi(0,0)$ (Table 8).

Table 8

n_{jo} - manometer reading	8	9	10	11	12
I_{jo} - interval of force values transmitted to the rail	1120-1280	1280-1440	1440-1600	1600-1760	1760-1920
N_{jo} - number of occurrences in each interval	1	9	41	8	1
P_{jo} - frequency of occurrence in each interval	0.017	0.150	0.683	0.133	0.017

Let us compute the expected value of $5\psi(0,0)$:

$$M5\psi(0,0) = \sum_{j=1}^{k} 5\tilde{\psi}_j(0,0)\,P^*_{j0} = 1\,200\cdot 0{,}017 + 1\,360\cdot 0{,}150 +$$
$$+ 1\,520\cdot 0{,}683 + 1\,680\cdot 0{,}133 + 1\,840\cdot 0{,}017 = 1\,518\,\mathbf{kg},$$

from which

$$M\psi(0,0) = \frac{1}{5}\,M5\psi(0,0) = \frac{1}{5}\,1518 = 506\ \text{kg}.$$

The variance of $5\psi(0,0)$ is given by

$$\partial 5\psi(0,0) = \sum_{j=1}^{5} [5\tilde{\psi}_j(0,0) - M5\psi(0,0)]^2\,P^*_{j0} =$$
$$= (1\,200 - 1\,518)^2\,0{,}017 + (1\,360 - 1\,518)^2\,0{,}150 +$$
$$+ (1\,520 - 1\,518)^2\,0{,}683 + (1680 - 1518)^2\,0{,}133 +$$
$$+ (1\,840 - 1\,518)^2\,0{,}017 = 10\,650\ \text{kg}^2.$$

From this we can compute the variance of $\psi(0,0)$:

$$\partial\psi(0,0) = \frac{1}{5}\,\partial 5\psi(0,0) = \frac{1}{5}\,10\,650 = 2\,130\ \text{kg}^2$$

2. $\lambda_i = 2$ mm

From the third column of Table 7 we construct the statistical series of the random variable $5\psi(2,0)$ (Table 9).

Table 9

n_{j_2}	14	15	16	17	18	19
I_{j2}	2 080— 2 240	2 240— 2 400	2 400— 2 560	2 560— 2 720	2 720— 2 880	2 880— 3 040
N_{j2}	3	10	28	15	2	2
P^*_{j2}	0,050	0,167	0,467	0,250	0,033	0,033

Let us compute the mathematical expectation of $\psi(2,0)$:

$$M5\psi(2,0) = \sum_{j=1}^{6} 5\tilde{\psi}_j(2,0)\,P^*_{j2} = 2\,160\cdot 0{,}050 + 2\,320\cdot 0{,}167 +$$
$$+2\,480\cdot 0{,}467 + 2\,640\cdot 0{,}250 + 2\,800\cdot 0{,}033 + 2\,960\cdot 0{,}033 = 2\,492\ \text{kg}.$$

We find the expected value to be

$$M\psi(2,0) = \frac{1}{5}\,M5\psi(2,0) = \frac{1}{5}\,2492 = 500\ \text{kg}.$$

The variance of $5\psi(2,0)$ is given by

$$\partial 5\psi(2,0) = \sum_{j=1}^{6} [5\tilde{\psi}_j(2,0) - M5\psi(2,0)]^2\,P^*_{j2}$$
$$= (2\,160 - 2\,492)^2\,0{,}050 + (2\,320 - 2\,492)^2\,0{,}167 +$$
$$+ (2\,480 - 2\,492)^2\,0{,}417 + (2\,640 - 2\,492)^2 \times$$
$$\times 0{,}250 + (2\,800 - 2\,492)^2\,0{,}033 + (2\,960 - 2492)^2\,0{,}033 = 31\,840\ \text{kg}^2.$$

The variance of $\psi(2,0)$ is

$$\partial\psi(2,0) = \frac{1}{5}\,\partial 5\psi(2,0) = \frac{1}{5}\,31840 = 6368\ \text{kg}^2.$$

3. $\lambda_i = 4$ mm

On the basis of the fourth column of Table 7, let us construct the statistical series of the random variable $5\psi(4,0)$ (Table 10).

Table 10

n_{j4}	18	19	20	21	22	23	24
l_{j4} . . .	2720—2880	2880—3040	3040—3200	3200—3360	3360—3520	3520—3680	3680—3840
N_{j4} . . .	2	1	19	16	12	7	3
$P^*_{l_4}$ . . .	0,033	0,017	0,317	0,267	0,200	0,116	0,05

The expected value of $5\psi(4,0)$ is given by

$$M5\psi(4,0) = 2\,800 \cdot 0{,}033 + 2\,960 \cdot 0{,}017 + 3\,120 \cdot 0{,}317 + 3\,280 \times \\ \times 0{,}267 + 3\,440 \cdot 0{,}200 + 3\,600 \cdot 0{,}116 + 3\,760 \cdot 0{,}05 = 3\,302 \text{ kg}.$$

We find the mathematical expectation of $\psi(4,0)$ to be

$$M\psi(4,0) = \frac{1}{5} M5\psi(4,0) = \frac{1}{5} 3\ 302 = 660 \text{ kg}.$$

The variance of $5\psi(4,0)$ is

$$\partial 5\psi(4,0) = \sum_{1}^{7} [5\tilde{\psi}_j(4,0) - M5\psi(4,0)]^2 P^*_{j4} = \\ = (2\,800 - 3\,302)^2 0{,}033 + (2\,960 - 3\,302)^2 0{,}017 + \\ + (3\,120 - 3\,302)^2 0{,}317 + (3\,280 - 3\,302)^2 0{,}267 + \\ + (3\,440 - 3302)^2 0{,}200 + (3\,600 - 3\,302)^2 0{,}116 + \\ + (3\,760 - 3\,302)^2 0{,}05 = 45\,570 \text{ kg}^2$$

Thus, the variance of $\psi(4,0)$ is

$$\partial\psi(4,0) = \frac{1}{5} \partial 5\psi(4,0) = \frac{1}{5} 45\ 570 = 9\ 100 \text{ kg}^2.$$

4. $\lambda_i = 6$ mm

Making use of column 5 of Table 7, we construct the statistical series of the random variable $5\psi(6,0)$ (Table 11).

Table 11

n_{j_6}	21	22	23	24	25	26	27
l_{j6} . . .	3 200—3 360	3 360—3 520	3 520—3 680	3 680—3 840	3 840—4 000	4 000—4 160	4 160—4 320
N_{j6} . . .	1	5	15	10	20	5	4
P^*_{j6} . . .	0,017	0,083	0,250	0,167	0,333	0,083	0,067

The expected value of $5\psi(6,0)$ is given by

$$M5\psi(6,0) = \sum_{j=1}^{7} 5\tilde{\psi}(6,0)\, P^*_{j6} = 3\,280 \cdot 0{,}017 + 3\,440 \cdot 0{,}083 + 3\,600 \cdot 0{,}250 + 3\,760 \cdot 0{,}167 + 3\,920 \cdot 0{,}333 + 4\,080 \cdot 0{,}083 + 4\,240 \cdot 0{,}067 = 3\,796 \text{ kg}.$$

Thus, the expected value of $\psi(6,0)$ is

$$M\psi(6,0) = \frac{1}{5} M5\psi(6,0) = \frac{1}{5} 3\,796 = 760 \text{ kg}.$$

The variance of $5\psi(6,0)$ is

$$\partial 5\psi(6,0) = \sum_{j=1}^{7} [5\tilde{\psi}_j(6,0) - M5\psi(6,0)]^2 P^*_{j6} = (3\,280 - 3\,796)^2 0{,}017 + (3\,440 - 3\,796)^2 0{,}083 + (3\,600 - 3\,796)^2 0{,}250 + (3\,760 - 3796)^2 0{,}167 + (3\,920 - 3\,796)^2 0{,}333 + (4\,080 - 3\,796)^2 0{,}083 + (4\,240 - 3\,796)^2 0{,}067 = 50\,030 \text{ kg}.$$

The variance of $\psi(6,0)$ is

$$\partial\psi(6,0) = \frac{1}{5} \cdot \partial 5\psi(6,0) = \frac{1}{5} \cdot 50\,030 = 10\,000 \text{ kg}^2$$

5. λ_i = 8 mm

Table 12

n_{j_8}	24	25	26	27	28	29	30
l_{j8} . . .	3 680—3 840	3 840—4 000	4 000—4 160	4 160—4 320	4 320—4 480	4 480—4 640	4 640—4 800
N_{j8} . . .	3	5	15	22	6	6	3
P^*_{j8} . .	0,050	0,083	0,250	0,367	0,100	0,100	0,150

The expected value of $5\psi(8,0)$

$$M5\psi(8,0) = \sum_{j=1}^{7} 5\tilde{\psi}_j(8,0)\, P^*_{j8} = 3\,760 \cdot 0{,}050 + 3\,920 \cdot 0{,}083 + 4\,080 \cdot 0{,}250 + 4\,240 \cdot 0{,}367 + 4\,400 \cdot 0{,}100 + 4\,560 \cdot 0{,}100 + 4\,720 \cdot 0{,}150 = 4\,222 \text{ kg}.$$

The expected falue of $\psi(8,0)$ is

$$M\psi(8,0) = \frac{1}{5} M5\psi(8,0) = \frac{1}{5} 4\,222 = 844 \text{ kg}.$$

The variance of $5\psi(8,0)$ is given by

$$\partial 5\psi(8,0) = \sum_{j=1}^{7} \left[5\tilde{\psi}_j(8,0) - M5\psi(8,0)\right]^2 P^*_{j8} =$$
$$= (3\,760 - 4\,222)^2 0{,}050 + (3\,920 - 4\,222)^2 0{,}083 +$$
$$+ (4\,080 - 4\,222)^2 0{,}250 + (4\,240 - 4\,222)^2 0{,}367 +$$
$$+ (4\,400 - 4\,222)^2 0{,}100 + (4\,560 - 4\,222)^2 0{,}100 +$$
$$+ (4\,720 - 4\,222)^2 0{,}050 = 50\,660 \text{ kg}^2$$

The variance of $\psi(8,0)$ is

$$\partial\psi(8,0) = \frac{1}{5} \partial 5\psi(8,0) = \frac{1}{5} 50\,660 = 10\,300 \text{ kg}.$$

6. $\lambda_i = 10$ mm

From column seven of Table 7 we construct the statistical series of the random variable $5\psi(10,0)$ (Table 13).

Table 13

n_{j10}	25	26	27	28	29	30	31
I_{j10} . . .	3 810— 4 000	4 000 – 4 160	4 160 – 4320	4 320 – 4 480	4 480 – 4 640	4 640 – 4 800	4 800 – 4 960
N_{j10} . .	1	4	7	18	15	9	6
P^*_{j10} . .	0,017	0,066	0,117	0,300	0,250	0,150	0,100

The expected value of $5\psi(10,0)$ is equal to

$$M5\psi(10,0) = \sum_{j=1}^{7} 5\tilde{\psi}_j(10,0)\, P^*_{j10} = 3\,920 \cdot 0{,}017 + 4\,080 \cdot 0{,}066 + 4\,240 \cdot 0{,}117 + 4\,400 \cdot 0{,}300 + 4\,560 \cdot 0{,}250 + 4{,}720 \cdot 0{,}150 + 4\,880 \cdot 0{,}100 + 4\,489 \text{ kg}.$$

We determine the expected value of $\psi(10,0)$ to be

$$M\psi(10,0) = \frac{1}{5} M5\psi(10,0) = \frac{1}{5} 4\ 489 = 900 \text{ kg}.$$

Now we can determine the variance of $5\psi(10,0)$

$$\partial 5\psi(10,0) = \sum_{j=1}^{7} [5\tilde{\psi}_j(10,0) - M5\psi(10,0)]^2 P^*_{j10} = (3\,920 - 4\,489)^2 0{,}017 + (4\,080 - 4\,489)^2 0{,}066 + (4\,240 - 4\,489)^2 0{,}117 + (4\,400 - 4\,489)^2 0{,}300 + (4\,560 - 4\,489)^2 0{,}250 + (4\,720 - 4\,489)^2 0{,}150 + (4\,880 - 4\,489)^2 0{,}100 = 51\,660 \text{ kg}^2.$$

The variance of $\psi(10,0)$ is

$$\partial\psi(10,0) = \frac{1}{5} \partial 5\psi(10,0) = \frac{1}{5} 51\ 660 = 10\ 600 \text{ kg}^2.$$

7. $\lambda_i = 12$ mm

Making use of column 8 of Table 7, we will construct the statistical series of $5\psi(12,0)$ (Table 14).

Table 14

$n_{j_{12}}$	26	27	28	29	30	31	32	33
l_{j12} . .	4 000 — 4 160	4 160 — 4 320	4 320 — 4 480	4 480 — 4 640	4 640 — 4 800	4 800 — 4 960	4 960 — 5 120	5 120 — 5 280
N_{j12} . .	3	2	4	12	23	9	4	3
P^*_{j12} . .	0,050	0,034	0,066	0,200	0,384	0,150	0,066	0,050

The expected value of $5\psi(12,0)$ is equal to

$$M5\psi(12,0) = \sum_{j=1}^{8} 5\tilde{\psi}_j(12,0)\, P^*_{j12} = 4\,080 \cdot 0{,}050 + 4\,240 \cdot 0{,}034 + \\ + 4\,400 \cdot 0{,}066 + 4\,560 \cdot 0{,}200 + 4\,720 \cdot 0{,}384 + 4\,880 \cdot 0{,}150 + \\ + 5\,040 \cdot 0{,}066 + 5\,200 \cdot 0{,}050 = 4\,684 \text{ kg}.$$

We find the expected value of $\psi(12,0)$ to be

$$M\psi(12,0) = \frac{1}{5} M5\psi(12,0) = \frac{1}{5} 4\ 684 - 937 \text{ kg}.$$

The variance of $5\psi(12,0)$ is equal to

$$\partial 5\psi(12,0) = \sum_{j=1}^{8} [5\tilde{\psi}_j(12,0) - M5\psi(12,0)]^2 P^*_{j12} = \\ = (4\,080 - 4\,684)^2 0{,}050 + (4\,240 - 4\,684)^2 0{,}034 + \\ + (4\,400 - 4\,684)^2 0{,}066 + (4\,560 - 4\,684)^2 0{,}200 + \\ + (4\,720 - 4\,684)^2 0{,}384 + (4\,880 - 4\,684)^2 0{,}15 + \\ + (5\,040 - 4\,684)^2 0{,}066 + (5\,200 - 4\,684)^2 0{,}050 = 63\,640 \text{kg}^2.$$

The variance of $\psi(12,0)$ is

$$\partial\psi(12,0) = \frac{1}{5} \partial 5\psi(12,0) = \frac{1}{5} 63\ 640 = 12\ 700 \text{ kg}^2.$$

8. $\lambda_i = 14$ mm

Making use of 9th column of Table 7, we obtain the statistical series of the random variable $5\psi(14,0)$ (Table 15).

Table 15

n_{j14}	27	28	29	30	31	32	33	34
I_{j14} . . .	4 160 – 4 320	4 320 – 4 480	4 480 – 4 610	4 610 – 4 800	4 800 – 4 960	4 960 – 5 120	5 120 – 5 280	5 280 – 5 440
N_{j14} . .	1	4	8	17	15	8	4	3
P^*_{j14} . .	0,017	0,066	0,133	0,284	0,250	0,133	0,067	0,050

Let us determine the expected value of $5\psi(14,0)$

$$M5\psi(14,0) = \sum_{j=1}^{8} 5\tilde{\psi}_j(14,0)\,P^*_{j14} = 4\,240\cdot 0{,}017 + 4\,400\cdot 0{,}066 +$$
$$+ 4\,560\cdot 0{,}133 + 4\,720\cdot 0{,}284 + 4\,880\cdot 0{,}250 + 5\,040\cdot 0{,}133 +$$
$$+ 5\,200\cdot 0{,}067 + 5\,360\cdot 0{,}050 = 4\,817 \text{ kg}.$$

The expected value of $\psi(14,0)$ is

$$M\psi(14,0) = \frac{1}{5}\,M5\psi(14,0) = \frac{1}{5}\,4\,817 = 963 \text{ kg}.$$

Now let us compute the variance of $5\psi(14,0)$

$$\partial 5\psi(14,0) = \sum_{j=1}^{8} [5\tilde{\psi}_j(14,0) - M5\psi(14,0)]^2\,P^*_{j14} =$$
$$= (4\,240 - 4\,817)^2\,0{,}017 + (4\,400 - 4\,817)^2\,0{,}066 +$$
$$+ (4\,560 - 4\,817)^2\,0{,}133 + (4\,720 - 4\,817)^2\,0{,}284 +$$
$$+ (4\,880 - 4\,817)^2\,0{,}250 + (5\,040 - 4\,817)^2\,0{,}133 +$$
$$+ (5\,200 - 4\,817)^2\,0{,}067 + (5\,360 - 4\,817)^2\,0{,}050 = 60\,580 \text{ kg}^2$$

The variance of $\psi(14,0)$ is

$$\partial\psi(14,0) = \frac{1}{5}\,\partial 5\psi(14,0) = \frac{1}{5}\,60\,580 = 12\,116 \text{ kg}^2.$$

9. $\lambda_i = 16$ mm

Column 10 of Table 7 yields the statistical series of the random variable $5\psi(14,0)$ (Table 16).

Table 16

n_{j16}	29	30	31	32	33	34	35
l_{j16} . . .	4 480 – 4 640	4 640 – 4 800	4 800 – 4 910	4 910 – 5 120	5 120 – 5 280	5 280 – 5 440	5 440 – 5 600
N_{j16} . .	5	6	26	12	11	6	4
P^*_{j16} . .	0,083	0,100	0,267	0,200	0,183	0,100	0,067

The expected value of the function $5\psi(16,0)$ is

$$M5\psi(16,0) = \sum_{j=1}^{7} 5\tilde{\psi}(16,0)\, P^{*}_{j16} = 4\,560 \cdot 0{,}083 + 4\,720 \cdot 0{,}100 +$$
$$+ 4\,880 \cdot 0{,}267 + 5\,040 \cdot 0{,}200 + 5\,200 \cdot 0{,}183 + 5\,360 \cdot 0{,}100 +$$
$$+ 5\,520 \cdot 0{,}067 = 5\,085 \text{ kg}.$$

The expected value of $\psi(16,0)$ is

$$M\psi(16,0) = \frac{1}{5} M5\psi(16,0) = \frac{1}{5} 5\ 085 = 1\ 017 \text{ kg}.$$

Let us compute the variance of $5\psi(16,0)$

$$\partial 5\psi(16,0) = \sum_{j=1}^{7} \left[5\tilde{\psi}_j(16,0) - M5\psi(16,0)\right]^2 P^{*}_{j16} =$$
$$= (4\,560 - 5\,085)^2\, 0{,}083 + (4\,720 - 5\,085)^2\, 0{,}100 +$$
$$+ (4\,880 - 5\,085)^2\, 0{,}267 + (5\,040 - 5\,085)^2\, 0{,}200 +$$
$$+ (5\,200 - 5\,085)^2\, 0{,}183 + (5\,360 - 5\,085)^2\, 0{,}100 +$$
$$+ (5\,520 - 5\,085)^2\, 0{,}067 = 60\,020 \text{ kg}^2.$$

The variance of $\psi(16,0)$ is equal to

$$\partial\psi(16,0) = \frac{1}{5} \partial 5\psi(16,0) = \frac{1}{5} 60\ 020 = 12\ 000 \text{ kg}.$$

10. λ_i = 18 mm

The statistical series of the random variable $5\psi(18,0)$, computed from column 11, Table 7, is shown in Table 17.

Table 17

n_{j18}	29	30	31	32	33	34	35	36
J_{j18} . . .	4 480 – 4 640	4 640 – 4 800	4 800 – 4 960	4 960 – 5 120	5 120 – 5 280	5 280 – 5 440	5 440 – 5 600	5 600 – 5 760
N_{j18} . .	4	4	10	15	15	7	3	2
P^{*}_{j18} . .	0,067	0,067	0,166	0,250	0,250	0,116	0,05	0,034

The mathematical expectation of $5\psi(18,0)$ is

$$M5\psi(18,0) = \sum_{j=1}^{8} 5\tilde{\psi}_j(18,0)\,P^{\bullet}_{j18} = 4\,560\cdot 0{,}067 + 4\,720\cdot 0{,}067 + 4\,880\cdot 0{,}166 + 5\,040\cdot 0{,}250 + 5\,200\cdot 0{,}250 + 5\,360\cdot 0{,}116 + 5\,520\cdot 0{,}05 + 5\,680\cdot 0{,}034 = 5\,084\ \text{kg}.$$

The mathematical expectation of $\psi(18,0)$ is

$$M\psi(18,0) = \frac{1}{5}\,M\psi(18,0) = \frac{1}{5}\,5\,084 = 1\,017\ \text{kg}.$$

The variance of $5\psi(18,0)$ is given by

$$\partial 5\psi(18,0) = \sum_{j=1}^{8} [5\tilde{\psi}_j(18,0) - M5\psi(18,0)]^2 P^{\bullet}_{j18} = (4\,560 - 5\,084)^2 \times 0{,}067 + (4\,720 - 5\,084)^2\,0{,}067 + (4\,880 - 5\,084)^2\,0{,}166 + (5\,040 - 5\,084)^2\,0{,}250 + (5\,200 - 5\,084)^2\,0{,}250 + (5\,360 - 5\,084)^2 \times 0{,}116 + (5\,520 - 5\,084)^2\,0{,}05 + (5\,680 - 5\,084)^2\,0{,}034 = 68\,450\ \text{kg}^2.$$

The variance of $\psi(18,0)$ is

$$\partial\psi(18,0) = \frac{1}{5}\,\partial 5\psi(18,0) = \frac{1}{5}\,68\,450 = 13\,690\ \text{kg}^2.$$

11. $\lambda_i = 20$ mm

The statistical series of the random variable $5\psi(20,0)$ is shown in Table 18.

Table 18

$n_{j_{20}}$	29	30	31	32	33	34	35	36
J_{j20} . . .	4 480—4 640	4 640—4 800	4 800—4 960	4 960—5 120	5 120—5 280	5 280—5 460	5 460—5 600	5 600—5 760
N_{j20} . .	4	5	8	18	15	5	2	3
$P^{\bullet}_{j20}$ . .	0,067	0,083	0,133	0,300	0,250	0,084	0,033	0,050

Let us determine the expected value of $5\psi(20,0)$

$$M5\psi(20,0) = \sum_{j=1}^{8} 5\tilde{\psi}(20,0)\, P^{*}_{j20} = 4\,560 \cdot 0{,}067 + 4\,720 \times$$
$$\times 0{,}083 + 4\,880 \cdot 0{,}133 + 5\,040 \cdot 0{,}300 + 5\,200 \cdot 0{,}250 + 5\,360 \cdot 0{,}084 +$$
$$+ 5\,520 \cdot 0{,}033 + 5\,680 \cdot 0{,}050 = 5\,086 \text{ kg}.$$

The expected value of $\psi(20,0)$ is

$$M\psi(20,0) = \frac{1}{5} M5\psi(20,0) = \frac{1}{5}\ 5\ 086 = 1\ 017 \text{ kg}.$$

The variance of $5\psi(20,0)$ is given by

$$\partial 5\psi(20,0) = \sum_{j=1}^{8} [5\tilde{\psi}_j(20,0) - M5\psi(20,0)]^2 P^{*}_{j20} = (4\,560 - 5\,086)^2 \times$$
$$\times 0{,}067 + (4\,720 - 5\,086)^2\, 0{,}083 + (4\,880 - 5\,086)^2\, 0{,}133 +$$
$$+ (5\,040 - 5\,086)^2\, 0{,}300 + (5\,200 - 5\,086)^2\, 0{,}250 + (5\,360 - 5\,086)^2 \times$$
$$\times 0{,}084 + (5\,520 - 5\,086)^2\, 0{,}033 + (5\,680 - 5\,086)^2\, 0{,}050 =$$
$$= 67\,595 \text{ kg}^2.$$

The variance of $\psi(20,0)$ is

$$\partial\psi(20,0) = \frac{1}{5}\ \partial 5\psi(20,0) = \frac{1}{5}\ 67\ 595 = 13\ 500 \text{ kg}^2.$$

Thus we have obtained the expected values and the variances of the random variables $\psi(\lambda_i,0)$ for different values of the displacement λ_i. Now let us verify that the distribution of the random variable $5\psi(\lambda_i,0)$ is normal, by using the χ^2 test. For the random variable $5\psi(0,0)$ this test is not applicable, since there are really only three interval ranges and the number of degrees of freedom in this case is zero.

Results of the application of the χ^2 test for the other values of the displacement are shown in Table 19. In constructing the table several of the interval ranges were combined so that the number of occurrences in each interval would be at least three. Column 4 of this table contains the theoretical frequency values P_j computed according to the formula

$$P_{jl} = \frac{1}{2}\Phi\left(\frac{5\psi_{j+1}(\lambda_l,0) - M5\psi(\lambda_l,0)}{\sqrt{\partial 5\psi(\lambda_l,0)}}\right) -$$
$$- \frac{1}{2}\Phi\left(\frac{5\psi_j(\lambda_l,0) - M5\psi(\lambda_l,0)}{\sqrt{\partial 5\psi(\lambda_l,0)}}\right),$$

where $\Phi(t) = \sqrt{2/\pi} \int_0^t e^{-s^2/2} ds$ is the well known integral of Laplace.

Table 19

Table 19

λ_i, μм	I_{ji}	N_{ji}	P_{ji}	60 P_{ji}	$N_{ji} - 60\,P_{ji}$	$(N_{ji} - 60\,P_{ji})^2$	$\frac{(N_{ji}-60\,P_{ji})^2}{60\,P_{ji}}$
2	2 080–2 240	3	0,068	4	−1	1	0,25
	2 240–2 400	10	0,2235	14	−4	16	1,15
	2 400–2 560	28	0,3465	21	7	36	2,34
	2 560–2 720	15	0,2520	15	0	0	0
	2 720–3 010	4	0,0986	6	−2	4	0,67
		$\Sigma = 60$		$\Sigma = 60$			$\chi^2 = 4,41$
4	2 720–3 040	3	0,1045	6	−3	9	1,5
	3 040–3 200	19	0,2080	13	+6	36	2,77
	3 200–3 360	16	0,2950	18	−2	4	0,22
	3 360–3 520	12	0,2380	14	−2	4	0,28
	3 520–3 680	7	0,1140	7	0	0	0
	3 680–3 840	3	0,0320	2	1	1	0,5
		$\Sigma = 60$		$\Sigma = 60$			$\chi^2 = 5,27$
6	3 200–3 520	6	0,1000	6	0	0	0
	3 520–3 680	15	0,1975	12	3	9	0,75
	3 680–3 840	10	0,2780	17	−7	49	2,88
	3 840–4 000	20	0,2390	14	6	36	2,56
	4 000–4 160	5	0,1341	8	−3	9	1,13
	4 160–4 320	4	0,0439	3	1	1	0,33
		$\Sigma = 60$		$\Sigma = 60$			$\chi^2 = 6,75$
8	3 680–3 840	3	0,0375	2	1	1	0,5
	3 840–4 000	5	0,1180	7	−2	4	0,57
	4 000–4 160	15	0,2300	14	1	1	0,07
	4 160–4 320	22	0,2730	17	5	25	1,47
	4 320–4 480	6	0,2065	12	−6	36	3,0
	4 480–4 640	6	0,0950	6	0	0	0
	4 640–4 800	3	0,0270	2	1	1	0,5
		$\Sigma = 60$		$\Sigma = 60$			$\chi^2 = 5,59$
10	3 840–4 160	5	0,0630	4	1	1	0,25
	4 160–4 320	7	0,1620	9	−2	4	0,45
	4 320–4 480	18	0,2575	17	1	1	0,06
	4 480–4 640	15	0,2645	16	−1	1	0,06
	4 640–4 800	9	0,1675	10	−1	1	0,01
	4 800–4 960	6	0,0660	4	2	4	1
		$\Sigma = 60$		$\Sigma = 60$			$\chi^2 = 1,92$
12	4 000–4 160	3	0,0155	1	2	4	4,0
	4 160–4 480	6	0,1930	12	−6	36	3,0
	4 480–4 640	12	0,2285	14	−2	4	0,28
12	4 640–4 800	23	0,2365	14	9	81	5,78
	4 800–4 960	9	0,1850	11	−2	4	0,36
	4 960–5 120	4	0,0960	6	−2	4	0,66
	5 120–5 280	3	0,0330	2	1	1	0,50
		$\Sigma = 60$		$\Sigma = 60$			$\chi^2 = 14,60$
14	4 160–4 480	5	0,0815	5	0	0	0
	4 480–4 640	8	0,1505	9	−1	1	0,11
	4 640–4 800	17	0,2360	14	3	9	0,64
	4 800–4 960	15	0,2470	15	0	0	0
	4 960–5 120	8	0,1715	10	−2	4	0,40
	5 120–5 280	4	0,0795	5	−1	1	0,20
	5 280–5 440	3	0,0245	2	1	1	0,5
		$\Sigma = 60$		$\Sigma = 60$			$\chi^2 = 1,85$
16	4 480–4 640	4	0,0330	2	2	4	2,0
	4 640–4 800	5	0,0930	6	−1	1	0,16
	4 800–4 960	8	0,1765	11	−3	9	0,82
	4 960–5 120	18	0,2395	15	3	9	0,60
	5 120–5 260	15	0,2220	13	2	4	0,31
	5 280–5 460	5	0,1515	9	−4	16	1,78
	5 460–5 760	5	0,0705	4	1	1	0,25
		$\Sigma = 60$		$\Sigma = 60$			$\chi^2 = 5,95$
18	4 480–4 640	5	0,0275	2	3	9	4,5
	4 640–4 800	6	0,0885	5	1	1	0,2
	4 800–4 960	16	0,1820	12	4	16	1,33
	4 960–5 120	12	0,2505	15	−3	9	0,60
	5 120–5 280	11	0,2295	14	−3	9	0,64
	5 280–5 440	6	0,1415	8	−2	4	0,50
	5 440–5 600	4	0,0565	4	0	0	0
		$\Sigma = 60$		$\Sigma = 60$			$\chi^2 = 7,77$
20	4 480–4 640	4	0,0340	2	2	2	2
	4 640–4 800	4	0,0935	5	−1	1	0,2
	4 800–4 960	10	0,1775	11	−1	1	0,91
	4 960–5 120	15	0,2400	14	+1	1	0,71
	5 120–5 280	15	0,2180	13	+2	4	0,31
	5 280–5 440	7	0,1410	8	−1	1	0,12
	5 440–5 760	5	0,1180	7	−2	4	0,57
		$\Sigma = 60$		$\Sigma = 60$			$\chi^2 = 4,82$

Now, having the values of χ^2 and r for each λ_i, we can use Table 6 in Venttsel's book [9] to find the probability that the value of the variable which obeys the χ^2 law will exceed this value. The results obtained are summarized in Table 20.

Table 20

λ_i, мм	0	2	4	6	8	10	12	14	16	18	20
χ^2	—	4,41	5,27	7,65	5,59	1,91	14,60	1,85	5,95	7,77	1,82
r	0	2	3	3	4	3	4	4	4	4	4
P	—	0,11	0,14	0,06	0,24	0,60	0,005	0,76	0,20	0,10	0,39

Except for the distribution of the random variable $5\psi(12,0)$, all the other distributions coincide with the Gaussian distribution since the threshold for agreement is usually taken to be $P = 0.05$.

In general, distributions are considered not coincident if $P < 0.001$, so that the question concerning the agreement of the distribution of the random variable $5\psi(12,0)$ with the normal distribution is a doubtful one. The poor agreement for the distribution of $5\psi(12,0)$ is probably caused by experimental errors; this explanation seems to be reasonable since the point $\partial 5\psi(12,0)$ falls off the curve of the variance of the random function $5\psi(\lambda_i,0)$.

Figure III.4, a and b, shows the graphs of $M\psi(\lambda,0)$ and $\partial\psi(\lambda,0)$, constructed from the experimental data.

In conclusion, let us note that in view of the poor accuracy of the measurements, the graph of the variance of the random function $\psi(\lambda,0)$ cannot be considered to be completely reliable.

2. Experimental determination of the expected value of the function $f(\theta,\lambda^*)$ for the case of second loading

The goal of this series of experiments was to demonstrate the character of the variation of the load transmitted from the rail to the tie, due to a displacement of the rail which had previously been displaced in the opposite direction by λ^* mm. The experiments were carred out in the summer of 1958 at the track stub of the Tsaritsin station on the Moscow line, on the same experimental stand which was used for the determination of the statistical characteristics of the function $\psi(\lambda,0)$. The stand was preserved intact, so that the track parameters remained the same: P50 rails; wooden ties, 1840 per km; ballast of crushed stone of medium hardness; fastenings of type K.

In the course of the experiment five ties were displaced simultaneously. The following procedure was followed: the track was displaced by an amount λ_i^* by means of a hydraulic jack equipped with a manometer, with a calibration of 160 kg per division; the jack was then moved to the other end of the rail, and the force transmitted to the rail was adjusted after every 2 mm of displacement, the initial force being considered that which initiates a displacement. (This first reference point cannot be considered reliable.) A displacement was produced in each rail line in turn, after which the experimental set up was restored to its original state and the experiment was repeated. For each of the values $\lambda^* = 4,8,12,16$ and 20 mm, both rails were displaced five times. The experimental data are reproduced in Table 21, with the even numbered experiments corresponding to displacements of the westward rail, and the odd numbered ones to those of the eastward rail.

Table 21

	N	$f(\theta, \lambda^*)$										
		$\lambda^* = 0$	$\lambda^* = 2$	$\lambda^* = 4$	$\lambda^* = 6$	$\lambda^* = 8$	$\lambda^* = 10$	$\lambda^* = 12$	$\lambda^* = 14$	$\lambda^* = 16$	$\lambda^* = 18$	$\lambda^* = 20$
	1	16	21	26	34	37	42	44	46	50	49	50
	2	15	26	28	34	37	43	44	46	49	49	49
	3	16	25	28	35	38	43	46	47	50	50	50
	4	16	27	25	35	37	44	46	48	50	50	50
4	5	14	26	28	36	38	44	46	47	50	49	50
	6	16	26	29	35	38	44	47	48	50	51	50
	7	17	28	28	35	38	44	46	48	52	50	52
	8	17	26	27	35	38	45	46	48	50	51	52
	9	16	26	27	37	37	44	46	49	52	50	50
	10	16	27	28	38	38	44	47	48	52	49	52
$\sum_1^{10} q_j$		159	261	274	354	376	437	458	476	505	498	505
$5 M f_1(\theta, 4)$		2 550	4 180	4 380	5 670	6 030	7 000	7 350	7 640	8 100	8 000	8 100
	1	15	24	28	30	32	39	43	48	50	52	54
	2	16	24	29	31	33	39	43	49	50	51	58
	3	16	25	28	32	34	39	43	49	51	51	54
	4	17	24	30	32	34	40	44	50	51	53	55
8	5	17	25	28	32	33	39	45	50	51	53	55
	6	15	25	30	31	34	40	45	51	51	53	55
	7	16	25	30	33	34	40	45	50	50	54	54
	8	16	25	30	32	34	40	46	50	52	55	56
	9	16	26	30	32	35	41	47	50	52	53	56
	10	15	25	30	33	35	40	48	51	52	53	57
$\sum_1^{10} q_j$		159	248	295	318	338	397	449	498	510	528	549
$5 M f_1(\theta, 8)$		2 550	3 980	4 730	5 100	5 420	6 360	7 200	8 000	8 170	8 460	8 800
	1	16	27	33	38	38	39	42	49	55	59	61
	2	17	28	34	37	38	40	41	50	56	60	62
	3	17	29	34	37	39	40	41	48	57	59	61
	4	16	28	35	37	39	41	43	50	56	59	59
12	5	17	28	34	38	38	40	43	50	57	62	61
	6	18	27	32	38	37	39	42	50	56	62	59
	7	15	29	33	39	39	40	42	51	56	59	61
	8	15	28	33	40	40	41	43	52	55	60	65
	9	16	28	33	37	39	40	41	52	58	60	62
	10	17	26	34	36	39	40	42	50	56	61	61
$\sum_1^{10} q_j$		164	278	335	377	386	400	420	502	562	597	610
$5 M f_1(\theta, 12)$		2 620	4 450	5 370	6 040	6 180	6 400	6 720	8 010	9 000	9 560	9 760

N: experiment number.

The values of $f(\theta, \lambda^*)$ correspond to manometer readings in divisions.

Table 21 (continued)

λ^*, mm	N	$f(\theta, \lambda^*)$										
		$\theta = 0$	$\theta = 2$	$\theta = 4$	$\theta = 6$	$\theta = 8$	$\theta = 10$	$\theta = 12$	$\theta = 14$	$\theta = 16$	$\theta = 18$	$\theta = 20$
16	1	17	27	31	36	39	39	40	40	41	48	51
	2	16	26	33	36	39	39	40	40	43	50	52
	3	16	25	30	37	39	40	41	42	43	51	53
	4	16	26	32	37	40	41	42	43	44	50	51
	5	17	26	33	36	38	39	40	40	42	51	53
	6	15	27	34	37	41	41	41	40	42	50	51
	7	14	26	35	36	37	38	40	39	41	48	51
	8	16	27	32	38	40	41	42	41	42	49	52
	9	17	28	32	38	42	43	43	44	43	51	55
	10	17	28	33	38	42	43	41	45	45	52	54
$\sum_1^{10} q_j$		161	266	325	369	397	401	413	414	426	500	529
$5 M f_1(\theta, 16)$		2 580	4 260	5 200	5 900	6 350	6 470	6 620	6 630	6 820	8 000	8 469
20	1	15	33	36	37	40	39	42	40	40	40	41
	2	15	33	36	37	40	40	42	40	41	42	43
	3	16	34	37	38	40	40	43	41	42	43	43
	4	17	34	38	40	41	41	42	43	42	42	43
	5	17	33	38	39	41	42	42	42	43	44	41
	6	17	34	38	40	42	42	43	43	43	41	43
	7	17	34	39	41	41	43	43	43	43	44	45
	8	18	35	38	42	41	44	43	44	44	44	45
	9	18	36	40	43	42	44	44	45	45	44	41
	10	19	37	40	43	41	43	44	45	46	45	46
$\sum_1^{10} q_j$		169	343	380	400	409	418	428	426	429	429	437
$5 M f_1(\theta, 20)$		2 710	5 500	6 080	6 400	6 550	6 700	6 870	6 830	6 860	6 860	7 000

At the end of each series of experiments carried out with a fixed value of the prior displacement λ_i^*, the sums $\sum_1^{10} q_j$ of the measurements of the force transmitted to the rail by the hydraulic jack are obtained for all values of the displacement θ, and, on the basis of these sums, the values of the function $Mf_1(\theta, \lambda_i^*)$ are computed according to the formula

$$5Mf_1(0, \lambda_i^*) = \frac{m_0}{10} \sum_{j=1}^{10} q_j - 16 \sum_{j=1}^{10} q_j,$$

where m_o = 160 kg, ocrresponding to one dividision of the manometer scale.

Let us recall that in the absence of any load the manometer reads half a division.

Making use of the data in Table 21, one can construct the graph of the function $5Mf_1(\theta,\lambda_i^*)$. Such graphs are shown in Figure III.5.

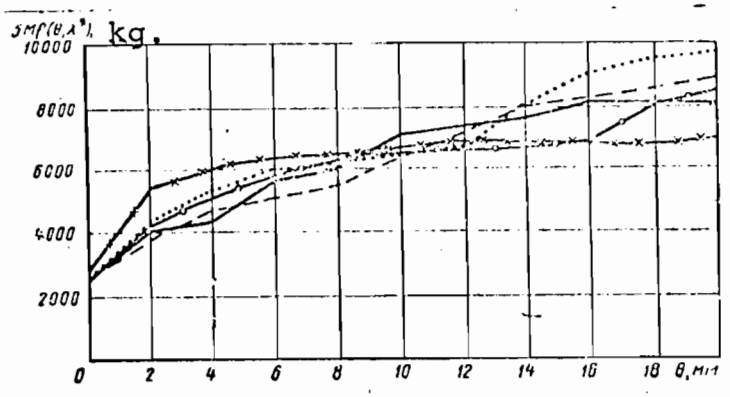

Fig. III.5. Graphs of the function $5Mf_1(\theta,\lambda_i^*)$: — $\lambda^* = 4$ mm; --- $\lambda^* = 8$ mm; ··· $\lambda^* = 12$ mm; -o- $\lambda^* = 16$ mm; - x - $\lambda^* = 20$ mm.

Finally, making use of the graphs of $M\psi(\lambda,0)$ and $Mf_1(\theta,\lambda_i^*)$, shown in Figures III.4a and III.5, let us construct the graph of $M\psi(\lambda, \lambda_i^*)$ for the case of the second loading according to the formula

$$M\psi(\lambda,\lambda_i^*) = M\psi(\lambda,0) - Mf_1(\theta,\lambda_i^*).$$

The graph of the function $\psi(\lambda,\lambda^*)$ for the second loading is shown in Figure III.6.

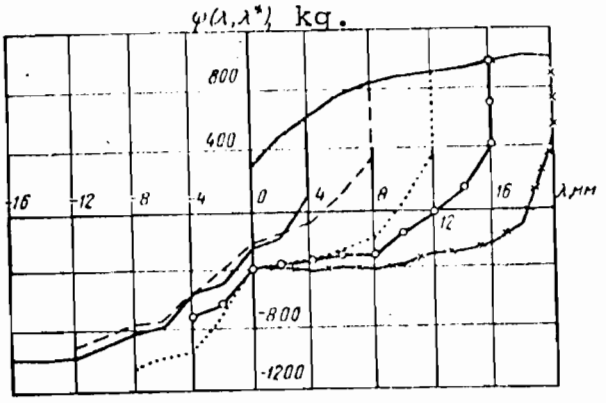

Fig. III.6. Graphs of the function $\psi(\lambda,\lambda^*)$: — $\lambda^* = 4$ mm; ---$\lambda^* = 8$ mm; ··· $\lambda^* = 12$ mm; -o- $\lambda^* = 16$ mm; -x- $\lambda^* = 20$ mm.

It is not without interest to note that for $\lambda = 0$ all the curves $\psi(\lambda,\lambda_i^*)$ have approximately equal values. Physically, this

corresponds to the fact that beginning with the point $\lambda = 0$, the tie displacements will take place in ballast which preserves its structure, independent of the prior displacements.

3. Determination of the linear resistance of continuous welded rails in station tracks with simple fastening assemblies

In April 1959 the author carried out experiments at the station Lublino on the Moscow line to determine the linear resistance in CWR track. These experiments were carried out on the operating first track of an unsymmetrical hump, on two strings of welded rails, 627 and 514 meters long. The ballast on this experimental section of the track consisted of very dirty sand, highly packed, and covering the ties above the upper bed level. Rails of type P50 were welded by the thermit process; there were 1600 ties per km. The track was anchored against creep by means of wedge-shaped anticreepers, installed in one direction at every tenth tie, and opposing the creep uphill. The force from each pair of anticreepers was transmitted to 5 ties connected together by spacers. Well worn tie plate fastening assemblies were used. The resistance was determined by two methods, neither one of which gave a high degree of accuracy with the measuring devices employed, so that the results of the experiments can be examined only as averaged results.

First method. Determination of the linear resistance in rail strings by making use of the second derivatives with respect to the temperature of the displacements of the ends of the rail strings. The method is based on the following considerations. Suppose a certain distribution of longitudinal rail forces in the track is produced by the first loading. (Fig. III.7). Let us assume that the linear resistance at every point of the track does not vary with the displacement.

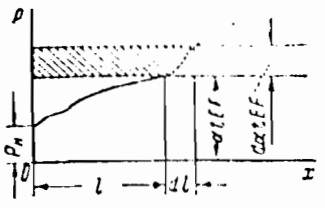

Fig. III.7. Longitudinal forces in the "transition" zone of the end of a rail string, assuming the linear resistance does not depend on the rail displacements.

At a distance ℓ, the length of the "transition" zone of the rail string, the longitudinal force is $P = \alpha t EF$.

Suppose now that the temperature of the string has been raised by an amount dt; then the longitudinal force in the middle portion of the rail string is increased by $\alpha EF dt$, and the end of the string is displaced by an additional amount, equal, to within a multiplying constant EF, to the shaded area in Figure III.7. Thus,

$$d\lambda_o = \frac{1}{EF} \ell \alpha EF \, dt = \alpha \ell dt,$$

or, dividing both sides of the equation by dt, we obtain

$$\frac{d\lambda_0}{dt} = \alpha l. \qquad \text{(III.1)}$$

Differentiating this equation, and taking note of the relation

$$\frac{dl}{dt} = \alpha EF \frac{1}{\rho(l)},$$

where $\rho(\ell)$ is the linear resistance at the point $x = \ell$, we obtain

$$\frac{d^2\lambda_0}{dt^2} = \alpha^2 EF \frac{1}{\rho(l)}. \qquad \text{(III.2)}$$

From this we obtain the expression for the linear resistance at the point $x = \ell$:

$$\rho(l) = \frac{\alpha^2 EF}{\frac{d^2\lambda_0}{dl^2}} \approx \frac{\alpha^2 EF \Delta l^2}{\Delta^2 \lambda}. \qquad \text{(III.3)}$$

Here $\Delta^2\lambda$ is the second difference of the displacement of the free end of the rail string, and Δt is the temperature increment.

According to (III.1), the quantity ℓ can be found from

$$l \approx \frac{1}{\alpha} \cdot \frac{\Delta\lambda_0}{\Delta t}.$$

Let us note that if $\rho(\ell) = \rho_o = \text{const}$, integration of (III.2) yields

$$\lambda_0 = \frac{\alpha^2 EF}{2\rho_0} t^2 + c_1 t + c_2. \qquad \text{(III.4)}$$

Differentiating this expression and making use of (III.1) gives

$$\frac{\alpha^2 EF}{\rho_o} + c_1 = \alpha \ell,$$

however, for $t = P_H/\alpha EF$ we have $\ell = 0$, from which it follows that

$$c_1 = - \frac{\alpha P_H}{\rho_o} .$$

Taking into account the condition $\lambda_o(P_H/\alpha EF) = 0$, we can determine

$$c_2 = \frac{P_H}{2\rho_o EF},$$

after which (III.4) takes the form

$$\lambda_0 = \frac{\alpha^2 EF}{2\rho_0}\left(t - \frac{P_H}{\alpha EF}\right)^2.$$

Solving this equation for t, we obtain

$$t = \frac{1}{\alpha}\sqrt{\frac{2}{EF}\lambda_0} + \frac{P_H}{\alpha EF},$$

i.e. we arrive at the previously obtained equation (II.32).

Let us note that our method is based on the assumption that the linear resistance at every point of the rail string does not depend on the displacement of the rail, so that the method is applicable only to investigations of track with well worn spike fastenings and without additional rail anchors, i.e. to the case when the linear resistance is determined by frictional forces between the rail and the tie plate.

During the experiment, the displacement of the ends of the rail strings was fixed by means of dial gauges (accurate to 0.003 cm) after every two degree rise in the rail temperature. The temperature was measured by means of a mercury thermometer graduated in $0.5^{\circ}C$.

Every day, before the experiments were carried out, the spikes in the experimental section were pulled up, the joint bars were disassembled, and wooden sledge hammers were used to eliminate the residual stresses in the rails; after this the spikes were driven in again, and the joint bars were bolted to the rails. At the time when the strings of rails were fastened, the positions of the ends were fixed, and were taken to be zero from then on.

The results of the measurements, and computations based on formula (III.3), are shown in Table 22.

Table 22

D	North end	t	Δt	λ_0, cm	$\Delta\lambda_0$, cm	$\Delta^2\lambda_0$, cm	$l = \frac{1}{\alpha}\cdot\frac{\Delta\lambda_0}{\Delta t}$	$\frac{\alpha^2 E F \Delta t^2}{\Delta^2 \lambda_0}$
15 June 1959 r.	R ($z = 514$ м)	14	2	0,027	0,040	0,030	1 700	2,5
		16	2	0,067	0,070	0,027	2 960	2,8
		18	2	0,137	0,097	0,027	4 100	2,8
		20	2	0,234	0,124	0,030	5 250	2,5
		22	2	0,358	0,154	0,030	6 530	2,5
		24	2	0,512	0,184	0,033	7 800	2,3
		26	2	0,596	0,217	—	—	—
		28	—	0,813	—	—	—	—
	L ($z = 627$ м)	14	2	0,027	0,040	0,033	1 700	2,3
		16	2	0,067	0,073	0,033	3 100	2,3
		18	2	0,140	0,106	0,030	4 500	2,5
		20	2	0,246	0,136	0,030	5 770	2,5
		22	2	0,382	0,166	0,027	7 040	2,8
		24	2	0,548	0,193	0,030	8 180	2,5
		26	2	0,741	0,223	—	—	—
		28	—	0,964	—	—	—	—
16 June 1959 r.	R ($z = 514$ м)	12	2	0,036	0,046	0,033	1 950	2,3
		14	2	0,082	0,079	0,033	3 350	2,3
		16	2	0,161	0,112	0,033	5 180	2,3
		18	2	0,273	0,145	0,030	6 150	2,5
		20	2	0,418	0,175	0,030	7 420	2,5
		22	2	0,593	0,205	0,027	8 700	2,8
		24	2	0,798	0,232	0,030	9 830	2,5
		26	2	1,030	0,262	—	—	—
		28	—	1,292	—	—	—	—
	L ($z = 627$ м)	12	2	0,030	0,043	0,030	1 820	2,5
		14	2	0,073	0,073	0,030	3 090	2,5
		16	2	0,146	0,103	0,033	4 370	2,3
		18	2	0,249	0,136	0,027	5 770	2,8
		20	2	0,385	0,163	0,027	7 090	2,8
		22	2	0,548	0,190	0,030	8 060	2,5
		24	2	0,738	0,220	0,027	9 310	2,8
		26	2	0,958	0,247	—	—	—
		28	—	1,205	—	—	—	—
17 June 1959 r.	R ($z = 514$ м)	14	2	0,027	0,043	0,033	1 800	2,3
		16	2	0,070	0,076	0,030	3 220	2,5
		18	2	0,146	0,106	0,027	4 510	2,8
		20	2	0,252	0,133	0,030	5 640	2,5
		22	2	0,385	0,163	0,030	6 920	2,5
		24	2	0,548	0,193	—	—	—
		26	—	0,741	—	—	—	—
	L ($z = 627$ м)	14	2	0,037	0,047	0,030	2 620	2,5
		16	2	0,084	0,077	0,030	3 260	2,5
		18	2	0,161	0,107	0,033	4 510	2,3
		20	2	0,268	0,140	0,030	5 930	2,5
		22	2	0,408	0,170	0,033	7 220	2,3
		24	2	0,578	0,203	—	—	—
		26	—	0,781	—	—	—	—

Remarks. R and L denote right and left rail strings.
The rail strings were fastened in such a way that the rail anchors did not impede their displacement.
D: date of experiment

Let us compute the mean value of the linear resistance of track with spike fastenings, for the case when the rail anchors do not impede the displacement of the rail strings:

$$\rho_a \frac{\sum_1^n \rho}{n} = \frac{10.2,3 + 18.2,5 + 8.2,8}{36} = 2,51 \text{ kg/cm}$$

The above method cannot be applied to determine the linear resistance in track which has rail anchors to prevent the displacement of the rails, since in this case the ties will be displaced, and this results in a variable linear resistance.

Second method. Determination of the linear resistance in rail strings by making use of the second derivatives of the displacement with respect to the length. The method is based on equation (III.25),

$$\frac{d^2\lambda}{dx^2} = \frac{1}{2EF\Delta x}\psi(\lambda, 0) = \frac{1}{EF}\rho(\lambda),$$

where $\rho(\lambda) = \Psi(\lambda,0)/2\Delta x$ is the linear resistance of the rail string during the first loading.

Substituting differences for derivatives in this equation, and solving it for $\rho(\lambda)$, we obtain

$$\rho(\lambda) = \frac{EF}{\Delta x^2}\,\Delta^2\lambda\,. \qquad \text{(III.5)}$$

Here $\Delta^2\lambda$ is the second difference of the displacement of the rail cross-section.

Since the accuracy in computing $\Delta^2\lambda$ is $m_1 = 0.003$ cm (accuracy of the gauge), the accuracy in computing the linear resistance is

$$m_2 = 0.003\ EF/\Delta\ x^2.$$

When the accuracy of computing the linear resistance is $m_2 < 0.2$ kg/cm, which yields a relative error of less than 10% the quantity Δx must satisfy the inequality

$$\Delta x > \sqrt{EF\frac{m_1}{m_2}} = \sqrt{2{,}1 \cdot 10^6 \frac{0{,}003}{0{,}2}} = 1410 \text{ см.}$$

In this case, the distance between the cross-sections at which the rail displacements were measured was taken to be $\Delta x = 1500$ cm. The arrangement of the dial gauges and the numbering of the stakes is shown in Figure III.8.

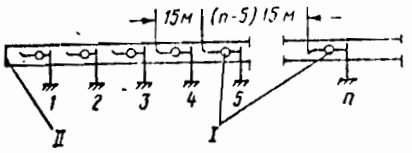

Fig. III.8. Arrangement of the dial gauges; I - dial gauges; II - end of the rail string; 1 - 5, n - number of the stake

As in the experimental set-up for the first method, some preparatory work was carried out before each experiment.

The position of the stakes was fixed at the time the rail string was installed in the track, and was taken to be zero subsequently.

The dial gauge reading were taken during the day, at the time when the temperature was at its maximum. The results of the measurements, and of the computations according to formula (III.5), are shown in table 23.

The mean value of the linear resistance is given by

$$\rho_a = \frac{\sum_1^n \rho}{n} = \frac{13.2{,}39+18.2{,}57+9.2{,}75}{40} = 2{,}55 \text{ kg/cm.}$$

Comparing the mean values of the linear resistance computed by the two different methods, we see that they are of the same order of magnitude.

Let us note that for both methods the linear resistance was averaged over x, utilizing the ergodic property of $\rho(x)$.

At the southern ends of the rail strings the rail anchors impede the displacement of the rails with respect to the ties; consequently, the ties are displaced in the ballast, and the linear resistance will depend not only on the location, but also on the displacement of the rail. Because of this, a realization of the random function $\rho(x)$ will not possess the ergodic property, and it is not possible to evaluate the statistical properties of the function from a small number of realizations. (To determine the statistical characteristics of an ergodic stationary random function, it is sufficient, in general, to have but one realization.)

If the linear resistance depends on the rail displacement (i.e. if $\rho(x)$ is not a stationary ergodic function), the mean value with respect to x (mean value "along" the process) does not coincide with the mean value over the ensemble (mean value "transverse" to the process). In this case the function

$$M\phi(\lambda,0) = \int_{-\infty}^{\infty} \phi(\lambda,0) f[\phi(\lambda,0)] d\phi(\lambda,0),$$

where $f[\phi(\lambda_i,0)]$ is the probability density of the random variable $\phi(\lambda_i,0)$, must be computed by averaging over the ensemble, i.e. on the basis of methods worked out in the first section of this chapter.

Table 23

D	T	North end	x, см	Δx, см	λ, см	$\Delta\lambda$, см	$\Delta^2\lambda$, см	$\varphi = EF\frac{\Delta\lambda}{\Delta x}$
10 June 1959 г.	12	R (z = 514 м)	0	1 500	0,738	0,226	0,040	2,39
			1 500	1 500	0,512	0,186	0,040	2,39
			3 000	1 500	0,326	0,146	0,043	2,57
			4 500	1 500	0,180	0,103	0,046	2,75
			6 000	1 500	0,077	0,057	0,040	2,39
			7 500	1 500	0,020	0,017	—	—
			9 000	—	0,003	—	—	—
	12	L (z = 627 м)	0	1 500	0,766	0,241	0,043	2,57
			1 500	1 500	0,525	0,198	0,043	2,57
			3 000	1 500	0,327	0,155	0,046	2,75
			4 500	1 500	0,172	0,109	0,046	2,75
			6 000	1 500	0,083	0,063	0,043	2,57
			7 500	1 500	0,020	0,020	—	—
			9 000	—	0	—	—	—
11 June 1959 г.	14	R (z = 514 м)	0	1 500	0,503	0,186	0,046	2,75
			1 500	1 500	0,317	0,140	0,043	2,57
			3 000	1 500	0,177	0,097	0,040	2,39
			4 500	1 500	0,080	0,057	0,040	2,39
			6 000	1 500	0,023	0,017	—	—
			7 500	—	0,006	—	—	—
	14	L (z = 627 м)	0	1 500	0,515	0,186	0,040	2,39
			1 500	1 500	0,329	0,146	0,043	2,57
			3 000	1 500	0,183	0,103	0,043	2,57
			4 500	1 500	0,080	0,060	0,043	2,57
			6 000	1 500	0,020	0,017	—	—
			7 500	—	0,003	—	—	—
12 June 1959 г.	13	R (z = 514 м)	0	1 500	0,512	0,186	0,040	2,39
			1 500	1 500	0,326	0,146	0,046	2,75
			3 000	1 500	0,180	0,100	0,040	2,39
			4 500	1 500	0,080	0,060	0,040	2,39
			6 000	1 500	0,020	0,020	—	—
			7 500	—	0	—	—	—
	13	L (z = 627 м)	0	1 500	0,548	0,198	0,043	2,57
			1 500	1 500	0,350	0,155	0,046	2,75
			3 000	1 500	0,195	0,109	0,046	2,75
			4 500	1 500	0,086	0,063	0,043	2,57
			6 000	1 500	0,023	0,020	—	—
			7 500	—	0,003	—	—	—

T- Temperature at which the rail strings were installed, °C.

D - date of the experiment

Table 23 (continued)

D	T	North end	x, см	Δx, см	λ, см	$\Delta\lambda$, см	$\Delta^2\lambda$, см	$p = EF\frac{\Delta^2\lambda}{\Delta x^2}$
13 June 1959 г.	14	R (z = 514 м)	0	1 500	0,509	0,189	0,046	2,75
			1 500	1 500	0,320	0,143	0,043	2,57
			3 000	1 500	0,177	0,100	0,040	2,39
			4 500	1 500	0,077	0,060	0,043	2,57
			6 000	1 500	0,017	0,017	—	—
			7 500	—	0	—	—	—
	14	L (z = 627 м)	0	1 500	0,518	0,186	0,040	2,39
			1 500	1 500	0,332	0,146	0,043	2,57
			3 000	1 500	0,186	0,103	0,043	2,57
			4 500	1 500	0,083	0,060	0,040	2,39
			6 000	1 500	0,023	0,020	—	—
			7 500	—	0,003	—	—	—
14 June 1959 г.	12	R (z = 514 м)	0	1 500	0,332	0,146	0,043	2,57
			1 500	1 500	0,186	0,103	0,040	2,39
			3 000	1 500	0,083	0,063	0,043	2,57
			4 500	1 500	0,020	0,020	—	—
			6 000	—	0	—	—	—
	12	L (z = 627 м)	0	1 500	0,329	0,149	0,046	2,75
			1 500	1 500	0,180	0,103	0,043	2,57
			3 000	1 500	0,077	0,060	0,043	2,75
			4 500	1 500	0,017	0,017	—	—
			6 000	—	0	—	—	—

CHAPTER IV

CONCERNING THE RELAXATION OF THE LONGITUDINAL FORCES IN CWR TRACK WHEN IT IS DEFORMED IN THE HORIZONTAL PLANE

1. Determination of the relaxation of the longitudinal forces in the course of analysing track stability by means of currently available methods

Investigation of the nature of the longitudinal forces in track which undergoes deformation is of considerable importance at the present time because the relaxation of the longitudinal forces is taken into account in one way or another in many currently used methods for analysing track stability.

At the same time, the problem of determining the nature of longitudinal track forces under deformations in the horizontal plane has not been solved completely, and somewhat arbitrary assumptions have to be made when the relaxation is taken into account.

In determining the stability of CWR track by means of the energy method, the relaxation of the longitudinal forces is accounted for in the following manner.

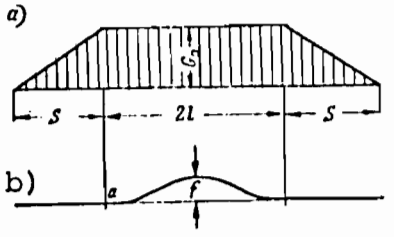

Fig. IV.1. Longitudinal force diagram (a) due to track deformation, (b) under the assumption of constant longitudinal forces in the deformed track section

Along the deformed length of the track (the shape of which might resemble the cosine curve, for example) the longitudinal relaxation forces are assumed to be constant, equal to G_o, and along adjacent sections they are assumed to decrease linearly, the slope being equal to the linear resistance to displacement of the track. (Fig. IV.1). In connection with this, the linear resistance is defined as the ratio of the force transmitted from rail to tie to the distance between the centerlines of adjacent ties, the resistance of the tie to rail displacement being assumed constant.

The displacement of the cross-section at the point α, where the straight and the deformed track sections join, caused by the variation of the longitudinal force on the straight track section, is determined according to Hooke's law by

$$\Delta l' = \frac{1}{EF}\int_0^S G dx = \frac{G_0^2}{2\rho_0 EF}, \qquad \text{(IV.1)}$$

where E = modulus of elasticity of rail steel, in kg/cm^2;

F = area of rail cross-section, in cm^2;

G = relaxation force, in kg;

S = length of the portion of straight track in which longitudinal displacements take place;

ρ_o = linear resistance to track displacements, in kg/cm.

At the same time, if we assume the middle portion of the deformed curve to be stationary in the horizontal direction, the displacement of the point α is the difference between the displacements $\Delta\ell$ and $\Delta\ell''$, where $\Delta\ell$ is the displacement produced by the elongation of the rail string due to its

deformation (half the difference in the lengths of the deformed and the undeformed centerlines of the rail string), and $\Delta\ell''$ is the displacement due to the action of the relaxation force G_o on the deformed track section.

In what follows, the magnitude of the change in the longitudinal force in the rail string, brought about by the deformation of the track, will be called the relaxation force.

Half of the difference between the lengths of the deformed and the initial centerlines is given by the expression

$$\Delta l = \int_{-l}^{0} \left(\sqrt{1 + (y')^2} - 1\right) dx. \qquad \text{(IV.2)}$$

Here ℓ is the length of half of the deformed wave.

Expanding the square root in a power series yields

$$\sqrt{1 + (y')^2} = 1 + \frac{1}{2}(y')^2 - \frac{1 \cdot 1}{2 \cdot 4}(y')^4 + \frac{1 \cdot 1 \cdot 3}{2 \cdot 4 \cdot 6}(y')^6 - \ldots$$

which converges for $(y')^2 \leq 1$.

Substituting this expression into (IV.2) and neglecting quantitites of degree greater than two results in

$$\Delta l = \int_{-l}^{0} \left[1 + \frac{1}{2}(y')^2 - 1\right] dx = \frac{1}{2}\int_{-l}^{0} (y')^2 dx. \qquad \text{(IV.3)}$$

If the deformation is described by *

$$y = \frac{f}{2}\left(1 + \cos\frac{\pi x}{\ell}\right), \qquad \text{(IV.4)}$$

---

* The exact shape of the deformed track has no importance in theoretical investigations of the question.

where f is the amplitude of the deformation curve, we obtain

$$\Delta l = \frac{\pi^2 f^2}{8l^2} \int_{-l}^{0} \sin^2 \frac{\pi x}{l} dx = \frac{\pi^2 f^2}{16l}. \qquad \text{(IV.5)}$$

The displacement, brought about by the appearance of the longitudinal relaxation force in the deformed part of the track, is given by

$$\Delta \ell'' \frac{G_o \ell}{EF}. \qquad \text{(IV.6)}$$

Thus, making use of (IV.4), (IV.5) and (IV.6), we arrive at

$$\frac{G_o^2}{2\rho_o EF} + \frac{G_o \ell}{EF} = \frac{\pi^2 f^2}{16\ell}, \qquad \text{(IV.7)}$$

where ρ_o is the linear resistance of the rail string.

Solving (IV.7) for G_o yields

$$G_0 = -\rho_0 l + \sqrt{\rho_0^2 l^2 + EF\rho_0 \frac{\pi^2 f^2}{16l}}. \qquad \text{(IV.8)}$$

Longitudinal relaxation forces computed from (IV.8) under the assumption that they are constant in the deformed section of the track, may differ considerably from those which actually exist. In this chapter an attempt is made to solve the problem of constructing longitudinal force diagrams, and track displacement diagrams, under the most general assumptions about the nature of the tie displacement dependence on the applied loads, and about the character of the track deformation

2. Derivation of the integro-differential equation for the longitudinal relaxation forces in CWR track when it is deformed in the horizontal plane

Let us examine an infinite string of welded rails in a deformed state, taking the originally straight centerline for the abcissa.

Under the deformation, an arbitrary point α is displaced to a new position. Let this new position be α', corresponding to a vertical displacement y and a horizontal displacement λ. If the rail string is cut at α', the left hand portion is discarded, and the right hand portion is straightened out without changing the longitudinal forces, the point α' will be displaced to a new position α".

The elongation ξ of a semi-infinite rail string is determined by the action of longitudinal tensile relaxation forces G^* and, according to Hooke's law, is given by

$$\xi = -\frac{1}{EF}\int_x^\infty G^* dS, \qquad \text{(IV.9)}$$

where dS is the element of length of the deformed rail string.

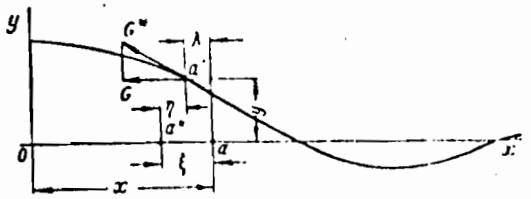

Fig. IV.2. Displacement of rail cross-section under transverse deformations of the rail string

Taking into account the relation

$$G^*(dx/dS) = G,$$

where G is the horizontal projection of the axial force, equation (IV.9) can be written in the form

$$\xi = -\frac{1}{EF}\int_x^\infty G[1 + (y')^2]dx,$$

or, neglecting the quantity $(y')^2$, which is small compared to one, we finally obtain

$$\xi = -\frac{1}{EF}\int_x^\infty G\,dx. \qquad \text{(IV.10)}$$

The difference between the length of the deformed semi-infinite rail string and its horizontal projection on the interval (α,∞) is given by

$$\eta = \int_x^\infty (\sqrt{1+(y')^2} - 1)\,dx \approx \frac{1}{2}\int_x^\infty (y')^2\,dx. \qquad \text{(IV.11)}$$

Clearly, the displacement λ of the rail string is the sum

$$\lambda = \xi + \eta,$$

which, in view of (IV.10) and (IV.11), can be expressed in the form

$$\lambda = -\int_x^\infty \left[\frac{G}{EF} - \frac{1}{2}(y')^2\right] dx. \qquad \text{(IV.12)}$$

Let us assume that the temperature induced longitudinal forces were constant along the length of the track before it was deformed. Under these conditions, the linear resistance to longitudinal displacements will be determined by the change in the magnitude of the relaxation forces G on an element of length dx, i.e.

$$\rho = dG/dx \qquad \text{(IV.13)}$$

On the other hand, it was indicated in Chapter II that in the absence of vertical loads and previous displacements, the linear resistance depends on the displacements of the rail cross-section i.e.

$$\rho = \phi(\lambda).$$

Combining this with (IV.12) and (IV.13), we obtain an integro-differential equation for the relaxation forces in a string of continuously welded rails:

$$\frac{dG}{dx} = \varphi\left\{-\int_{x}^{\infty}\left[\frac{G}{EF} - \frac{i}{2}(y')^2\right]dx\right\}. \qquad \text{(IV.14)}$$

The equation (IV.14) will be solved below for special cases of functions $\phi(\lambda)$ and $y(x)$.

3. Integration of the equation for the relaxation forces in a string of continuous welded rails for the case when the linear resistance to longitudinal displacement is determined by dry friction

For this case we assume the existence of dry friction forces between the rail and the underlying foundation.

In all the previous solutions, it was agreed that the linear resistance has the same sign as the increment in the longitudinal force. Neglect of the actual sign of the linear resistance is traditional, and all existing formulas which relate the longitudinal force to the linear resistance omit the negative sign; furthermore, the graphs of the force transmitted from rail to tie are called linear resistance graphs in the existing literature.

Let us note that if the derivative of the longitudinal force is related to the force transmitted from rail to tie through the linear resistance, the twofold neglect of the sign of the linear resistance does not alter the final result.

In order for an element Δx of a rail string to be displaced horizontally, it is necessary to apply a force ΔG in the direction of the expected displacement. Thus, in the presence of dry friction, the increment in the longitudinal force has the same sign as the longitudinal velocity of the rail cross-section.

Since the velocity has the same sign as the displacement, we can write

$$\frac{dG}{dx} = |\rho_o| \text{sign } \lambda, \qquad \text{(IV.15)}$$

where the signum function is determined by

$$\text{sign}\,\lambda = \frac{1}{\pi}\int_{-\infty}^{\infty} \frac{\sin \lambda t}{t}\, dt = \begin{cases} 1 \text{ for } & \lambda > 0 \\ 0 \text{ for } & \lambda \quad 0 \\ -1 \text{ for } & \lambda < 0 \end{cases}. \qquad \text{(IV.16)}$$

The constant linear resistance ρ_o is determined as the product of the coefficient of friction between the rail and the rail supporting foundation (including the friction due to the fastenings) and the compression force per unit length between the rail and the foundation.

Substituting for λ from (IV.12) into (IV.15), we obtain

$$\frac{dG}{dx} = |\rho_0| \,\text{sign} \int_x^{\infty} \left[-\frac{G}{EF} + \frac{1}{2}(y')^2 \right] dx. \qquad \text{(IV.17)}$$

Equation (IV.17) can be obtained directly from (IV.14) by setting

$$\phi(\lambda) = |\rho_o| \text{ sign } \lambda .$$

If the CWR track has the same elasticity in the longitudinal and transverse directions, the deformation which results when the track undergoes buckling in the horizontal plane is either symmetric or antisymmetric. Under these conditions, the longitudinal relaxation force diagram will always be symmetric, while the displaement diagram, obtained by integration of a symmetric one, will be antisymmetric. It follows from this, in particular, that $\lambda(0) = 0$ (the coordinate origin is at the center of symmetry).

The physical significance of this is that the midpoint is stationary. Consequently, investigation of a semi-infinite rail string is sufficient for computational purposes.

It follows from (IV.15) and (IV.16) that the function $\rho_0 = dG/dx$ has jump discontinuities at those points where $\lambda(x)$ changes sign. Thus, the longitudinal force diagram, being obtained by integrating the linear resistance $\rho(x)$, will have corners at these points.

If $\lambda(x)$ changes sign only at the origin, the longitudinal force diagram will have a corner only for $x = 0$.

The longitudinal force in the right half of the rail string can be represented in the form

$$G(x) = \begin{cases} |\rho_0|(z - x) & \text{for } x < z \\ 0 & \text{for } x > z. \end{cases} \qquad \text{(IV.18)}$$

The longitudinal force and longitudinal displacement diagrams for the case examined above are shown in Figure IV.3.

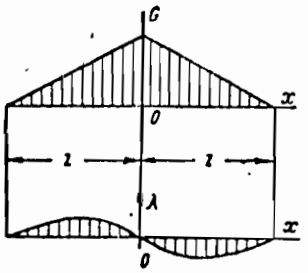

Fig. IV.3. Diagram of longitudinal forces due to track deformations when the rail-foundation interaction is frictional, and when $\lambda(x)$ has one change of sign

When the function $\lambda(x)$ has two changes of sign, at $x = 0$ and at $x = b$, the longitudinal relaxation force diagram will have two corners.

The longitudinal force in the right half of the rail string can be represented analytically in the form

$$G(x)=\begin{cases}|\rho_0|(z-2b+x) & \text{for } x<b\\ |\rho_0|(z-x) & \text{for } b<x<z.\\ 0 & \text{for } x>z\end{cases} \qquad \text{(IV.19)}$$

The longitudinal force and displacement diagrams for this case are shown in Figure IV.4.

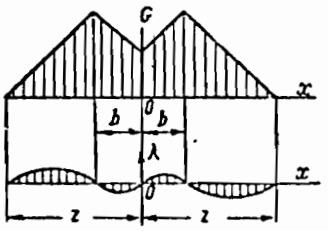

Fig. IV.4 Diagram of longitudinal forces due to track deformations when the rail-foundation interaction is frictional, and when $\lambda(x)$ has three changes of sign

The solution to (IV.17) can be found by a method of selection applied in the following way.

Let us suppose that the function $\lambda(x)$ has n changes of sign in the semi-infinite rail string, at $x = 0$, and at $x = b_i$ ($i = 1, 2, \ldots, n-1$). Then, it follows from (IV.12) that we will have n equations:

$$\left.\begin{aligned}\frac{1}{EF}\int_0^z G(x)\,dx &= -\frac{1}{2}\int_0^\infty (y')^2\,dx;\\ \frac{1}{EF}\int_{b_i}^z G(x)\,dx &= -\frac{1}{2}\int_{b_i}^\infty (y')^2\,dx.\end{aligned}\right\} \qquad \text{(IV.20)}$$

Here G(x) is determined by the formula for the case when the longitudinal force diagram has n corners, similar to (IV.19) for the case of three corners in $-\infty<x<\infty$.

Having determined z and b_i ($i = 1, 2, \ldots, n-1$) from (IV.20), we can construct the longitudinal force diagram. Let us note that for the right half (left half) of the rail string $b_k \geq 0$ ($b_k \leq 0$). If this condition is not satisfied, the number of

changes of sign of $\lambda(x)$ must be different from n.

Knowing the longitudinal force diagram, one can determine $\lambda(x)$ from (IV.12). If the function $\lambda(x)$ so obtained has the values b_i for its roots, the function G(x) must satisfy (IV.17), otherwise it becomes necessary to recompute, assuming that the function $\lambda(x)$ has m changes of sign, at $x = 0$, and at $x = b_i$ $(i = 1, 2, \ldots, m-1)$. Let us study two examples.

Example 1. Let us construct the longitudinal force diagram when the deformation is given by

$$y = \frac{f}{2}\left(1 + \cos\frac{\pi x}{\ell}\right),$$

with $f = 11.3$ cm, $\ell = 800$ cm, $\rho_o = 10$ kg/cm, $E = 21 \cdot 10^5$ kg/cm^2, $F = 128$ cm^2 (cross-sectional area of two P50 rails). The deformation curve is shown in Figure IV.5.

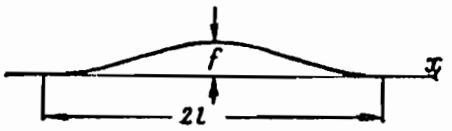

Fig. IV.5. Deformation of the rail line

Let us assume that the function $\lambda(x)$ changes sign twice in half of the rail string. The longitudinal force diagram has the form shown in Figure IV.6.

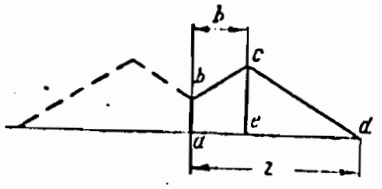

Fig. IV.6. Areas in the longitudinal force diagram, which determine the longitudinal deformations of the rails

Making use of (IV.20), we form the two equations

$$\begin{cases} \int\limits_0^z G(x)\,dx = \dfrac{EF}{2}\int\limits_0^l (y')^2\,dx; \\ \int\limits_b^z G(x)\,dx = \dfrac{EF}{2}\int\limits_b^l (y')^2\,dx. \end{cases}$$

The integral on the left hand side of the first equation is equal to the area abcd (see Fig. IV.6). Thus,

$$\int\limits_0^z G(x)\,dx = \frac{\rho_0 z^2}{2} - \rho_0 b^2 = 5z^2 - 10\,b^2.$$

Let us now compute the integral on the right hand side of the first equation:

$$\frac{EF}{2}\int\limits_0^l (y')^2\,dx = EF\,\frac{\pi^2 f^2}{8l^2}\int\limits_0^l \sin^2\frac{\pi x}{l}\,dx = EF\,\frac{\pi^2 f^2}{16\,l} =$$

$$= \frac{2{,}1\cdot 10^6\cdot 128\,\pi^2\cdot 11{,}3^2}{16\cdot 800} = 2{,}65\cdot 10^7.$$

The integral on the left hand side of the second equation is equal to the area ecd. Consequently,

$$\int\limits_b^z G(x)\,dx = \rho_0\,\frac{(z-b)^2}{2} = 5z^2 - 10zb + 5b^2.$$

Let us compute the integral on the right hand side of the second equation:

$$\frac{EF}{2}\int\limits_0^l (y')^2\,dx = EF\,\frac{\pi^2 f^2}{8l^2}\int\limits_b^l \sin^2\frac{\pi x}{l}\,dx =$$

$$= EF\,\frac{\pi^2 f^2}{8l^2}\left(\frac{l-b}{2} + \frac{l}{4\pi}\sin\frac{2\pi b}{l}\right) = \frac{2{,}1\cdot 10^6\cdot 128\,\pi^2\cdot 11{,}3^2}{8\cdot 800^2}\left(\frac{800\,b}{2} + \right.$$

$$\left. + \frac{800}{4\pi}\sin\frac{2\pi}{800}b\right) = 2{,}65\cdot 10^7 - 3{,}3\cdot 10^1\,b + 4{,}2\cdot 10^6\sin 7{,}85\cdot 10^{-3}b.$$

This yields two equations

$$\begin{cases} 5z^2 - 10\,b^2 - 2{,}65\cdot 10^7 = 0; \\ 5z^2 + 5b^2 - 2{,}65\cdot 10^7 + 3{,}3\cdot 10^1\,b - 4{,}2\cdot 10^6\sin 7{,}8\cdot 10^{-3}\,b - 10zb = 0. \end{cases}$$

Solving these, we obtain

$$z = 2300 \text{ cm}$$

$$b = 300 \text{ cm}.$$

Having the values of z and b, we can construct the longitudinal force diagram (Fig. IV.7).

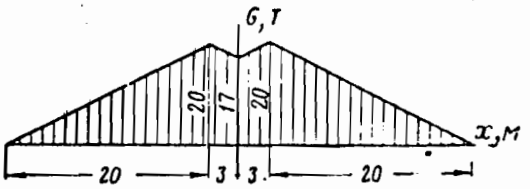

Fig. IV.7. Longitudinal force diagram for the first example

Except for the multiplying constant (1/EF), the displacement of the track cross-section produced by the appearance of the force G(x) is, according to (IV.10), equal to the area under the longitudinal force diagram to the right of point x (Fix. IV.8).

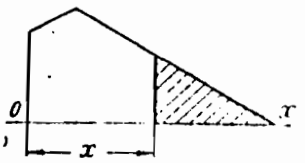

Fig. IV.8. Area in the longitudinal force diagram which determines the longitudinal deformation at the point x

The difference between the lengths of the deformed rail string on $0<x<\ell$ and its horizontal projection can be found from (IV.11):

$$\eta = \int_0^\infty (y')^2\,dx = \frac{\pi^2 f^2}{8l^2}\int_x^l \sin^2\frac{\pi x}{l}\,dx = \frac{\pi^2 f^2}{8l^2}\left(\frac{l-x}{2} + \frac{l}{4\pi}\sin\frac{2\pi x}{l}\right)$$

$$= \frac{\pi^2 \cdot 11{,}3^2}{8\cdot 800^2}\left(\frac{800-x}{2} + \frac{800}{4\pi}\sin\frac{2\pi x}{800}\right)$$

$$= 0{,}098 - 1{,}22\cdot 10^{-4}\,x + 0{,}0156\sin 7{,}8\cdot 10^{-3}\,x.$$

The η diagram is shown in Figure IV.9.

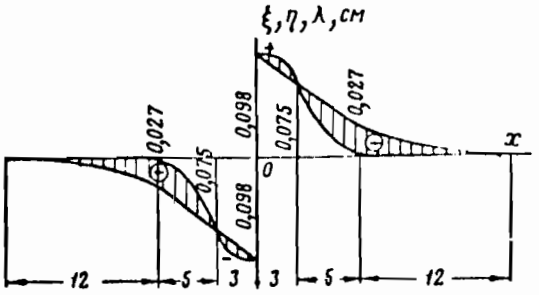

Fig. IV.9. Longitudinal displacement diagram for Example 1

The difference between the ξ and the η curves, shown shaded in Figure IV.9, represents the longitudinal displacements of the track cross-sections. The resulting λ(x) curve has zeros only at 0 and at 300. Consequantly, the assumption of two sign changes in λ(x) is correct.

It is evident from Figure IV.9 that the displacements caused by the relaxation of the forces are directed away from the center of the deformed curve in the section $|x| < 300$ cm, and towards the center in $|x| > 300$ cm.

Example 2. Let us construct the longitudinal force diagram in the deformed track on the basis of equation (IV.4), assuming $f = 3$ cm, $\ell = 800$ cm, $\rho_0 = 20$ kg/cm, $E = 2 \cdot 10^6$ kg/cm^2, $F = 128$ cm^2 (cross-sectional area of two rails).

The deformation curve is shown in Figure IV.5. Let us assume that the function λ(x) changes sign only once, λ(0) = 0.

From (IV.20) it follows that

$$\int_0^z G(x)\,dx = \frac{EF}{2}\int_0^{\ell} (y')^2 dx,$$

The integral on the right hand side is equal to half the area of the triangle in Figure IV.3. Consequently,

$$\int_0^z G(x)\,dx = \frac{p_0 z^2}{2} = \frac{20 z^2}{2} = 10 z^2.$$

Let us compute the integral on the right hand side:

$$\frac{1}{2} EF \int_0^l (y')^2\,dx = EF\,\frac{\pi^2 f^2}{4l^2} \int_0^l \sin^2 \frac{\pi x}{l}\,dx = EF\,\frac{\pi^2 f^2}{16 l} =$$

$$= \frac{2{,}1 \cdot 10^6 \cdot 128\,\pi^2 \cdot 3^2}{16 \cdot 800} = 1{,}85 \cdot 10^6.$$

We obtain the following equation:

$$10\ z^2 = 1.85.10^6.$$

Thus, the abscissa of the end point of the longitudinal force diagram is given by

$$z = \sqrt{18.5} \cdot 10^2 = 430 \text{ cm}.$$

Having obtained the value of z, we construct the longitudinal force diagram (Fig. IV.10).

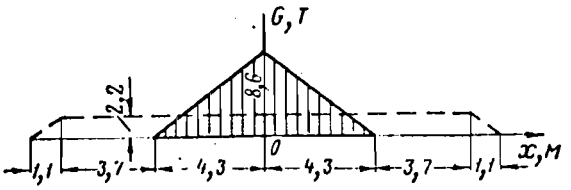

Fig .IV.10. Longitudinal force diagram for Example 2. The dotted curve shows the force computed according to the presently used method

Except for a multiplying constant, the displacement of the track cross-section at x, produced by the appearance of a longitudinal force according to (IV.10), is equal to the area under the longitudinal force diagram to the right of point x.

The difference between the length of the deformed rail string on (x,∞) and its horizontal projection can be found from (IV.11):

$$\tau_1 = \int_x^{\infty} (y')^2\, dx = \frac{\pi^2 f^2}{8l^2}\left(\frac{l-x}{2} + \frac{l}{4\pi}\sin\frac{2\pi x}{l}\right) =$$

$$= \frac{3^2\pi^2}{8\cdot 800^2}\left(\frac{800-x}{2} + \frac{800}{4\pi}\sin\frac{2\pi x}{800}\right) =$$

$$= 6{,}88\cdot 10^{-3} - 8{,}60\cdot 10^{-6}\, x + 1{,}09\cdot 10^{-3}\sin 7{,}8\cdot 10^{-3}\, x.$$

Figure IV.11 shows the ξ and η curves, and their difference λ.

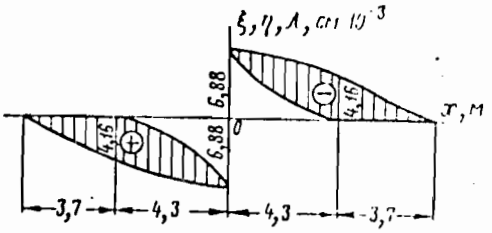

Fig. IV.11. Longitudinal displacement diagram for Example 2

It is clear from Figure IV.11 that the only zero of the function $\lambda(x)$ is the one at zero. Consequently, our assumption that $\lambda(x)$ changes sign only once is correct.

For comparison, let us compute the longitudinal relaxation force by means of the presently employed method. According to formula (IV.8)

$$G_0 = -p_0 l + \sqrt{p_0^2 l^2 + EFp_0\frac{\pi^2 f^2}{8l}} =$$

$$= -20\cdot 800 + \sqrt{20^2\cdot 800^2 + 2{,}1\cdot 10^6\cdot 128\cdot 20\frac{\pi^2\cdot 3^2}{8\cdot 800}} = 2\,200\,\text{kg}.$$

Figure IV.10 shows the results obtained from the presently used method and the method proposed here.

The solutions of each problem is unique. The hypothesis n = 1 will lead to a contradiction in the first example, since the number of roots is two. In example two, an attempt to assume two sign changes will lead to a contradiction, since the roots of $\lambda(x)$ in the right half of the rail string will turn

out to be negative.

4. Integration of the relaxation force equation for CWR track for the case when the linear resistance to longitudinal displacement is a linear function of the displacement

Frequently, the function $\phi(\lambda)$ can be represented as a linear function of the displacement,

$$\phi(\lambda) = k_1\lambda.$$

In this case (IV.14), after differentiation, takes the form

$$\frac{d^2G}{dx^2} - \frac{k_1}{EF}G = -\frac{k_1}{2}(y')^2. \qquad \text{(IV.21)}$$

It is not difficult to solve (IV.21) for an arbitrary function y'(x). In chapter VI it will be shown that the eigengunctions of the stability problem for CWR track can be expressed in terms of hyperbolic and trigonometric functions. When the buckled surface is symmetrical, the slope y' of the deformed rail string can be represented in the form

$$y' = Ae^{-\alpha x}\sin\beta x. \qquad \text{(IV.22)}$$

In this case one should look for a particular solution of (IV.21) in the form

$$G = B_1e^{-2\alpha x}\sin^2\beta x + B_2e^{-2\alpha x}\sin 2\beta x + B_3e^{-2\alpha x}\cos 2\beta x.$$

Substituting this expression in (IV.21) and equating the coefficients of like functions on both sides of the equation, one can determine the constant B_i:

$$B_1 = A^2 \frac{k_1}{2(\gamma^2 - 4\alpha^2)} = A^2\omega_1;$$

$$B_2 = -A^2 \frac{2\alpha\beta\, k_1}{4n^2 + m^2} = A^2\omega_2;$$

$$B_3 = \frac{nB_1 + mB_2}{2n} = A^2\omega_3,$$

where $n = 4\alpha\beta$, $m = 4\beta^2 - 4\alpha^2 + \gamma^2$, and $\gamma = \sqrt{k_1/EF}$.

It should be noted that the constants ω_i depend only on the track parameters and not on the shape of the deformation.

The general solution of (IV.21) with y' specified by (IV.22) can be written in the form

$$G = B_4 e^{-\gamma x} + B_5 e^{\gamma x} + B_1 e^{-2\alpha x} \sin^2 \beta x + B_2 e^{-2\alpha x} \sin 2\beta x + B_3 e^{-2\alpha x} \cos 2\beta x. \qquad \text{(IV.23)}$$

Making use of the condition $G(\infty) = 0$, we get $B_5 = 0$.

Now let us determine $\lambda(x)$. Substituting (IV.22) and (IV.23) into (IV.12), we obtain

$$\lambda = \left(\frac{B_1}{EF} - \frac{A^2}{2}\right)\int_x^\infty e^{-2\alpha x} \sin^2 \beta x\, dx + \frac{\beta_2}{EF}\int_x^\infty e^{-2\alpha x} \sin 2\beta x\, dx + \\ + \frac{B_3}{EF}\int_0^\infty e^{-2\alpha x} \cos 2\beta x\, dx + \frac{\beta_4}{EF}\int_x^\infty e^{-\gamma x}\, dx. \qquad \text{(IV.24)}$$

The condition $\lambda(0) = 0$ can be used to evaluate B_4:

$$B_4 = -\frac{\left(\frac{A^2EF}{2} - B_1\right)\int_0^\infty e^{-2\alpha x} \sin^2 \beta x\, dx - B_2\int_0^\infty e^{-2\alpha x} \sin 2\beta x\, dx}{\int_0^\infty e^{-\gamma x}\, dx} - \\ - \frac{B_3\int_0^\infty e^{-2\alpha x} \cos 2\beta x\, dx}{\int_0^\infty e^{-\gamma x}\, dx},$$

or, after performing the integration,

$$B_4 = A^2\omega_4 = \frac{\beta}{2(\alpha^2+\gamma^2)}\left[\left(\frac{A^2EF}{2}-B_1\right)\frac{\gamma^2}{2\alpha}-B_2\gamma-B_3\alpha\right],$$

where ω_4 is a constant which depends only on the track parameters.

Substituting the values of the coefficients B_i into (IV.23), we obtain the expression for the relaxation forces in CWR track:

$$G = A^2(\omega_4 e^{-\gamma x} + \omega_1 e^{-2\alpha x}\sin^2\beta x + \omega_2 e^{-2\alpha x}\sin 2\beta x + \omega_3 e^{-2\alpha x}\cos 2\beta x). \qquad \text{(IV.25)}$$

It follows from (IV.25) that for small track deformations the longitudinal relaxation force is a quantity of second order with respect to the maximum value of the slope of the deformation curve.

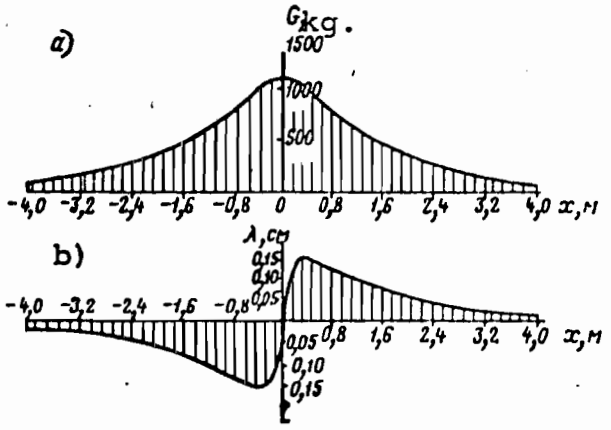

Fig. IV.12. (a) Force and (b) displacement diagrams for the example used to illustrate the case of elastic rail-foundation interaction

Figure IV.12 shows the longitudinal force and displacement diagrams resulting from the action of a concentrated force

$k = 48$ kg/cm^2, $E = 2.1\cdot10^6$ kg/cm^2, $F = 64$ cm^2,

$\alpha = \beta = 0.01$ cm^{-1}, $\gamma = 6.10^{-4}$ cm^{-1}, $A = 0.05$.

In conclusion, we note that the presently employed formulas for the determining the relaxation forces, according to which

the longitudinal forces in the deformed section are constant, can give results which differ from the actual results not only quantitatively, but qualitatively. This was particularly evident in example two. The proposed method allows one to determine the track forces and displacements more accurately.

CHAPTER V
CONCERNING LONGITUDINAL FORCES IN CWR TRACK IN THE ZONE OF THE MOVING TRAIN

In studying rail creep produced by forces which arise in CWR track, it is important to take into account a special property which influences the creep forces, as well as the displacements induced by these forces. This special property is the continuity of the longitudinal rail deformations in CWR track.

For conventional jointed track, the theory of rail creep was developed by V. G. Al'brecht [1].

An attempt is made below to understand the character of the longitudinal forces in CWR track in the zone of the moving train, under the most general assumptions concerning the nature of the resistance of the ties to displacement along the track, and of the form of the rail deformation due to vertical forces.

1. Derivation of the equation for the longitudinal displacements of CWR track in the zone of the moving train

We will assume that a string of welded rails can be treated as an infinite beam in bending under the action of vertical forces. Let us examine it in a coordinate system x, y, moving with the train with speed v cm/sec. Let us take the undeformed rail axis for the abscissa (Fig. V.1).

Due to the motion of the train, a point α on the neutral axis is displaced to position α'. If the part of the rail string to the right of α' were straightened out while maintaining the

axial forces, the point α' will be displaced to α".

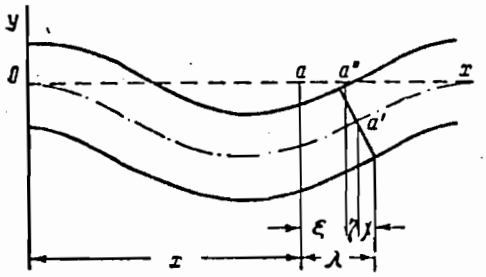

Fig. V.1. Displacement of the rail base under the action of longitudinal and transverse loads

Clearly, the displacement ξ produced by the longitudinal forces can be obtained from Hooke's law:

$$\xi = \frac{-1}{EF}\int_{x}^{\infty} P\,dx, \qquad \text{(V.1)}$$

where P is the axial force in the track (tension).

The difference between the length of a curve and its horizontal projection is given by (IV.11). Finally, the displacement of the rail base χ, due to a rotation of the cross-section through an angle y', can be found from

$$\chi = by', \qquad \text{(V.2)}$$

where b is the distance between the rail neutral axis and the rail base.

In the first approximation this distance can be taken to be half the rail height. Consequently, the displacement of the rail base is given by

$$\lambda = \xi + \eta + \chi.$$

Substituting for the quantities on the right hand side from (V.1), (IV.11), and (V.2) yields

$$\lambda = -\int_{x}^{\infty} \frac{P}{EF}\,dx + \frac{1}{2}\int_{x}^{\infty} (y')^2\,dx + by'. \qquad \text{(V.3)}$$

In the solution of problems connected with rail creep, we will take the tensile forces to be positive. Let us now move on to the examination of the forces transmitted to the rail.

The longitudinal force increment ΔP in a section of length Δx is given by the sum of the force ΔG, which acts at the rail-tie interface, the tensile force ΔR of the anticreep system over the length Δx, and also the inertia force ΔI, acting at the center of gravity of the element Δx, minus the incremental creep force ΔT, produced by the train deceleration and transmitted to the rail head.

The force ΔG is a function of the vertical and the horizontal displacements of the rail cross-sections, and of their derivatives. Since the time derivative of the quantity λ is, to within a multiplying constant v, equal to the derivative of λ' with respect to the abscissa x of the moving coordinate system, we can write

$$\Delta G = \Delta G(\lambda,\lambda',\lambda'',\ldots,y,y',y'',\ldots), \tag{V.4}$$

or, taking into account (V.3),

$$\Delta P = \Delta G(\xi,\xi',\xi'',\ldots,y,y',y'',\ldots) - \Delta T + \Delta R + \Delta I.$$

Dividing this equation by Δx, we obtain

$$\frac{\Delta P}{\Delta X} = \phi(\xi,\xi',\xi'',\ldots,y,y',y'',\ldots) - \tau + r + i, \tag{V.5}$$

where

$$\frac{\Delta T}{\Delta x} = \tau; \quad \frac{\Delta G}{\Delta x} = \phi(\xi,\xi',\xi'',\ldots,y,y',y'',\ldots);$$

$$\frac{\Delta R}{\Delta x} = r; \quad \frac{\Delta I}{\Delta x} = i.$$

In view of the fact that the track is divided into intervals of equal length Δx, which is considerably smaller than the length of the train, the ratio of the increments can be approximated by the derivative. Thus,

$$\frac{dP}{dx} \approx \frac{\Delta P}{\Delta x} = \phi_1(\xi,\xi',\xi'',\ldots,y,y'y'',\ldots) - \tau + r + i. \qquad (V.6)$$

Let us determine the inertial forces i per unit length, which arise due to track displacement in the direction of creep. When the track is subjected to a longitudinal force P and a vertical load, the cross-section at x is displaced by the amount $\xi + \eta$, so that the inertial force I is determined by the following expression:

$$\Delta I = \frac{1}{2}\, m\Delta x \frac{d^2(\xi + \eta)}{dt^2},$$

where m is the mass per unit length of track in kg sec^2/cm^2. Since $t = x/v$, where v is the train speed, we obtain

$$i = \frac{1}{2}\, mv^2\, \frac{d^2(\xi + \eta)}{dx^2} \qquad (V.7)$$

Differentiating (V.1) and IV.11) twice, and substituting the results in (V.7), we finally obtain

$$i = \frac{1}{2}\, mv^2\left(\frac{1}{EF} \cdot \frac{dP}{dx} + y'y''\right).$$

When the deformations are small, the quantity $d^2\eta/dx^2 = y'y''$ is small to second order and can be neglected, so that

$$i = \frac{mv^2}{2EF} \cdot \frac{dP}{dx}. \qquad (V.8)$$

Substituting (V.8) into (V.6), we obtain

$$\frac{dP}{dx} = \alpha_o\, [\phi_1(\xi,\xi',\xi'',\ldots,y,y',y'',\ldots) - \tau + r].$$

Here

$$\alpha_o = \frac{2EF}{2EF - mv^2}.$$

For speeds less than 200 km/hr, the coefficient α_o is, for all practical purposes, equal to one, so that we can write

$$\frac{dP}{dx} \approx \phi_1(\xi,\xi',\xi'',\ldots,y,y',y'',\ldots) - \tau + r.$$

Differentiating (V.1) twice, and substituting (V.9) in the right hand side, yields

$$\frac{d^2\xi}{dx^2} = \frac{1}{EF}\,\phi_1(\xi,\xi',\xi'',\ldots,y,y'y'',\ldots) - \frac{\tau - r}{EF}\,. \qquad (V.10)$$

The solution of (V.10) can be considerably simplified by means of a method which will now be described.

Suppose, for example, that the train consists of identical cars of length δx. Then, the longitudinal force increment in a section of rail of length δx will be given, according to (V.9), by the expression

$$\delta P = \int_0^{\delta x} \phi_1(\xi,\xi',\xi'',\ldots,y,y',y'',\ldots)dx - \delta T + r\delta x, \qquad (V.11)$$

where $\delta T = \tau\delta x$ is the force on the rail head produced by the friction in the journal boxes and brake shoes of one car.

In contrast to the rapidly oscillating functions y, y', y'', ..., the functions $\xi,\xi',\xi'',\ldots$ vary slowly, so that their values can be considered constant on an interval of length δx. Thus, the integral in (V.11) becomes a function of the parameters $\xi,\xi',\xi'',\ldots$. Dividing (V.11) by δx, we obtain

$$\frac{\delta P}{\delta x} = \frac{1}{\delta x}\int_0^{\delta x} \varphi_1(\xi,\xi',\xi'',\ldots,y,y',y'',\ldots)\,dx - \frac{\delta\tau}{\delta x} + r = \\ = \frac{1}{\delta x}\psi_1(\xi,\xi',\xi'',\ldots) - \frac{\delta T}{\delta x} + r. \qquad (V.12)$$

Since the length of the train is considerably greater than the length of a single car, we can set

$$\frac{dP}{dx} \approx \frac{\delta P}{\delta x} = \frac{1}{\delta x}\,\psi_1(\xi,\xi',\xi'',\ldots) - \tau + r. \qquad (V.13)$$

Here

$$\tau = \frac{\Delta T}{\Delta x} = \frac{\delta T}{\delta x} .$$

Now, making use of (V.1) and (V.13), we obtain

$$\frac{d^2\xi}{dx^2} = \frac{1}{EF\delta x}\psi_1(\xi, \xi', \xi'', \ldots) - \frac{\tau - \ddot{r}}{EF} . \qquad (V.14)$$

We will call equation (V.14) the longitudinal displacement equation for CWR track in the zone of the moving train. It is very much simpler than equation (V.10) since it does not contain the functions y, y', y",... .

2. Integration of the longitudinal displacement equation for CWR track in the zone of the moving train when the interaction between the rail and the rail supporting foundation is purely frictional.

For the case when the force between the rail and the rail supporting foundation is that of dry friction, the function ϕ_1 has the form

$$\phi_1(\xi,\xi',\xi'',\ldots,y,y',y'',\ldots) = - k_f g \operatorname{sign} \frac{d\lambda}{dt} . \qquad (V.15)$$

Here k_f is the coefficient of friction between the rail and the foundation, including the friction in the intermediate fasteners; g is the distributed vertical load due to the train; and $d\lambda/dt$ is the time derivative of the rail base displacement. The function $\operatorname{sign} \dot{\lambda}$ is defined by

$$\operatorname{sign}\dot{\lambda} = \frac{1}{\pi}\int_{-\infty}^{\infty} \frac{\sin \dot{\lambda} t}{t} dt = \begin{cases} 1 \text{ при } \dot{\lambda} > 0 \\ 0 \text{ при } \dot{\lambda} = 0 . \\ -1 \text{ при } \dot{\lambda} < 0 \end{cases}$$

The formula (V.15) states that the frictional force which arises at the interface between the rail base and the foundation is proportional to the vertical load, and that its direction depends on the direction of the displacement of the rail base.

The minus sign shows that its direction is opposite to that of the rail base displacement.

Let us compute the derivative $d\lambda/dt$. Since $dx/dt = v$, we obtain

$$\dot{\lambda} = v\frac{d\lambda}{dx} = v\left(\frac{P}{EF} - \frac{1}{2}(y')^2 + by''\right),$$

from (V.3); or, neglecting the second order quantity $(y')^2$, and approximating b by means of h/2, where h is the rail height, we are led to

$$\dot{\lambda} = v\left(\frac{P}{EF} + \frac{h}{2}y''\right). \qquad (V.16)$$

Let us make some transformations:

$$\operatorname{sign}\dot{\lambda} = \operatorname{sign} v\left(\frac{P}{EF} + \frac{h}{2}y''\right) = \operatorname{sign}\left(\frac{P}{EF} - \frac{h}{2}\cdot\frac{M}{EI}\right)$$
$$= \operatorname{sign}\left(\frac{2EI}{hEF}P - M\right) = \operatorname{sign}\left(\frac{2i_0^2}{h}P - M\right),$$

where i_o = radius of gyration of the rail for bending in the vertical plane;

M = rail bending moment;

I = moment of inertia of the rail for bending in the vertical plane.

The ratio i_o/h is approximately the same for all rails, $i_o/h = 0.37$. Thus, we obtain

$$\operatorname{sign}\dot{\lambda} = -\operatorname{sign}(M - 0.27\,hP). \qquad (V.17)$$

Let us construct the function ψ:

$$\psi(\xi, \xi', \xi'', \ldots) = \frac{k}{\delta x}\xi\int_0^{\delta x} g(x)\operatorname{sign}(M - 0{,}27\,hP)\,dx. \qquad (V.18)$$

For a particular car, the function ψ can be computed for various values for the force P.

The general technique for computing the integral in (V.18) is illustrated in Figure V.2.

Having determined the values of $\psi_1(\xi,\xi',\xi'',\ldots) = \psi_2(P)$ for different values of the longitudinal force P, one can construct the graph of $\psi_2(P)$. The general form of such a graph is shown in Figure V.3.

For our case, the differential equation (V.9) for the longitudinal forces has the form

$$\frac{dP}{dx} = \psi_2(P) - \tau + r, \qquad (V.19)$$

and can be integrated by quadratures:

$$x = \int \frac{dP}{\psi_2(P) - \tau + r} + c, \qquad (V.20)$$

where the constant c is determined by the boundary conditions.

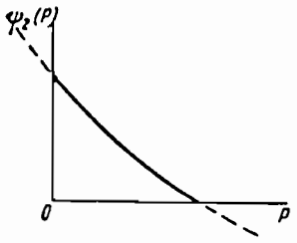

Fig. V.3. Graph of creep force due to one car vs. the mean value over its length of the longitudinal force

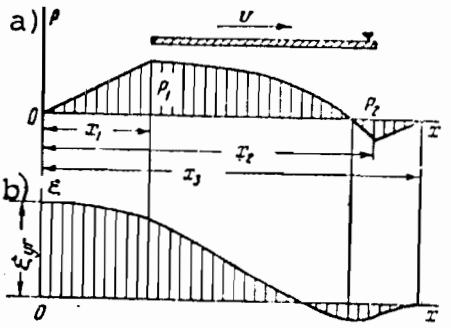

Fig. V.4 Graphs of longitudinal forces (a) and displacements (b) in the moving train zone, with frictional interaction between the rail and the rail supporting foundation

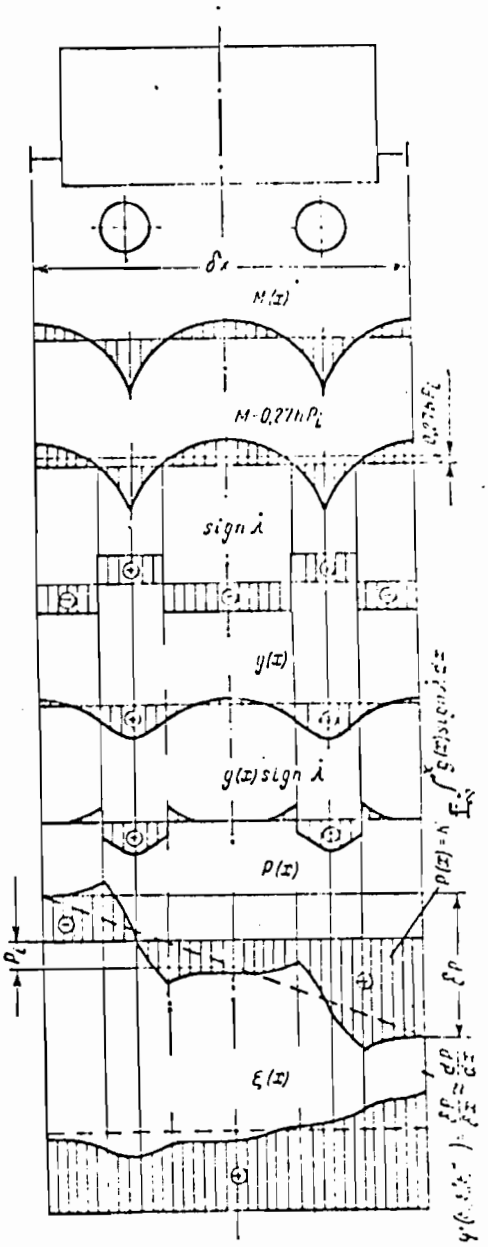

Fig. V.2 Construction of graphs of longitudinal forces and displacements in the zone of one moving car, assuming frictional interaction between the rail and the rail supporting foundation

If we adopt the approximation

$$\psi_2 (P) = d - bP,$$

then the equation (V.19) for the longitudinal forces takes the form

$$\frac{dP}{dx} + bP = \alpha - \tau + r. \qquad (V.21)$$

The solution is given by

$$P = Be^{-bx} + \frac{\alpha - \tau + r}{b}, \qquad (V.22)$$

where the coefficient B is determined by the boundary conditions.

Let us construct the graphs of longitudinal forces and displacements in the track. The general form of such graphs is shown in Figure V.4. The figure shows that for $x < o$ the rails are displaced by an amount ξ_c, which represents the rail creep.

Assuming values for P_2, one can construct the graph of $P(x)$. Indeed, in the section $x_2 \leq x \leq x_3$ in front of the moving train, the longitudinal forces are given by

$$\begin{aligned} P &= - g_o k_f (x_3 - x) \\ &= \rho_o (x - x_3), \end{aligned} \qquad (V.23)$$

where g_o is the force per meter of length which presses the rail to the foundations in the absence of loading due to the train. The length of the section in front of the train in which the longitudinal forces are damped out is determined by the formula

$$\ell_3 = x_3 - x_2 = \frac{P_2}{\rho_o}. \qquad (V.24)$$

In the section $x_1 \leq x \leq x_2$ underneath the moving train, the longitudinal forces can be found from the expression

$$P = Be^{-b(x_2 - x)} + \frac{\alpha - \tau + r}{b}. \qquad (V.25)$$

The value of B is found by making use of the condition

$$P_2 = B + b^{-1}(\alpha - \tau + r),$$

which yields

$$B = P_2 - b^{-1}(\alpha - \tau + r).$$

In the cross-section $x = x_1$, the longitudinal force is given by

$$P_1 = P(x_1) = \left(P_2 - \frac{a - \tau + r}{b}\right) e^{b(x_1 - x_2)} + \frac{a - \tau + r}{b}.$$

In the section $0 \leq x \leq x_1$ behind the moving train, the longitudinal forces can be computed from

$$P = P_1 - \rho_o(x_1 - x). \qquad (V.26)$$

The length of the zone behind the train in which the longitudinal forces are damped out is determined by

$$\ell_1 = x_1 = \frac{P_1}{\rho_o} \qquad (V.27)$$

Every value of P_2 determines a longitudinal force graph. To find out which graph is the correct one, i.e. to resolve the static indeterminacy of the system, let us make use of the principle of least work, which states that the partial derivative of the system potential energy U with respect to the redundant unknown quantity P_2 must vanish, i.e.

$$\frac{\partial U}{\partial P_2} = 0. \qquad (V.28)$$

The potential energy of the longitudinally deformed CWR track is given by [17]

$$U = \frac{1}{2EF} \int_{-\infty}^{\infty} P^2 dx. \qquad (V.29)$$

Let us split the integral in (V.29) into a sum of three integrals:

$$\int_{-\infty}^{\infty} P^2\,dx = \int_0^{x_1} P^2\,dx + \int_{x_1}^{x_2} P^2\,dx + \int_{x_2}^{x_3} P^2\,dx.$$

Let us compute the first integral on the right hand side:

$$2EFU_1 = \int_0^{x_1} P^2\,dx = \int_0^{\frac{1}{\rho_0}[(P_2-\gamma)e^{-bl}+\gamma]} \rho_0^2 x^2\,dx = \frac{1}{3\rho_0} \times$$
$$\times [P_2 e^{-bl} + \gamma(1-e^{-bl})]^3,$$

where $\gamma = b^{-1}(\alpha - \tau + r)$, $l = x_2 - x_1$.

Evaluation of the second integral yields

$$2EFU_2 = \int_{x_1}^{x_2} P^2\,dx = \int_0^{l} [(P_2-\gamma)e^{-b\xi} + \gamma]^2\,d\xi =$$
$$= \int_0^{l} (P_2-\gamma)^2 e^{-2b\xi}\,d\xi + \int_0^{l} 2\gamma(P_2-\gamma)e^{-b\xi}\,d\xi + \int_0^{l} \gamma^2\,d\xi =$$
$$= (P_2-\gamma)^2 \frac{1}{2b}(1-e^{-2bl}) + 2\gamma(P_2-\gamma)\frac{1}{b}[1-e^{-bl}] + \gamma^2 l.$$

Finally, the third integral is equal to

$$2EFU_3 = \int_{x_2}^{x_3} P^2\,dx = \int_0^{\frac{P_3}{\rho_0}} \rho_0^2 x^2\,dx = \frac{1}{3\rho_0} P_3^3.$$

Differentiating these expressions with respect to P_2,

$$\frac{\partial 2EFU_1}{\partial P_2} = \frac{1}{\rho_0} e^{-bl}[P_2 e^{-bl} + \gamma(1-e^{-bl})]^2;$$

$$\frac{\partial 2EFU_2}{\partial P_2} = \frac{1}{b}(1-e^{-2bl})(P_2-\gamma) + 2\gamma\frac{1}{b}(1-e^{-bl});$$

$$\frac{\partial 2EFU_3}{\partial P_2} = \frac{1}{\rho_0} P_2^2,$$

and making use of (V.28) results in

$$\frac{0}{\rho_0}[P_2 0 + \gamma(1-0)]^2 + \frac{1}{\rho_0}P_2^2 + (P_2 - \gamma)\frac{1}{b}(1-0^2) +$$
$$+ 2\gamma\frac{1}{b}(1-0) = 0,$$

where $\theta = e^{-b\ell}$. This equation has the form

$$P_2^2 + CP_2 + D = 0,$$

where

$$\left.\begin{aligned} C &= \frac{20^2\gamma(1-0) + \frac{\rho_0}{b}(1-0^2)}{1+0^3}; \\ D &= \frac{0\gamma^2(1-0)^2 - \frac{\rho_0\gamma}{b}(1-0^2) + 2\frac{\rho_0\gamma}{b}(1-0)}{1+0^3}. \end{aligned}\right\} \qquad (V.30)$$

If the length of the train is large, $\theta \approx 0$, which leads to the approximations:

$$C \approx \frac{\rho_0}{b}; \quad D \approx \frac{\gamma\rho_0}{b}.$$

The solution of (V.30)

$$P_2 = -\frac{C}{2} + \sqrt{\left(\frac{C}{2}\right)^2 - D}$$

determines the actual value of P_2 [the negative sign in front of the square root corresponds to the maximum of $U(P_2)$].

After the construction of the longitudinal force graph, let us determine the longitudinal displacement of the neutral axis of the rail. With our choice of the coordinate system (see Fig.4), the displacement ξ can be found from the expression

$$\xi = \frac{1}{EF}\int_x^{x_0} P dx,$$

where $\xi(x_3) = 0$. It should be noted that the graphs shown in Figure V.4 describe only the smoothed out variation of the longitudinal force and displacement along the length of the rail string. However, one can construct such graphs taking into account the variation of the load (per unit length) on the rail base over a distance equal to a car length.

In order to accomplish this, it is sufficient to subdivide the longitudinal force graph into sections of length δx, and on each of these to replace the smoothed out curve by the actual one. The following procedure can be used. The increment δP_i in the longitudinal force is measured in each section, and the graph V.3 is used to find the average value of the longitudinal force* on the interval P_i by means of the expression $\psi_2(P_i) = \delta P_i/\delta x$. Now, using the procedures shown in Figure V.2, one can construct the graph of the actual longitudinal forces on the i-th section. Having performed this operation on every section, we will obtain a more accurate graph of the longitudinal forces in the zone of the moving train, and, after integrating it, a more accurate graph of the longitudinal displacements. Now there is no difficulty in constructing the graph of the longitudinal displacements of the rail base. To do this it is only necessary to add the graph of displacements ξ of the neutral axis to the graph of the angle through which the rail is rotated multiplied by the constant $h/2$.

---

* Here the average is, in general, not the average value over an interval with unit weight, although it must satisfy the inequality $A_i \leq P_i \leq B_i$, where A_i and B_i are respectively the smallest and the largest value of the force on the i-th section.

Example. Let us construct the graphs of the longitudinal force and displacement in the zone of the moving train. Let us suppose the train consists of 80 two-axle cars, each of length 16 m, with 8 m between axles. Assume the following data:

Load per axle, P_o = 10 T; $k = (U/4EI)^{1/4} = 0.01\ cm^{-1}$; $K_f = 0.25$; h = 152 mm; r = 0; $\tau = 0$; $\rho_o = 0.6$ T/m.

In this example it is convenient to take δx to be the distance between adjacent axles, and δP to be the creep force due to one axle. The functions M(x) and g(x) are plotted in Figure V.5. In view of their symmetry, only the values for positive x are shown.

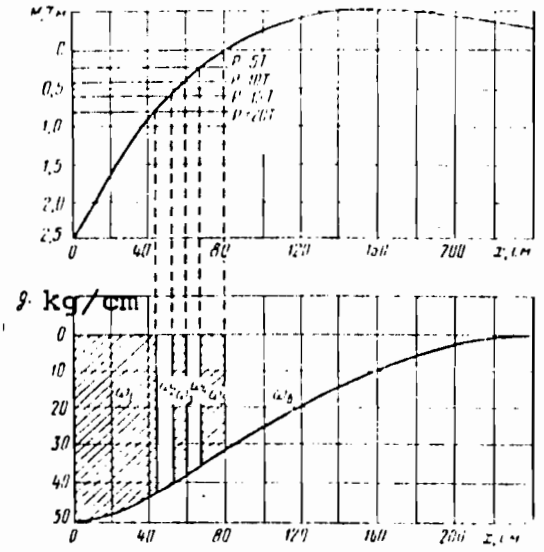

Fig. V.5. Calculation of the creep force due to one wheel for different values of the longitudinal force in the rail, assuming frictional interaction between the rail and the rail supporting foundation (corresponding to the first example).

On the graph of M(x), let us draw a sequence of horizontal lines with ordinates equal to $0.27\ hP_i$, for P_i = 5, 10, 15, and 20 T. The abscissas of the points of intersection between the graph of M(x) and the straight lines, determine the sign of the

frictional force per unit length between the rail and the foundation.

Let ω_1 denote the area bounded by the curve g(x), the horizontal axis, the vertical axis, and a vertical line with the same abscissa as the point of intersection between M(x) and the horizontal line corresponding to P_i = 20 T. Let ω_2 denote the area bounded by g(x), the horizontal axis, and the two vertical lines corresponding to P_i = 20T and 15 T, etc. (see Fig. V.5). It is found that ω_1 = 2.11 T; ω_2 = 0.33 T; ω_3 = 0.31 T; ω_4 = 0.25 T; ω_5 = 0.43 T; ω_6 = 1.86 T.

Consequently, the creep forces produced by one axle, for various values of the force P_i, will be given by

$$\delta P_i(0) = 2k_{rp}(\omega_1 + \omega_2 + \omega_3 + \omega_4 + \omega_5 - \omega_6) = 2\cdot 0{,}25\,(2{,}11 + 0{,}33 + 0{,}31 + 0{,}25 + 0{,}43 - 1{,}86) = 0{,}79\ T;$$

$$\delta P_i(5) = 2k_{rp}(\omega_1 + \omega_2 + \omega_3 + \omega_4 - \omega_5 - \omega_6) = 2\cdot 0{,}25\,(2{,}11 + 0{,}33 + 0{,}31 + 0{,}25 - 0{,}43 - 1{,}86) = 0{,}35\ T;$$

$$\delta P_i(10) = 2k_{rp}(\omega_1 + \omega_2 + \omega_3 - \omega_4 - \omega_5 - \omega_6) = 2\cdot 0{,}25\,(2{,}11 + 0{,}33 + 0{,}31 - 0{,}25 - 0{,}43 - 1{,}86) = 0{,}11\ T;$$

$$\delta P_i(15) = 2k_{rp}(\omega_1 + \omega_2 - \omega_3 - \omega_4 - \omega_5 - \omega_6) = 2\cdot 0{,}25\,(2{,}11 + 0{,}33 - 0{,}31 - 0{,}25 - 0{,}43 - 1{,}86) = -0{,}21\ T;$$

$$\delta P_i(20) = 2k_{rp}(\omega_1 - \omega_2 - \omega_3 - \omega_4 - \omega_5 - \omega_6) = 2\cdot 0{,}25\,(2{,}11 - 0{,}33 - 0{,}31 - 0{,}25 - 0{,}43 - 1{,}86) = -0{,}56\ T.$$

Figure V.6 shows that the graph of $\delta P_i(P_i)$ is very close to that of a straight line. Let us approximate it by the straight line

$$\delta P_i(P_i) = 0.78 - 0.065\ P_i,\ T.$$

Taking into account that δx = 8 m for our case, we obtain the expression for the function $\psi_2(P_i)$

$$\psi_2(P_i) = \frac{\delta P_i}{\delta x} = 0.095 - 0.0081\ P_i,\ T/m.$$

Thus, we will have two additional parameters: $a = 0.095\ T \cdot m^{-1}$ and $b - 0.0081\ m^{-1}$.

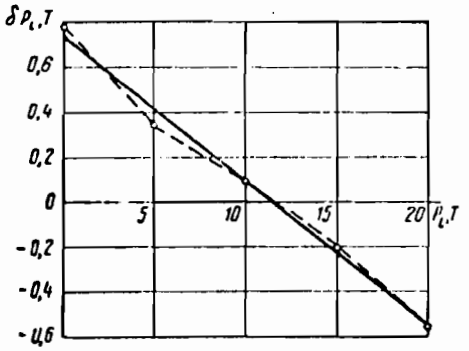

86 T.

Fig. V.6. The graph of the creep force due to one pair of wheels as a function of the longitudinal force in the rail, assuming frictional interaction between the rail and the foundation (for the first example).

Let us determine the parameters C and D in equation (V.30) from the approximate expressions previously introduced:

$$\theta = \exp(-0.008 \times 80 \times 16) \approx 0 ;$$

$$C = \rho_0/b = 0.6/0.0081 = 74\ T ;\ \gamma = b^{-1}(\alpha-\tau+r) = 0.095/0.0081 = 11.7\ T;$$

$$D = \tau\rho_0/b = 11.7 \times 0.6/0.0081 - 865\ T^2 .$$

Let us compute P_2:

$$P_2 = -\frac{1}{2} C + [(C/2)^2-D]^{1/2} = -14.5T.$$

The quantity P_1 can now be determined from

$$P_1 = (P_2 - 1)e^{-b\ell} + \gamma \approx \gamma = 11.7\ T$$

The length of the zone in front of the train in which the longitudinal forces decay can be computed from (V.24):

$$\ell_3 = P_2/\rho_0 = 14.5/0.6 = 24\ m.$$

The length of the zone behind the train in which the longitudinal forces decay is determined from (V.27):

$$\ell_1 = P_1/\rho_0 = 11.7/0.6 = 19.5\ m.$$

Now we have all the necessary data to construct the longitudinal force diagram. Dividing the graph of the longitudinal forces into subintervals (Figure V.7), and constructing on each of these a new graph by taking into account the creep forces along the length of a car, we will obtain a more accurate graph of the longitudinal forces. In view of the complexity of the computations required, we indicate the high frequency oscillations produced by the forces which vary along the length of a car, superimposed on the averaged graph, in a qualitative way only in Figure V.7.

The graph of the longitudinal displacements is also shown in Figure V.7. Here the amplitude of the oscillations about the averaged curve is much smaller.

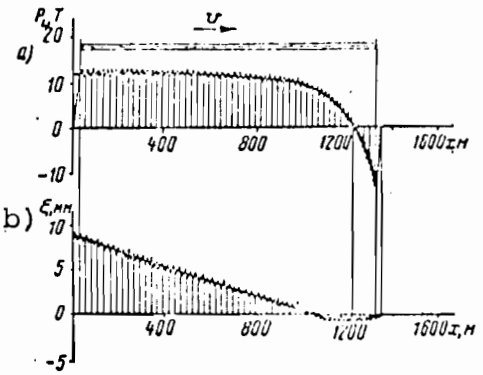

Fig. V.7. Graphs of the longitudinal forces (a) and displacements (b) in the zone of the moving train, with frictional interaction between the rail and the rail supporting foundation (for the first example).

In conclusion, let us note that we have investigated forces only in infinite rail strings without joints. In the presence of joints between separate strings of rails, the boundary conditions which determine the graphs of the longitudinal forces and displacements will be different from the ones we have used.

3. Integration of the longitudinal displacement equation for CWR track in the moving train zone with elastic interaction between the rail and the rail supporting foundation

If a spring type intermediate fastener is strong enough to prevent the relative displacement of the rail and the tie, the results of V. G. Al'brecht [1], on the determination of the modulus of elasticity of the rail foundation in the horizontal plane, show that the function ϕ can be represented in the form

$$\phi_1(\xi,\xi',\xi'',\ldots,y,y',y'',\ldots) = -(n+mg)\,\lambda, \qquad (V.31)$$

where n and m are constants, and g is the distributed vertical load. According to Al'brecht's data for medium grained sand ballast, $n = 48$ kg/cm^2, $m = 4.56$ cm. The minus sign in (V.31) indicates that the elastic reaction of the foundation at the rail-foundation interface opposes the displacement of the rail, i.e. that the reaction force acts in the direction opposite to the creep.

Let us compute the function ψ_1:

$$\psi_1(\xi,\xi',\xi'',\ldots) = \int_0^{\delta x} \varphi_1(\xi,\xi',\xi'',\ldots,y,y',y'',\ldots)\,dx =$$
$$= -\int_0^{\delta x} (n+mg)(\xi+\eta+\chi)\,dx.$$

Neglecting the quantity η, which is small to second order compared to the displacements ξ and χ, we obtain

$$\psi_1(\xi,\xi',\xi'',\ldots) \approx -\xi\int_0^{\delta x}(n+mg)\,dx - \int_0^{\delta x}\chi(n+mg)\,dx.$$

The second integral on the right hand side is equal to zero since the integrand is a product of functions orthogonal on the

interval $0<x<\delta x$ (the function n+mg is symmetric, while χ is inverse skew-symmetric on the interval). Thus,

$$\psi_1(\xi, \xi', \xi'', \ldots) = -\xi(n\delta x + mQ_1) = -c_1\xi, \qquad (V.32)$$

where Q_1 is the weight of the car, and c_1 is a constant.

Substituting the expression (V.32) into (V.14), and taking into account the absence of anticreep devices (r = 0), we obtain

$$\frac{d^2\xi}{dx^2} - \frac{c_1}{EF\delta x}\xi = -\frac{\tau}{EF}. \qquad (V.33)$$

This equation has solutions of the form

$$\xi = A_1 sh\gamma_1 x + A_2 ch\gamma_1 x + \frac{\delta T}{c_1}, \qquad (V.34)$$

where $\delta T = \tau\delta x$ kg, and $\gamma_1 = \sqrt{c_1/EF\delta x}$ cm^{-1}.

Differentiating (V.34) and making use of (V.1) yields

$$P = (A_1\gamma_1 ch\gamma_1 x + A_2\gamma_1 sh\ \gamma_1 x)EF. \qquad (V.35)$$

Now, let us address ourselves to the problem of determining the constants A_1 and A_2.

Let the origin of the coordinate system be at the mid-point of the train, which has length 2ℓ (Fig. V.8).

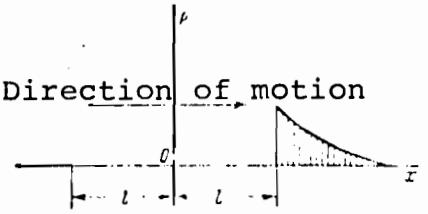

Fig. V.8. Diagram of longitudinal track forces in front of the moving train, with elastic-frictional interaction between the rail and the supporting foundation.

In the interval $\ell < x < \infty$, in front of the moving train, the conditions $g = 0$, $\tau = 0$ must hold. Then, according to (V.33) and (V.32), we obtain

$$\frac{d^2\xi}{dz^2} - \frac{c_2}{EF\delta x}\xi = 0. \qquad \text{(V.36)}$$

Here $z = x - \ell$ and $c_2 = n\delta x$. Solutions of (V.36) have the form

$$\xi = D_1 e^{-\gamma_2 z} + D_2 e^{\gamma_2 z}, \qquad \text{(V.37)}$$

where $\gamma_2 = \sqrt{n/EF}$. From the condition $\xi(\infty) = 0$, it follows that $D_2 = 0$, and we obtain

$$\xi = D_1 \exp(-\gamma_2 z). \qquad \text{(V.38)}$$

Differentiating this expression and making use of (V.1), we obtain

$$P = EF\frac{d\xi}{dz} = -\gamma_2 EFD_1 e^{-\gamma_2 z} = -\gamma_2 EF\xi. \qquad \text{(V.39)}$$

In particular, for $x = \ell$,

$$P(\ell) = -\gamma_2 EF\xi(\ell). \qquad \text{(V.40)}$$

If the elasticity of the track is uniform, we can write

$$P(-\ell) = \gamma_2 EF\ \xi(-\ell). \qquad \text{(V.41)}$$

The minus sign in (V.40) indicates that the forces at $x = \ell$ are compressive.

Substituting (V.40) and (V.41) into (V.34) and (V.35) when $x = \ell$ and $x = -\ell$, we obtain two equations:

$$-A_1\gamma_1 \operatorname{ch}\gamma_1\ell - A_2\gamma_1 \operatorname{sh}\gamma_1\ell = A_1\gamma_2 \operatorname{sh}\gamma_1\ell + A_2\gamma_2 \operatorname{ch}\gamma_1\ell + \gamma_2\delta T/c_1$$

$$-A_1\gamma_1 \operatorname{ch}\gamma_1\ell + A_2\gamma_1 \operatorname{sh}\gamma_1\ell = A_1\gamma_2 \operatorname{sh}\gamma_1\ell - A_2\gamma_2 \operatorname{ch}\gamma_1\ell - \gamma_2\delta T/c_1.$$

Solving these, we obtain

$$A_1 = 0;\ A_2 = -\gamma_2\delta T/c_1(\gamma_1 \operatorname{sh}\gamma_1\ell + \gamma_2 \operatorname{ch}\gamma_1\ell).$$

Substituting these constants into (V.34) and (V.35), we finally obtain

$$\left.\begin{aligned} \xi &= \frac{-\gamma_2 \delta T}{c_1(\gamma_2 \operatorname{ch}\gamma_1 l + \gamma_1 \operatorname{sh}\gamma_1 l)} \operatorname{ch}\gamma_1 x + \frac{\delta T}{c_1} \quad (-l < x < l); \\ P &= \frac{-\gamma_1 \gamma_2 EF\delta T}{c_1(\gamma_2 \operatorname{ch}\gamma_1 l + \gamma_1 \operatorname{sh}\gamma_1 l)} \operatorname{sh}\gamma_1 x \qquad (-l < x < l). \end{aligned}\right\} \tag{V.42}$$

Let us note that the inverse symmetry of the longitudinal force diagram was to be expected in view of the symmetry of the system and the inverse symmetry of the externally applied loads τ.

Formula (V.42) shows that in the absence of additional creep forces produced by the friction in the brake shoes and the journal boxes, P and ξ must vanish. Furthermore, because of the inverse symmetry of the longitudinal forces on the interval $-\infty < x < \infty$, it follows that when the interaction between the rail and the supporting foundation is elastic, there is no creep even in the presence of forces τ applied by the train to the rail head, since the magnitude of the creep ξ_c is, except for the multiplying constant 1/EF, equal to the area under the longitudinal force curve.

Setting z = 0 in (V.42), we determine the value of the constant D_1:

$$D_1 = \frac{-\gamma_2 \delta T \operatorname{ch}\gamma_1 l}{c_1(\gamma_2 \operatorname{ch}\gamma_1 l + \gamma_1 \operatorname{sh}\gamma_1 l)} + \frac{\delta T}{c_1} = \frac{\gamma_1 \operatorname{sh}\gamma_1 l\, \delta T}{c_1(\gamma_2 \operatorname{ch}\gamma_1 l + \gamma_1 \operatorname{sh}\gamma_1 l)}.$$

Substituting this value of D_1 into (V.38) yields the expression for the displacements in the region $l < x < \infty$ in front of the moving train,

$$\xi = \frac{\delta T \gamma_1 \operatorname{sh}\gamma_1 l}{c_1(\gamma_2 \operatorname{ch}\gamma_1 l + \gamma_1 \operatorname{sh}\gamma_1 l)} e^{-\gamma_1(x-l)} \quad (l < x < \infty). \tag{V.43}$$

Finally, making use of (V.39), we can determine the expression for the longitudinal forces in front of the moving train:

$$P = \frac{-\gamma_2 \tau \operatorname{sh} \gamma_1 l}{\gamma_1 (\gamma_2 \operatorname{ch} \gamma_1 l + \gamma_1 \operatorname{sh} \gamma_1 l)} e^{-\gamma_1 (x-l)} \quad (l < x < \infty). \qquad (V.44)$$

It should be noted that

$$\gamma_1^2 = c_1/EF\delta x \; ; \quad \delta T = \tau \delta x.$$

For $x = \ell$ the values of the longitudinal force P_1 computed according to the formulas (V.42) and (V.44) coincide, which provides a convenient check on our calculations.

There is no need to construct longitudinal force and longitudinal displacement diagrams for the region $-\infty < x < -\ell$ behind the moving train in view of the symmetry of ξ and the inverse symmetry of P.

Let us estimate the creep force $P(\ell)$ in the rail cross-section underneath the first axle of the locomotive. Substituting $x = \ell$ into (V.44), we obtain

$$P(l) = \frac{-\gamma_2 \tau \operatorname{sh} \gamma_1 l}{\gamma_1 (\gamma_2 \operatorname{ch} \gamma_1 l + \gamma_1 \operatorname{sh} \gamma_1 l)}. \qquad (V.45)$$

Let us compute the argument $\gamma_1 \ell$ of the hyperbolic functions for the following values of the track and rolling stock characteristics: rails - P50; $F = 64$ cm^2; $E = 2.1 \times 10^6$ kg/cm^2; wooden ties, 1840 per km; fasteners of type K; medium grained sand ballast; $n = 48$ kg/cm^2; $m = 4.56$ cm; train length, $2\ell = 80000$ cm; car length, $\delta x = 1400$ cm; car weight, $Q_1 = 60000$ kg.

Load per unit length of rail head produced by train deceleration: $\tau = 1.0$ kg/cm, which corresponds to a load of 2.5 T per 12.5 m rail length.

Auxilliary parameters:

$c_1 = n\delta x + mQ_1 = 340\ 000$ kg/cm:

$\gamma_1 = \sqrt{c_1/EF\delta x} = 1.34 \times 10^{-3}$ cm^{-1}; $\gamma_1 \ell = 53.6$.

For such large values of the argument one can use the approximations

$$\text{sh } \gamma_1 \ell \simeq \text{ch } \gamma_1 \ell \simeq 0.5 \exp \gamma_1 \ell,$$

which reduce (V.45) to

$$P(\ell) = -\gamma_2 \tau / \gamma_1 (\gamma_2 + \gamma_1).$$

For the value of γ_2 we obtain

$$\gamma_2 = \sqrt{n/EF} = 6 \times 10^{-4} \text{ cm}^{-1}.$$

Substituting the values of all the parameters into the formula for the longitudinal force at $x = \ell$, we finally obtain

$$P(\ell) = -230 \text{ kg}.$$

Thus, when the interaction between the rail and the rail supporting foundation is elastic, the maximal forces in the moving train zone are insignificant, and need not be considered.

CHAPTER VI

STABILITY QUESTIONS FOR CWR TRACK

At the present time CWR track is a reality. Because of its technical and economic superiority, CWR track is beginning to displace jointed track. Practical experience indicates that under certain conditions the track is stable. However, the stability problems for CWR track has not been completely solved.

Scientific investigators in the Soviet Union and abroad have been studying the stability problem for CWR track over a period of thirty years. Among the most important investigations we can single out those of K. N. Mishchenko, C. P. Pershin, A. A. Krivobodrova, A. Bloch, G. Zanden, I. J. Nemesdy-Nemesek, R. Levi, and M. Numata. Investigators working on the stability problems for CWR track have been making an incorrect assumption - they have been replacing the actual track parameters at the moment of buckling by the parameters which characterize the neutral equilibrium state, i.e. by parameters obtained by averaging with respect to the deformations which arise when the track is in the process of losing its stability, while these averaged quantities were found to depend on the parameters of the track before and after the onset of buckling. Even if we assume that the neutral equilibrium state, which corresponds to the moment at which buckling is initiated, depends on the past history of the system before buckling, we cannot possibly admit that it depends on the future states of the system.

Present day stability calculations do not take into account the effect of the moving train, which changes many of the track parameters in the regions in front of the locomotive and behind the last car. The solution of the stability problem in the presence of additional creep forces, which arise in the region in front of the moving train, deserves special attention.

1. Determination of stability conditions for CWR track

The problem will be solved under the following assumptions: 1) the longitudinal forces P are the same in both rail lines; 2) the radius of curvature R of both rail lines is the same, R = const; 3) as the track is deformed, the ties are displaced parallel to themselves.

It follows from the second assumption, which is justified by the fact that the radius of curvature is considerably larger (hundreds of times, or even thousands) than the track gauge, that the bending moments M and the shear forces Q are the same in both rail lines.

Let us isolate a track element of length Δx, equal to the distance between adjacent ties, and let us examine its equilibrium (Fig. VI.1).

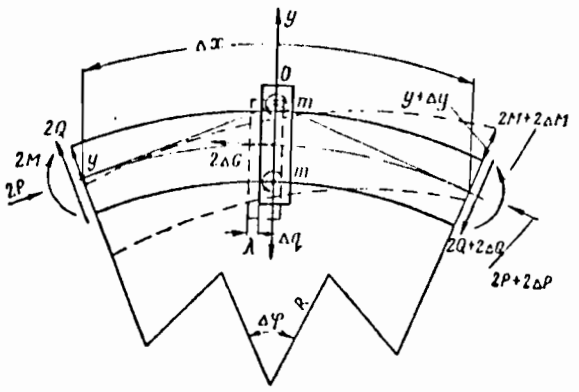

Fig. VI.1. Equilibrium conditions for a deformed track elements under the action of longitudinal and transverse forces

Summing up the moments about the point 0, we obtain

$$\sum M_o = 2\Delta M + 2m - 2Q \cdot 2R \tan \frac{\Delta\phi}{2} - 2Py + 2(P+\Delta P)\ (y+\Delta y) = 0.$$

Dividing this equation by $2\Delta x$, and taking into account the approximations

$$2R \tan(\Delta\phi/2)/\Delta x \approx \tan \Delta\phi/\Delta\phi \approx 1$$

and

$$2(P+\Delta P)\ (y+\Delta y) \approx 2Py + 2P\Delta y + 2y\Delta P$$

yields the equation

$$\frac{\Delta M}{\Delta x} + \frac{m}{\Delta x} - Q + P\frac{\Delta y}{\Delta x} + y\frac{\Delta P}{\Delta x} = 0.$$

Replacing the ratios of increments by derivatives, and introducing the notation

$$m/\Delta x = - f_1(y'),$$

which expresses the fact that the moment applied by the rail to the fastener is proportional to the angle of twist of the rail with respect to the tie, we finally obtain

$$\frac{dM}{dx} = f_1(y') + Q - Py' - yP'. \qquad \text{(VI.1)}$$

Let us find the sum of the vertical components of the forces:

$$\sum y = -\Delta q - 2\Delta Q\cos\frac{\Delta\phi}{2} + 2P\sin\frac{\Delta\phi}{2} = 0.$$

Here we have neglected the term $2\Delta P\sin(\Delta\phi/2) \approx \Delta P\Delta\phi$, since it is small compared to the others. Dividing the equation by $2\Delta x$, and taking into account the approximations

$$2\sin\frac{1}{2}\Delta\phi/\Delta x \approx \sin\Delta\phi/R\Delta\phi \approx R^{-1}; \cos\frac{1}{2}\Delta\phi \approx 1$$

we obtain

$$- \Delta Q/\Delta x - \Delta q/2\Delta x + P/R = 0.$$

Now, replacing the ratios of the increments by derivatives, and introducing the notation

$$q/2\Delta x = f_2(y),$$

according to which the force applied to the tie depends on the displacement, we are led to

$$dQ/dx = -f_2(y) + P/R \qquad \text{(VI.2)}$$

Differentiating (VI.1) and substituting for dQ/dx from (VI.2)

$$d^2M/dx^2 = f'_1(y') - f_2(y) + P/R - 2P'y' - Py'' - yP'' \qquad \text{(VI.3)}$$

Finally, making use of the relation which determines the bending moment in a curved beam (see Fig. VI.1)

$$M = EIy'' + EI(\lambda/R)',$$

where λ is the longitudinal displacement of the rail cross-section, we obtain

$$EI\left[y^{IV} + (\lambda/R)''\right] - f'_1(y') + f_2(y) + Py'' + 2P'y' + P''y = P/R \qquad \text{(VI.4)}$$

Here R and P are, in general, random functions of x, and $f_1(y')$ and $f_2(y)$ are also random functions.

A special case of this equation is derived in the paper of Ignyatich [14], with some errors in sign, however.

Now, let us find the sum of the horizontal components of the forces,

$$\sum x = -2\Delta P - \Delta G - 2Q\sin(\Delta\phi/2) = 0.$$

Dividing the equation by $2\Delta x$, and making the same approximations as before, we arrive at

$$\Delta P/\Delta x - \Delta G/\Delta x - Q/R = 0.$$

Finally, replacing the ratios of increments by derivatives, and taking into account the fact that

$$\Delta G/\Delta x = \phi(\lambda),$$

where λ is the displacement of the tie along the track, we obtain

$$dP/dx = -\phi(\lambda) - Q/R. \qquad \text{(VI.5)}$$

In discussions of track stability, we will consider compressive rail forces to be positive.

Integrating the expression for the derivative of the longitudinal force, we obtain

$$P = B + c.$$

Here $B = G + \int (Q/R)dx$; G is the force which results from the elongation of the rail axis due to transverse track deformations; c is an arbitrary constant. Furthermore, let us assume that

$$P = P(x,y,y',y'',y''',y^{IV}),$$

$$B = B(x,y,y',y'',y''',y^{IV}).$$

It is not difficult to see that when $y \equiv 0$,

$$G|_{y\equiv 0} \equiv 0; \qquad Q|_{y\equiv 0} \equiv 0.$$

From this, it follows that

$$B(x,0,0,0,0,0) \equiv 0.$$

Furthermore, one can write

$$P(x,0,0,0,0,0) \equiv P_o,$$

where P_o is the rail force in the undeformed track. Consequently, the constant of integration is $c = P_o$, and the longitudinal rail force can be determined from the expression

$$P(x,y,y',y'',y''',y^{IV}) = P_o + B(x,y,y',y'',y''',y^{IV}). \qquad (VI.6)$$

The function B is continuous and infinitely differentiable. Let us find the second derivative. Making use of (VI.2) and (VI.5), we can write

$$d^2B/dx^2 = \phi'(\lambda) + (1/R)f_2(y) - P_o - B/R^2. \qquad (VI.7)$$

It can be seen from Figure VI.2 that the elongation of the rail axis is given by the expression

$$\varepsilon = d\lambda/dx + d\eta/dx + y/R.$$

On the other hand, since the elongation results from the action of the force B,

$$\varepsilon = B/EF.$$

Consequently, making use of the expression (IV.11) for the difference η between the length of the curve and its projection, we obtain an expression for the displacement of the rail along the track,

$$\lambda = -\int_x^\infty \left[\frac{B}{EF} - \frac{1}{2}(y')^2 - \frac{y}{R}\right] dx. \qquad \text{(VI.8)}$$

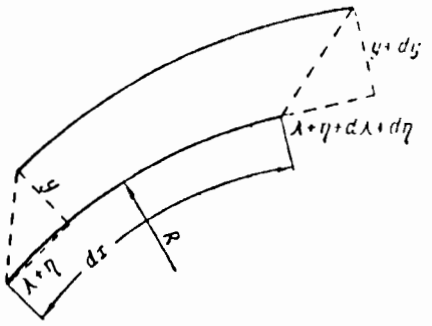

Fig. VI.2. Elongation of the neutral axis when the rail line is displaced

Let $\phi(\lambda)$ be represented by a power series

$$\phi(\lambda) = \sum_{i=0}^{\infty} a_i \lambda^i.$$

Substituting for λ from (VI.8) and differentiating $\phi(\lambda)$, we obtain

$$\begin{aligned}\varphi'(\lambda) &= \lambda'(a_1 + 2a_2\lambda + 3a_3\lambda^2 + \ldots + na_n\lambda^{n-1} + \ldots) = \\ &= -\left(\frac{B}{EF} - \frac{1}{2}(y')^2 - \frac{y}{R}\right)\left[a_1 - 2a_2\int_x^\infty \left[\frac{B}{EF} - \frac{1}{2}(y')^2 - \frac{y}{R}\right] dx + \right. \\ &\left. + \ldots + na_n\left\{-\int_x^\infty \left[\frac{B}{EF} - \frac{1}{2}(y')^2 - \frac{y}{R}\right] dx\right\}^{n-1} + \ldots\right] = \\ &= \frac{a_1}{EF} B - \frac{a_1}{R} y + \theta_1(x, y, y', y'', y''', y^{IV}).\end{aligned} \qquad \text{(VI.9)}$$

Here θ_1 is a nonlinear function of the transverse displacement

y and its derivatives. Substituting from (VI.9) into (VI.7), we finally obtain

$$\frac{d^2B}{dx^2} - \left(\frac{a_1}{EF} + \frac{1}{R^2}\right) B - \frac{1}{R}[f_2(y) - a_1 y] + \frac{P_0}{R^2} - \theta_1 = 0. \qquad \text{(VI.10)}$$

This equation describes the process of longitudinal force relaxation due to track deformation.

An analysis of (VI.9) shows that the function θ_1 is of degree two or higher in y and its derivatives.

Let us return to the examination of equation (VI.4). This equation is not homogeneous; consequently, $y \equiv 0$ is not an equilibrium solution. Because of the continuous increase in the compressive forces due to rising temperature, the deformations grow and the curve is displaced toward the outside. However, no bifurcation from one equilibrium form to another takes place. The deformation process proceeds in one direction, the track being displaced from an initially undeformed state. Such an instability is frequently called an instability of the second kind. It is due to the presence of active forces.

As the track deformation increases, so does the reaction of the ballast to the displacement of the ties, as a result of which an equilibrium is established, a different equilibrium state corresponding to different values of compressive force. It should be noted that the equilibrium state established in the process may be stable or unstable. Whether it is stable or not depends on the parametric loads. When there is a loss of stability due to the action of parametric loads, a bifurcation from one form of equilibrium to another takes place. In other words, it may happen that

for certain values of parameters the system has several qualitatively different equilibrium states, and the transition from one such state to another takes place discontinuously.

Substituting into (VI.4) the value of λ''' from (VI.6), and taking into account the fact that R = const, we will obtain

$$EIy^{IV} - f_1'(y') + f_2(y) + y''\left(P - \frac{EI}{R^2}\right) + 2y'P' + P''\left(y - \frac{i_0^2}{R}\right) - \\ - \frac{EI}{R}\left[y'y''' + (y'')^2\right] = \frac{P}{R},$$

where $i_o = \sqrt{I/F}$ is the radius of gyration of the rail for track deformations in the horizontal plane.

Suppose the longitudinal force is P and the track is displaced to the outside of the curve by an amount $y = \delta$. Let us measure the transverse displacements of the track from its axis in the equilibrium state. Introduce the new coordinate, $u = y - \delta$. Then, the equation derived above takes the form

$$EIu^{IV} - f_1'(u') + f_2(u+\delta) + u''\left[P(x, u+\delta, u', u'', u''', u^{IV}) - \frac{EI}{R^2}\right] + \\ + 2u'P'(x, u+\delta, u', u'', u''', u^{IV}) + \\ + \left(u + \delta - \frac{i_0^2}{R}\right)P''(x, u+\delta, u', u'', u''', u^{IV}) - \\ - \frac{EI}{R}\left[u'u''' - (u'')^2\right] = \frac{1}{R}P(x, u+\delta, u', u'', u''', u^{IV}). \quad \text{(VI.11)}$$

Now, let us expand $f_2(u+\delta)$ in a Taylor series,

$$f_2(u+\delta) = f_2(\delta) + \frac{u}{1!}\cdot\frac{df_2(u)}{du}\bigg|_{u=\delta} + \ldots + \frac{u^m}{m!}\cdot\frac{d^{(m)}f_2(u)}{du}\bigg|_{u=\delta} + \ldots = \quad \text{(VI.12)}$$
$$= f_2(\delta) + uf_{2,u}'(\delta) + \theta_2(u^2, u^3, \ldots, u^n, \ldots).$$

The nonlinear function θ_2 is of degree higher than one in u, and can be neglected when considering small deformations.

From Figure VI.3 it is easy to determine the elongation of the rail axis caused by its displacement by an amount δ to the outside of the curve. The magnitude of this elongation is

$$\varepsilon = \delta/R.$$

Taking this into account, we obtain:

$$B(x,0+\delta,0,0,0,0) \equiv EF\delta/R,\ P(x,0+\delta,0,0,0,0) \equiv P_o - EF\delta/R,$$

$$P'(x,0+\delta,0,0,0,0) \equiv 0,\ P''(x,0+\delta,0,0,0,0) \equiv 0.$$

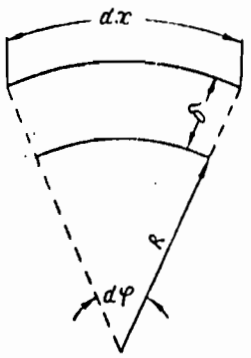

Fig. VI.3. Diagram for the elongation of the neutral axis due to a displacement by an amount δ of an element of the rail line from its initial position, assuming the angle which subtends the arc does not change

Substituting from (VI.12) into (VI.11), setting $u \equiv 0$, and taking into account the expressions just derived, we obtain

$$f_2(\delta) = P_o R^{-1} - EF\delta R^{-2}. \qquad \text{(VI.13)}$$

Thus, when conditions (VI.13) is satisfied, the equation (VI.11) has the trivial solution, the system described by this equation is in equilibrium, and the load which satisfies (VI.13) is a parametric load.

Substituting (VI.12) into (VI.10) and changing over to the variable $u = y - \delta$, we obtain

$$B''(x,u+\delta,u',u'',u''',u^{IV}) - (a_1/EF)B(x,u+\delta,u',u'',u''',u^{IV})$$

$$- R^{-1}\left[uf'_{2,u}(\delta) - a_1(u+\delta)\right] = \theta_1 + R^{-1}\theta_2. \qquad \text{(VI.14)}$$

It is easy to see that when $B = B(x,0+\delta,0,0,0,0) = EF\delta/R$, equation (VI.14) becomes an identity.

Let us represent $f_1(u')$ in the form of a power series,

$$f_1(u') = \sum_{i=0}^{\infty} b_i u'^i.$$

Differentiating yields

$$f_1'(u') = b_1 u'' + b_2 \cdot 2u'u'' + b_3 \cdot 3(u')^2 u'' + \ldots + b_n n (u')^{n-1} u'' + \ldots = b_1 u'' + \theta_3(u', u'', u''', u^{IV}), \quad \text{(VI.15)}$$

where θ_3 is a nonlinear function of the derivatives of the transverse rail displacement. Now, substituting into (VI.11) for the parametric load $P(x,u+\delta,u',u'',u''',u^{IV}) = P_o - EF\delta/R$, and taking into account the expansions (VI.12) and (VI.15), we can write

$$EIu^{IV} + u''\left(P_0 - b_1 \frac{EF}{R}\delta - \frac{EI}{R^2}\right) + uf_{2,u}'(\delta) = \theta_4, \quad \text{(VI.16)}$$

where

$$\theta_4 = \theta_3 - \theta_2 + EIR^{-2}\left[u'u''' + (u'')^2\right].$$

Since the nonlinear function θ_4 is continuous, a complete solution of the problem of finding the boundary of the domains of instability in this case can be based on the linear equation in the variations. This is quite evident on physical grounds since the function θ_4 is small at least to second order. Consequently, the critical parameters of the system described by (VI.16) can be found from

$$EIu^{IV} + u''\left(P_0 - b_1 \frac{EF}{R}\delta - \frac{EI}{R^2}\right) + uf_{2,u}'(\delta) = 0. \quad \text{(VI.17)}$$

To obtain the general solution of (VI.17), we must solve the equation

$$EIz^4 + \left(P_0 - b_1 - \frac{EF}{R}\delta - \frac{EI}{R^2}\right) z^2 + f'_{2,u}(\delta) = 0.$$

The roots of this equation are $z = \pm(\alpha \pm \beta_i)$, where

$$\alpha = \sqrt{\sqrt{\frac{f'_{2,u}(\delta)}{4EI}} - \frac{P_0 - b_1 - \frac{EI}{R}\delta - \frac{EF}{R^2}}{4EI}};$$

$$\beta = \sqrt{\sqrt{\frac{f'_{2,u}(\delta)}{4EI}} + \frac{P_0 - b_1 - \frac{EF}{R}\delta - \frac{EI}{R^2}}{4EI}}.$$

The general solution of (VI.17) will have the form

$$u = C_1 \sinh\alpha x \sin\beta x + C_2 \sinh\alpha x \cos\beta x + C_3 \cosh\alpha x \sin\beta x + C_4 \cosh\alpha x \cos\beta x \qquad \text{(VI.18)}$$

Here C_i are constants of integration.

Let us consider the infinitely long track to be divided into two parts, and let us examine the semi-infinite curved beam on the right. Geometrically, the semi-infinite curved beam can be represented by a spiral of radius R and infinitesimally small pitch.

Let us place the origin at the free end of the semi-infinite length of track, and let us assume that there is no deflection at infinity. The solution u will then have the form

$$u = A_1 e^{-\alpha x} \sin \beta x + A_2 e^{-\alpha x} \cos \beta x . \qquad \text{(VI.19)}$$

Differentiating this expression, we obtain

$$u' = A_1(-\alpha e^{-\alpha x}\sin\beta x + \beta e^{-\alpha x}\cos\beta x) + A_2(-\alpha e^{-\alpha x}\cos\beta x - \beta e^{-\alpha x}\sin\beta x);$$

$$u'' = A_1[(\alpha^2 - \beta^2)e^{-\alpha x}\sin\beta x - 2\alpha\beta e^{-\alpha x}\cos\beta x] + A_2[(\alpha^2 - \beta^2)e^{-\alpha x}\cos\beta x - 2\alpha\beta e^{-\alpha x}\sin\beta x];$$

$$u''' = A_1[(-\alpha^3 + 3\alpha\beta^2)e^{-\alpha x}\sin\beta x + (3\alpha^2\beta - \beta^3)e^{-\alpha x}\cos\beta x] + A_2[(-\alpha^3 + 3\alpha\beta^2)e^{-\alpha x}\cos\beta x + (3\alpha^2\beta + \beta^3)e^{-\alpha x}\sin\beta x].$$

At the free and x = 0 we have

$$
\begin{aligned}
&u(0) = A_2 = u_0;\\
&u'(0) = \beta A_1 - \alpha A_2 = u_0';\\
&u''(0) = -2\alpha\beta A_1 + (\alpha^2 - \beta^2) A_2 = u_0'';\\
&u'''(0) = (3\alpha^2\beta - \beta^3) A_1 + (3\alpha\beta^2 - \alpha^3) A_2 = u_0'''.
\end{aligned}
\qquad \text{(VI.20)}
$$

The buckled shape of the track can be symmetric or antisymmetric. We obtain

$y(0) = y''(0) = 0$ for the antisymmetric case,

$y'(0) = y'''(0) = 0$ for the symmetric case.

Substituting the boundary conditions into (VI.20) results in two equations for the determination of the critical parameters for each of the two cases.

For the antisymmetric case

$$y(0) = A_2 = 0, \quad y''(0) = -2\alpha\beta A_1 = 0,$$

from which it follows that $\alpha\beta = 0$, and, after some simplifications,

$$P_0 = 2\sqrt{EIf_{2,u}(\delta) + b_1 + \frac{EF}{R}\delta + \frac{EF}{R^2}}.$$

The buckled form is shown in Figure VI.4,a.

For the symmetric case

$$y'(0) = \beta A_1 - \alpha A_2 = 0,$$

$$y'''(0) = (3\alpha^2\beta - \beta^3)A_1 + (3\alpha\beta^2 - \alpha^3)A_2 = 0.$$

Setting the discriminant equal to zero yields

$$\beta(3\alpha\beta^2 - \alpha^3) + \alpha(3\alpha^2\beta - \beta^3) = 0,$$

or

$$2\alpha\beta(\alpha^2 + \beta^2) = 0.$$

Thus, $\alpha\beta = 0$ as for the antisymmetric case, and

$$P_0 = 2\sqrt{EIf_{2,u}(\delta) + b_1 + \frac{EI}{R}\delta + \frac{EF}{R^2}}.$$

Thus, the critical load is the same for the symmetric and the antisymmetric buckled forms.

For the symmetric case, the buckled shape is shown in Figure VI.4,b. The solutions obtained do not given any information about the amplitude of the deflection during the critical and the post critical phases. To obtain the complete solution it is necessary to take into account the nonlinear terms.

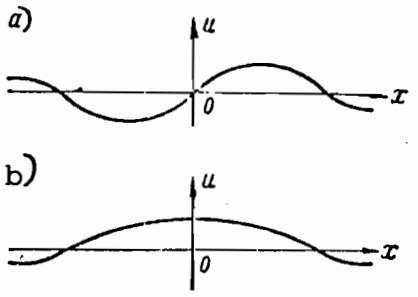

Fig. VI.4. Buckled forms of the track; (a) antisymmetric; (b) symmetric.

To summarize, we have obtained two equations which connect the parameters P_o, R, and δ:

$$f_2(\delta) = \frac{P_0}{R} - EF\frac{\delta}{R^2};$$
$$P_0 = 2\sqrt{EIf_{2,u}(\delta)} + b_1 + \frac{EF}{R}\delta + \frac{EI}{R^2}. \qquad \text{(VI.21)}$$

Let us recall that $b_1 = df_1(u')/du'|_{u'=0} = f'_{1,u'}(0)$, and represents the slope of the curve $f_1(u')$ at $u' = 0$. Thus, in order to construct the domains of instability it is sufficient to know the graph of $\Delta q(y)$, i.e. the dependence of the transverse force transmitted from the rail to the tie on the transverse rail displacement, and the parameter $f'_{1,u'}(0) = m'(0)/\Delta x$ ($m'(0)$ is the slope of the curve of the moment transmitted from the rail to the tie, as a function of the angle of twist of the rail with respect to the tie at the point $u' = 0$).

The functions $\Delta q(y)$ and $m(y')$ have been experimentally investigated fairly thoroughly, both in the Soviet Union (P.F. Isakov, C. P. Pershin, M. S. Bochenkov) and abroad (Birman, Raab, Nemesdy-

Nemesek). Figure VI.5 shows the function $\Delta q/\Delta x = 2f_2(y)$ for track with fasteners of type K, constructed on the basis of experiments and calculations of Raab.

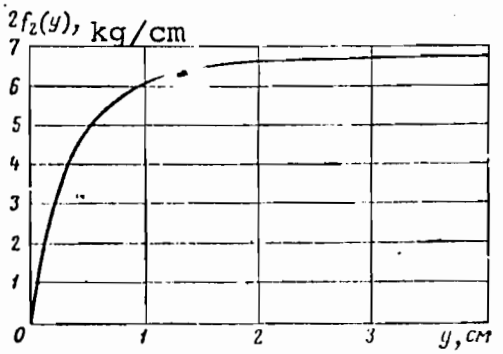

Fig. VI.5. Graph of the resistance per unit length to track displacement as a function of rail displacement (based on experiments and calculations of Raab for a track with fasteners of type K)

Figure VI.6 shows the graph of the function m(u') for a superstructure with hardwood ties and fasteners of type K, based German experimental data [27].

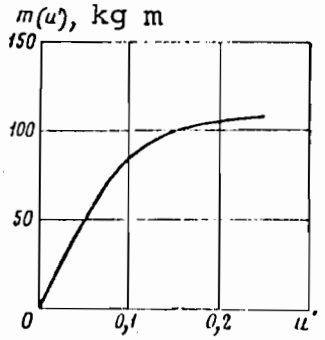

Fig. VI.6. Graph of the distributed passive moment transmitted from the tie to the rail, as a function of the angle of twist of the rail with respect to the tie

For making calculations it is convenient to write (VI.21) in the form

$$\left.\begin{aligned} R^3 - \frac{2[EIf_{2,u}(\delta) + f_{1,u'}(0)]}{f_2(\delta)} R^2 - \frac{EI}{f_2(\delta)} = 0; \\ P_0 = Rf_2(\delta) + EF\frac{\delta}{R}. \end{aligned}\right\} \qquad \text{(VI.22)}$$

The first equation does not depend on P_o, and can be easily solved for every value of δ, with the help of a slide rule, for example. After this, the second equation can be solved. For each value of δ we can find the relation between the curvature 1/R and the longitudinal force P_o, which corresponds to the elimination of the parameter δ from the system (VI.22), and thus obtain the function $P_o = \Phi\ (1/R)$, which defines the boundary between the zones of stability and instability. Figure VI.7 shows this function for a track with the following parameters: P50 rails; $I_2 = 416\ cm^4$; $F = 64\ cm^2$; $E = 2.1\ 10^6\ kg/cm^2$; wooden ties, 1840 per km; type K fasteners; crushed stone ballast.

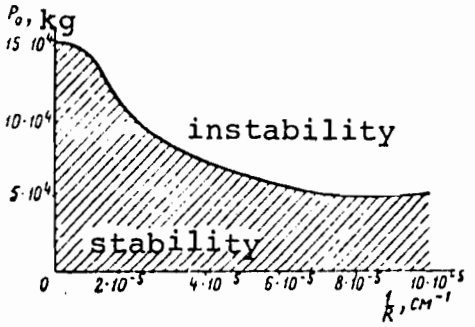

Fig. VI.7. Zone of stability in the P_o, R^{-1} space

The functions $f_2(y)$ and m(u') were taken according to the graphs in Figures VI.5 and VI.6. To compute the relation $P_o = \Phi\ (1/R)$ it is necessary to construct an auxilliary graph (Fig. VI.8) of the function $f_2'(y)$. The computations are shown in Table 24.

Table 24

δ, cm	$f_2(\delta)$, kg/cm	$f'_{2,u}(\delta)$, kg/cm^2	$f'_{1,u'}(0)$, kg	$\frac{EI}{f_2(\delta)}$, cm^3	$2\sqrt{\frac{EIf'_{2,u}(\delta)+f'_{1,u'}(0)}{f_2(\delta)}}$	R, cm	P_0, kg
0,0	0	6,85	1850	—	—	∞	156 300
0,1	0,69	6,85	1850	$12,67\cdot10^3$	$22,7\cdot10^1$	227 000	156 300
0,2	1,37	6,30	1850	$6,38\cdot10^3$	$10,9\cdot10^1$	109 000	149 800
0,3	1,95	4,40	1850	$4,48\cdot10^3$	$6,46\cdot10^1$	61 600	126 400
0,4	2,25	3,00	1850	$3,89\cdot10^3$	$4,62\cdot10^1$	46 200	105 000
0,5	2,50	2,00	1850	$3,50\cdot10^3$	$3,42\cdot10^1$	34 200	87 400
0,6	2,65	1,50	1850	$3,30\cdot10^3$	$3,17\cdot10^1$	28 000	76 600
0,8	2,82	1,00	1850	$3,10\cdot10^3$	$2,16\cdot10^1$	21 600	65 800
1,0	3,00	0,67	1850	$2,92\cdot10^3$	$1,67\cdot10^1$	16 700	58 100
1,2	3,08	0,42	1850	$2,84\cdot10^3$	$1,30\cdot10^1$	13 000	52 500
1,4	3,17	0,30	1850	$2,76\cdot10^3$	$1,08\cdot10^1$	10 800	51 500
1,6	3,20	0,20	1850	$2,73\cdot10^3$	$0,89\cdot10^1$	8 900	52 500

An analysis of Table 24 shows that the quantity $EI/f_2(\delta)$ can be neglected in equations (VI.22), after which the equations take the form

$$\left.\begin{aligned} R &= \frac{2\sqrt{EIf'_{2,u}(\delta)+f'_{1,u'}(0)}}{f_2(\delta)};\\ P_0 &= Rf_2(\delta)+EF\frac{\delta}{R}. \end{aligned}\right\} \qquad \text{(VI.23)}$$

A noteworthy observation is that for small radii of curvature (in our case for R = 100 m) the critical force P_o decreases together with the decrease in the radius. This can be explained by the sizable displacement, when the radius is small, of the track towards the outside of the curve due to the active force $P_o = \alpha tEF$ (α - coefficient of linear expansion of steel), and the consequent appreciable relaxation of the longitudinal force.

The curvature of the track is not constant. Consequently, in the stability calculations, one should take the maximum curvature connected with the presence of track nonuniformities. For example, if a straight section of the track has a nonuniformity as shown in Figure VI.9, the curvature $R^{-1} = 2f/\ell^2 = 1.6 \times 10^{-5}$ should be used

in the computation of the critical force.

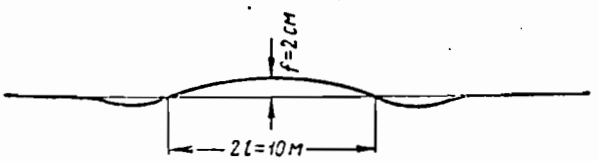

Fig. VI.9. Track nonuniformity with constant curvature along the chord

The dependence of the critical value of the longitudinal rail force $P_o = \alpha t EF$ on the curvature agrees well with experimental data obtained in West Germany [42] by means of artificially induced buckling of track with superstructure of type K. The calculated value is for the critical force in one rail line. Consequently, in comparing with experimental data, this value should be doubled since the longitudinal forces in both rail lines were measured.

If in (VI.23) we make the assumption that

$$f_2(\delta) = q_o = \text{const}, \quad f'_{2,u}(\delta) = k = \text{const}, \quad \delta = 0,$$

$$f'_{1,u'}(0) = f'_{1,u'}(u'_o) = c/\Delta x, \quad \ell = \ell_{oc}/2,$$

where u'_o is the average value of the rail twist with respect to the tie during the buckling process, we obtain

$$P_o = \sqrt{EIk} + c/\Delta x, \quad f = q_o \ell_{oc}^2/8P_o.$$

Except for multiplying constants, these formulas are precisely those which are used at the present time in track stability calculation. The slightly higher values obtained with the formulas in current use result from the fact that they are derived by using energy methods and approximating the buckled shape.

In [14] Ignyatich derives the following formula for the critical force:

$$P_c = \frac{m(0)}{y_0} + \frac{\bar{q}_0}{y_0' + \frac{1}{R^*}},$$

where y_o is the initial nonuniformity in the track, $\bar{q}_o$ is the tie resistance to displacement (const), R^* is the radius of curvature of the curve, and $m(y')$ is the moment of the fastener resistance to twist. Using our notation, one can write

$$y_o' + 1/R^* = 1/R,$$

where R is the local radius of curvature. If one takes into account the fact that the first term in the expression for the critical force was erroneously obtained by examining the system when it is not in equilibrium, one can write the expression for the critical force in the form

$$P_c = \bar{q}_o R.$$

It is easy to see that this expression is a particular case of the second of the formulas (VI.23), with $\delta = 0$.

An analysis of the data in Table 24 shows that over the range of the values of the curvature encountered in railroad track, the parameters $f_2(\delta)$ and particularly $f_{2,u}'(\delta)$ vary considerably (by a factor of several tens). Consequently, the utilization of the exact formulas (VI.23), and the subsequent construction of the stability regions in the parameter space P_o, R, yields a more reliable determination of the stability conditions for CWR track.

It should be taken into account that when the track is in operation there can occur hereditary phenomena when the ties are displaced not only along the track, but also in a direction perpendicular to it. In connection with this, the function $f_2(\delta)$

should be regarded as an average, taking into account the hereditary processes.

2. Stability of CWR track in the section in front of the moving train

From the point of view of stability, the most unfavorable section of track is the one directly in front of the locomotive. Here the longitudinal forces are augmented by the creep forces, and the track is weakened by the vibration of the rails.

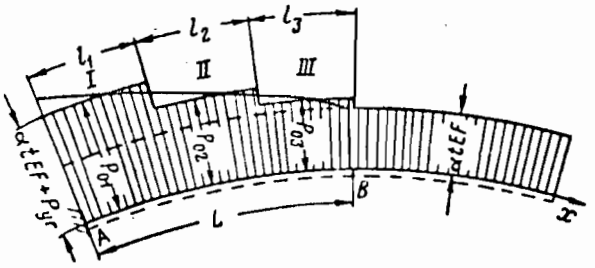

Fig. VI.10. Subdivision into sections with constant parameters of the longitudinal force diagram for the track in front of the moving train

Let us use the method of initial parameters to determine the values which characterize the neutral equilibrium. Suppose the longitudinal force diagram is subdivided into sections, on each of which the longitudinal force can be considered constant (Fig. VI.10). The deflection on the i-th interval can be determined from

$$u = A_1 e^{-\alpha x} \sin \beta x + A_2 e^{-\alpha x} \cos \beta x + A_3 e^{\alpha x} \sin \beta x + A_4 e^{\alpha x} \cos \beta x \quad \text{(VI.24)}$$

which can be obtained from (VI.18) by means of elementary transformations. Differentiating this expression successively we obtain

$$u' = A_1(-\alpha e^{-\alpha x}\sin\beta x + \beta e^{-\alpha x}\cos\beta x) + A_2(-\alpha e^{-\alpha x}\cos\beta x - \beta e^{-\alpha x}\sin\beta x) + A_3(\alpha e^{\alpha x}\sin\beta x + \beta e^{\alpha x}\cos\beta x) + A_4(\alpha e^{\alpha x}\cos\beta x - \beta e^{\alpha x}\sin\beta x);$$

$$u'' = A_1[(\alpha^2-\beta^2)e^{-\alpha x}\sin\beta x - 2\alpha\beta e^{-\alpha x}\cos\beta x] + A_2[(\alpha^2-\beta^2)e^{-\alpha x}\cos\beta x + 2\alpha\beta e^{-\alpha x}\sin\beta x] + A_3[(\alpha^2-\beta^2)e^{\alpha x}\sin\beta x + 2\alpha\beta e^{\alpha x}\cos\beta x] + A_4[(\alpha^2-\beta^2)e^{\alpha x}\cos\beta x - 2\alpha\beta e^{\alpha x}\sin\beta x];$$

$$u''' = A_1[(-\alpha^3+3\alpha\beta^2)e^{-\alpha x}\sin\beta x + (3\alpha^2\beta+\beta^3)e^{-\alpha x}\cos\beta x] + A_2[(-\alpha^3+3\alpha\beta^2)e^{-\alpha x}\cos\beta x + (-3\alpha^2\beta+\beta^3)e^{-\alpha x}\sin\beta x] + A_3[(\alpha^3-3\alpha\beta^2)e^{\alpha x}\sin\beta x + (3\alpha^2\beta-\beta^3)e^{\alpha x}\cos\beta x] + A_4[(\alpha^3-3\alpha\beta^2)e^{\alpha x}\cos\beta x + (-3\alpha^2\beta+\beta^3)e^{\alpha x}\sin\beta x].$$

At the free and x = 0 we obtain

$$\left.\begin{aligned} u(0) &= A_2 + A_4 = u_0;\\ u'(0) &= \beta A_1 - \alpha A_2 + \beta A_3 + \alpha A_4 = u_0';\\ u''(0) &= -\alpha\beta A_1 + (\alpha^2-\beta^2)A_2 + 2\alpha\beta A_3 + (\alpha^2-\beta^2)A_4 = u_0'';\\ u'''(0) &= (3\alpha^2\beta+\beta^3)A_1 + (-3\alpha\beta^2-\alpha^3)A_2 + \\ &\quad + (3\alpha^2\beta-\beta^3)A_3 + (-3\alpha\beta^2+\alpha^3)A_4 = u_0'''. \end{aligned}\right\} \qquad \text{(VI.25)}$$

Let us solve these equations for A_1, A_2, A_3, A_4. We can transform the augmented matrix of the system (VI.25):

$$\left\|\begin{array}{cccc|c} 0 & 1 & 0 & 1 & u_0 \\ \beta & -\alpha & \beta & \alpha & u_0' \\ -2\alpha\beta & \alpha^2-\beta^2 & 2\alpha\beta & \alpha^2-\beta^2 & u_0'' \\ 3\alpha^2\beta-\beta^3 & 3\alpha\beta^2-\alpha^3 & 3\alpha^2\beta-\beta^3 & \alpha^3-3\alpha\beta^2 & u_0''' \end{array}\right\| \rightarrow$$

$$\rightarrow \left\|\begin{array}{cccc|c} 0 & 1 & 0 & 1 & u_0 \\ \beta & 0 & \beta & 2\alpha & u_0' + u_0\alpha \\ 0 & 0 & 4\alpha\beta & 4\alpha^2 & u_0'' + u_0' \cdot 2\alpha + u_0(\alpha^2+\beta^2) \\ 0 & 0 & 0 & -4\alpha(\alpha^2+\beta^2) & u_0''' - u_0'(3\alpha^2-\beta^2) - u_0 \cdot 2\alpha(\alpha^2+\beta^2) \end{array}\right\|$$

Consequently, we obtain the system of equations:

$$\begin{aligned} A_2 + A_4 &= u_0;\\ \beta A_1 + \beta A_3 + 2\alpha A_4 &= u_0' + u_0\alpha;\\ 4\alpha\beta A_3 + 4\alpha^2 A_4 &= u_0'' + u_0' \cdot 2\alpha + u_0(\alpha^2+\beta^2);\\ -4\alpha(\alpha^2+\beta^2)A_4 &= u_0''' - u_0'(3\alpha^2-\beta^2) - u_0 \cdot 2\alpha(\alpha^2+\beta^2), \end{aligned}$$

which has the unique solution:

$$\left.\begin{aligned}
A_1 &= -u_0\frac{\beta^2-\alpha^2}{4\alpha\beta}+u_0'\frac{3\beta^2-\alpha^2}{4\beta(\alpha^2+\beta^2)}-u_0''\frac{1}{4\alpha\beta}+u_0'''\frac{1}{4\beta(\alpha^2+\beta^2)};\\
A_2 &= u_0\frac{1}{2}-u_0'\frac{3\alpha^2-\beta^2}{4\alpha(\alpha^2+\beta^2)}+u_0'''\frac{1}{4\alpha(\alpha^2+\beta^2)};\\
A_3 &= u_0\frac{\beta^2-\alpha^2}{4\alpha\beta}+u_0'\frac{3\beta^2-\alpha^2}{4\beta(\alpha^2+\beta^2)}+u_0''\frac{1}{4\alpha\beta}+u_0'''\frac{1}{4\beta(\alpha^2+\beta^2)};\\
A_4 &= u_0\frac{1}{2}+u_0'\frac{3\alpha^2-\beta^2}{4\alpha(\alpha^2+\beta^2)}-u_0'''\frac{1}{4\alpha(\alpha^2+\beta^2)}.
\end{aligned}\right\} \qquad \text{(VI.26)}$$

Substituting the values of the constants A_i into (VI.24), we obtain, after some simple calculations,

$$\begin{aligned}
u = {} & u_0'''\frac{\alpha\sin\beta x\operatorname{ch}\alpha x-\beta\cos\beta x\operatorname{sh}\alpha x}{2\alpha\beta(\alpha^2+\beta^2)}+u_0''\frac{\sin\beta x\operatorname{sh}\alpha x}{2\alpha\beta}+\\
& +u_0'\frac{(3\alpha\beta^2-\alpha^3)\sin\beta x\operatorname{ch}\alpha x+(3\alpha^2\beta-\beta^3)\cos\beta x\operatorname{sh}\alpha x}{2\alpha\beta(\alpha^2+\beta^2)}+\\
& +u_0\frac{(\beta^2-\alpha^2)\sin\beta x\operatorname{sh}\alpha x+2\alpha\beta\cos\beta x\operatorname{ch}\alpha x}{2\alpha\beta}.
\end{aligned} \qquad \text{(VI.27)}$$

Let us introduce a fictitious longitudinal force defined by

$$P_f = P - f'_{1,u'}(0) = P_0 - f'_{1,u'}(0) - \frac{EI}{R}\delta.$$

From an analysis of (VI.16) it follows that under the action of the fictitious force P_f, the curved beam (with radius R) undergoes the same deformations as the system being investigated, which represent a hinged framework with friction (here we have in mind small deformations).

Let Q_o denote the vertical component of the sum of all the forces to the left of x = 0, and M_o - the sum of the moments of these forces with respect to the point x = 0, u = 0:

$$Q_o = Q_o^v + Q_o^h \text{ and } M_o = M_o^v + M_o^h .$$

The superscripts v and h indicate that these components of Q_o and M_o are produced by vertical and horizontal forces respectively.

It is easy to see that the projection of the horizontal forces $Q_o^h = 0$, and that $M_o^h = - P_f u_o$. On the other hand, one can write (assuming that a positive moment produces a negative curvature)

$$M_o^v = - EIu_o'' - EI(\lambda/R)' \Big|_{x = 0} \text{ and } Q_o^v = - EIu_o''' - P_f u_o',$$

or, discarding the term $EI(\lambda/R)' \Big|_{x=0}$, which, was previously shown to have no influence on the critical parameters for curvatures appropriate to railroad track, we obtain

$$Q_o = - EIu_o''' - P_f u_o' \quad \text{and} \quad M_o = - EIu_o'' - P_f u_o,$$

from which it follows that

$$u_o''' = - (Q_o/EI) - (P_f/EI) u_o' \; ; \quad u_o'' = -(M/EI) - (P_f/EI) u_o.$$

Substituting the expressions from u_o''' and u_o'' into (VI.27), we obtain

$$u = -\frac{Q_0}{EI} \cdot \frac{\alpha \sin \beta x \operatorname{ch} \alpha x - \beta \cos \beta x \operatorname{sh} \alpha x}{2\alpha\beta (\alpha^2 + \beta^2)} - \frac{M_0}{EI} \cdot \frac{\sin \beta x \operatorname{sh} \alpha x}{2\alpha\beta} + \\ + u_0' \frac{\alpha \sin \beta x \operatorname{ch} \alpha x + \beta \cos \beta x \operatorname{sh} \alpha x}{2\alpha\beta} + \\ + u_0 \frac{(\alpha^2 - \beta^2) \sin \beta x \operatorname{sh} \alpha x + 2\alpha\beta \cos \beta x \operatorname{ch} \alpha x}{2\alpha\beta}. \tag{VI.28}$$

Let us denote the term which multiplies $-(Q_o/EI)$ by H_x:

$$H_x = \frac{\alpha \sin \beta x \operatorname{ch} \alpha x - \beta \cos \beta x \operatorname{sh} \alpha x}{2\alpha\beta (\alpha^2 + \beta^2)}.$$

It is clear that the terms which multiply $-(M_o/EI)$, u_o' and u_o are the successive derivatives of H_x. Consequently, we can write

$$u = -\frac{Q_o}{EI} H_x - \frac{M_o}{EI} H_x' + u_o' H_x'' + u_o H_x'''. \tag{VI.29}$$

The quantities which multiply the initial parameters are linearly independent. Each one of these functions represent the influence on the deflection of one of the initial parameters with the other three being zero.

Let us compute the first three derivatives of u with respect to x:

$$\left.\begin{aligned} u &= -\frac{Q_0}{EI} H_x - \frac{M_0}{EI} H_x' + u_0' H_x'' + u_0 H_x''';\\ u' &= -\frac{Q_0}{EI} H_x' - \frac{M_0}{EI} H_x'' + u_0' H_x''' + u_0 H_x^{IV};\\ u'' &= -\frac{Q_0}{EI} H_x'' - \frac{M_0}{EI} H_x''' + u_0' H_x^{IV} + u_0 H_x^{V};\\ u''' &= -\frac{Q_0}{EI} H_x''' - \frac{M_0}{EI} H_x^{IV} + u_0' H_x^{V} + u_0 H_x^{VI}. \end{aligned}\right\} \qquad \text{(VI.30)}$$

Let us also write down the expressions for H_x and its derivatives:

$$H_x = \frac{\alpha \sin \beta x \operatorname{ch} \alpha x - \beta \cos \beta x \operatorname{sh} \alpha x}{2\alpha\beta(\alpha^2 + \beta^2)};$$

$$H_x' = \frac{\sin \beta x \operatorname{sh} \alpha x}{2\alpha\beta};$$

$$H_x'' = \frac{\beta \cos \beta x \operatorname{sh} \alpha x + \alpha \sin \beta x \operatorname{ch} \alpha x}{2\alpha\beta};$$

$$H_x''' = \frac{(\alpha^2 - \beta^2) \sin \beta x \operatorname{sh} \alpha x + 2\alpha\beta \cos \beta x \operatorname{ch} \alpha x}{2\alpha\beta};$$

$$H_x^{IV} = \frac{\alpha(\alpha^2 - 3\beta^2) \sin \beta x \operatorname{ch} \alpha x + \beta(3\alpha^2 - \beta^2) \cos \beta x \operatorname{sh} \alpha x}{2\alpha\beta};$$

$$H_x^{V} = \frac{4\alpha\beta(\alpha^2 - \beta^2) \cos \beta x \operatorname{ch} \alpha x + (\alpha^4 - 6\alpha^2\beta^2 + \beta^4) \sin \beta x \operatorname{sh} \alpha x}{2\alpha\beta};$$

$$H_x^{VI} = \frac{(\beta^5 - 10\beta^3\alpha^2 + 5\beta\alpha^4) \cos \beta x \operatorname{sh} \alpha x}{2\alpha\beta} +$$

$$+ \frac{(\alpha^5 - 10\alpha^3\beta^2 + 5\beta^4\alpha) \sin \beta x \operatorname{ch} \alpha x}{2\alpha\beta}.$$

It should be noted that directly in front of the train, where the longitudinal force attains its maximum value, it may happen that $P_0 > 2\sqrt{EIf'_{2,u}(\delta)} + f'_{1,u}(0) + EF\delta/R$. In this case, the general solution of (VI.17) can be expressed in terms of trigonometric functions:

$$u = B_1 \sin \gamma_1 x + B_2 \cos \gamma_1 x + B_3 \sin \gamma_2 x + B_4 \cos \gamma_2 x,$$

where

$$\gamma_1 = \sqrt{\frac{P_0 - b_1 - \frac{EF}{R}\delta}{2EI} - \sqrt{\frac{\left(P_0 - b_1 - \frac{EF}{R}\delta\right)^2}{4E^2I^2} - \frac{f'_{2,u}(\delta)}{EI}}};$$

$$\gamma_2 = \sqrt{\frac{P_0 - b_1 - \frac{EF}{R}\delta}{2EI} + \sqrt{\frac{\left(P_0 - b_1 - \frac{EF}{R}\delta\right)^2}{4E^2I^2} - \frac{f'_{2,u}(\delta)}{EI}}}.$$

However, in the method of initial parameters the expressions for the deflection and its derivatives can be written in the form (VI.30). In this case the function H_x and its derivatives are given by [32]:

$$H_x = \frac{\frac{1}{\gamma_1}\sin\gamma_1 x - \frac{1}{\gamma_2}\sin\gamma_2 x}{\gamma_2^2 - \gamma_1^2};$$

$$H'_x = \frac{\cos\gamma_1 x - \cos\gamma_2 x}{\gamma_2^2 - \gamma_1^2};$$

$$H''_x = \frac{-\gamma_1\sin\gamma_1 x + \gamma_2\sin\gamma_2 x}{\gamma_2^2 - \gamma_1^2};$$

$$H'''_x = \frac{-\gamma_1^2\cos\gamma_1 x + \gamma_2^2\cos\gamma_2 x}{\gamma_2^2 - \gamma_1^2};$$

$$H^{IV}_x = \frac{\gamma_1^3\sin\gamma_1 x - \gamma_2^3\sin\gamma_2 x}{\gamma_2^2 - \gamma_1^2};$$

$$H^{V}_x = \frac{\gamma_1^4\cos\gamma_1 x - \gamma_2^4\cos\gamma_2 x}{\gamma_2^2 - \gamma_1^2};$$

$$H^{VI}_x = \frac{-\gamma_1^5\sin\gamma_1 x + \gamma_2^5\sin\gamma_2 x}{\gamma_2^2 - \gamma_1^2}.$$

Equations (VI.30) constitute a special case of more general equations investigated by Rippenbein [32]. We stress the fact that the quantity M_o, which enters into this equation, is not the bending moment at the cross-section x = 0, but is the sum of the moments of the forces about the point x = 0, u = 0.

Let us return to the problem of deriving the equilibrium equations for the track, with the assumed force diagram (see

Fig. VI.10). Suppose the train is moving towards the right, and that in the section where the first locomotive axle is located, the creep force is P_{cr}. Furthermore, let us assume that the creep force decays over a distance of length z, its law of variation being specified for any given type of superstructure. In addition to this, the track is affected by the temperature, which produces in it a longitudinal force $P_t = \alpha t EF$. Adding up the creep force and the temperature induced force, we obtain the actual longitudinal force diagram in the section of the track in front of the moving train.

Since the track is firmly pressed to the subgrade by the train, it can be considered fixed at the point A where the first locomotive axle is located. Let us subdivide the longitudinal force diagram into several parts, and determine the parameter values for which determine the stability conditions on each of these.

If the load has the critical value, it must, according to (VI.13), satisfy the condition

$$f_2(\delta_i) = \frac{P_{oi}}{R} - EF\,\frac{\delta_i}{R^2}\,. \qquad \text{(VI.31)}$$

Since the quantities P_{oi} and R are known, the parameter δ_i can be determined for each interval.

Since the train is moving, we can consider the rigid constraint at the point A to be applied after the transverse displacement of the track into its equilibrium position. Thus, the constraint does not produce any stresses due to the displacement of the curve by an amount δ.

Knowing the value of δ_i, one can determine the values of all the remaining parameters for the i-th section. Such quantities

are $f_2(\delta_i)$ and $f'_{2,u}(\delta_i)$, and also the parameter $b_1 = f'_{1,u'}(0)$, which has the same value for all intervals.

The boundary values at the left hand end-point of the first interval can be expressed in terms of the initial parameters u_o, u'_o, M_o and Q_o in the following way:

$$\left.\begin{aligned} u_{10} &= 0; \\ u'_{10} &= 0; \\ M_{10} &= M_0; \\ Q_{10} &= Q_0. \end{aligned}\right\} \qquad \text{(VI.32)}$$

Letting M_o and Q_o be the two fundamental parameters to be determined, let us denote by the symbol [V] the transformation (VI.32), with the matrix of coefficients

$$\|V\| = \begin{Vmatrix} 0 & 0 \\ 0 & 0 \\ 1 & 0 \\ 0 & 1 \end{Vmatrix}. \qquad \text{(VI.33)}$$

Furthermore, making use of (VI.30), and taking into account that $P_f = P_o - b_1 = EF\delta/R - EI/R^2 = 2EI(\alpha^2-\beta^2)$, we will obtain equations which connect the parameters corresponding to the two end-points of the first interval:

$$\left.\begin{aligned} u_{1l} &= u_{10}H_1''' + u'_{10}H_1'' - \frac{M_{10}}{EI}H_1' - \frac{Q_{10}}{EI}H_1; \\ u'_{1l} &= u_{10}H_1^{IV} + u'_{10}H_1''' - \frac{M_{10}}{EI}H_1'' - \frac{Q_{10}}{EI}H_1'; \\ M_{1l} &= u_{10}EI\left[2(\alpha_1^2-\beta_1^2) - H_1^V\right] - u'_{10}EIH_1^{IV} + M_{10}H_1''' + Q_{10}H_1''; \\ Q_{1l} &= -u_{10}EIH_1^{VI} + u'_{10}EI\left[2(\alpha_1^2-\beta_1^2) - H_1^V\right] + M_{10}H_1^{IV} + Q_{10}H_1'''. \end{aligned}\right\} \qquad \text{(VI.34)}$$

Let us denote by $[A_1]$ the transformation (VI.34), with the matrix

$$\|A_1\| = \begin{vmatrix} H_1''' & H_1^* & -\frac{H_1'}{EI} & -\frac{H_1}{EI} \\ H_1^{IV} & H_1''' & -\frac{H_1''}{EI} & -\frac{H_1'}{EI} \\ EI\left[2(\alpha_1^2-\beta_1^2) - H_1^V\right] & -EIH_1^{IV} & H_1''' & H_1^* \\ -EIH_1^{VI} & EI\left[2(\alpha_1^2-\beta_1^2) - H_1^V\right] & H_1^{IV} & H_1''' \end{vmatrix} \qquad \text{(VI.35)}$$

In order to obtain the quantities $u_{1\ell}, u'_{1\ell}, M_{1\ell}, Q_1$ in terms of M_o and Q_o, one must multiply the transformation [V] by the transformation $[A_1]$:*

$$[V\ A_1] = [V] \times [A_1].$$

The matrix of the coefficients of the transformation $[VA_1]$ can be easily found by multiplying the matrices:

$$\|VA_1\| = \begin{vmatrix} -\frac{H_1'}{EI} & -\frac{H_1}{EI} \\ -\frac{H_1^*}{EI} & -\frac{H_1'}{EI} \\ H_1''' & H_1^* \\ H_1^{IV} & H_1''' \end{vmatrix}. \qquad \text{(VI.36)}$$

The transition from the end of the first interval to the beginning of the second one is effected by means of forumlas connecting these intervals. Since the parameters u, u', M, and Q do not change in going from one interval to the next one, the transition matrix $\|B_1\|$ corresponds to the transformation

$$\begin{vmatrix} u_{20} & u_{1\ell} \\ u'_{20} & u'_{1\ell} \\ M_{20} & M_{1\ell} + (P_{f_1} - P_{f_2})\, u_{1\ell} \\ Q_{20} & Q_{1\ell} \end{vmatrix} \qquad \text{(VI.37)}$$

---

* In mathematics a different notation is employed. The matrix which is multiplied is placed last, while the multiplier matrix is placed first. However, in problems of structural mechanics the notation used above is more convenient [31].

and has the form

$$\|B_1\| = \begin{Vmatrix} 1 & 0 & 0 & 0 \\ 0 & 1 & 0 & 0 \\ P_{f_1} & -P_{f_1} & 0 & 1 & 0 \\ 0 & 0 & 0 & 1 \end{Vmatrix} \tag{VI.38}$$

The expressions for the parameters u_{20}, u_{20}, M_{20} and Q_{20} in terms of the initial parameters can be obtained by performing the multiplication

$$[VA_1] \times [B_1] = [VA_1B_1]. \tag{VI.39}$$

We can get to the end of the second interval by performing the multiplication

$$[VA_1B_1] \times [A_2] = [VA_1B_1A_2], \tag{VI.40}$$

where $[A_2]$ is the tranformation which connects the end points of the second interval. It can be obtained from (VI.34) by replacing the index 1 by 2. Continuing in the same way, we can reach the end of the n-th interval by means of the transformation

$$[VA_1B_1A_2B_2 \ldots B_{n-1}A_n]. \tag{VI.41}$$

This transformation expressed the parameters of the end of the last interval, which is siutated in the zone of decay of the longitudinal creep forces, in terms of the fundamental parameters M_o and Q_o. The matrix of this transformation will have two columns and four rows. Multiplying (VI.41) by the matrix

$$\|B_n\| = \begin{Vmatrix} 1 & 0 & 0 & 0 \\ 0 & 1 & 0 & 0 \\ P_{f_n} & -P_{f_{n+1}} & 0 & 1 & 0 \\ 0 & 0 & 0 & 1 \end{Vmatrix},$$

we will obtain the initial parameters of the semi-infinite track, which can be considered to be the (n-1)st interval.

The initial parameters of the semi-infinite track will be:

$$\left.\begin{aligned} &u_{n+1,0};\\ &u'_{n+1,0};\\ &M_{n+1,0} = -EIu''_{n+1,0} + 2EI(\alpha_{n+1}^2 - \beta_{n+1}^2)u_{n+1,0};\\ &Q_{n+1,0} = -EIu'''_{n+1,0} + 2EI(\alpha_{n+1}^2 - \beta_{n+1}^2)u'_{n+1,0}. \end{aligned}\right\} \qquad \text{(VI.42)}$$

Substituting into (VI.42) the values of $u''_{n+1,0}$ and $u'''_{n+1,0}$ from (VI.20), we obtain

$$M_{n+1,0} = EI(3\alpha_{n+1}^2 - \beta_{n+1}^2)u_{n+1,0} + 2EI\alpha_{n+1}u'_{n+1,0};$$
$$Q_{n+1,0} = -2\alpha_{n+1}EI(\alpha_{n+1}^2 + \beta_{n+1}^2)u_{n+1,0} - EI(\alpha_{n+1}^2 + \beta_{n+1}^2)u'_{n+1,0},$$

or, solving the resulting equations for $u_{n+1,0}$ and $u'_{n+1,0}$, we obtain the expressions:

$$u_{n+1,0} = -M_{n+1,0}\frac{1}{EI(\alpha_{n+1}^2 + \beta_{n+1}^2)} - Q_{n+1,0}\frac{2\alpha_{n+1}}{EI(\alpha_{n+1}^2 + \beta_{n+1}^2)};$$

$$u'_{n+1,0} = M_{n+1,0}\frac{2\alpha_{n+1}}{EI(\alpha_{n+1}^2 + \beta_{n+1}^2)} + Q_{n+1,0}\frac{3\alpha_{n+1}^2 - \beta_{n+1}^2}{EI(\alpha_{n+1}^2 + \beta_{n+1}^2)}.$$

Let us rewrite these expressions so that the right hand sides are zero:

$$\left.\begin{aligned} &u_{n+1,0} + M_{n+1,0}\frac{1}{EI(\alpha_{n+1}^2 + \beta_{n+1}^2)} + Q_{n+1,0}\frac{2\alpha_{n+1}}{EI(\alpha_{n+1}^2 + \beta_{n+1}^2)} = 0;\\ &u'_{n+1,0} - M_{n+1,0}\frac{2\alpha_{n+1}}{EI(\alpha_{n+1}^2 + \beta_{n+1}^2)} - Q_{n+1,0}\frac{3\alpha_{n+1}^2 - \beta_{n+1}^2}{EI(\alpha_{n+1}^2 + \beta_{n+1}^2)} = 0. \end{aligned}\right\} \qquad \text{(VI.43)}$$

Let us denote this transformation by [W]. The corresponding matrix is

$$\|W\| = \begin{Vmatrix} 1 & 0 & \dfrac{1}{EI(\alpha_{n+1}^2 + \beta_{n+1}^2)} & \dfrac{2\alpha_{n+1}}{EI(\alpha_{n+1}^2 + \beta_{n+1}^2)} \\ 0 & -1 & \dfrac{2\alpha_{n+1}}{EI(\alpha_{n+1}^2 + \beta_{n+1}^2)} & \dfrac{3\alpha_{n+1}^2 - \beta_{n+1}^2}{EI(\alpha_{n+1}^2 + \beta_{n+1}^2)} \end{Vmatrix}.$$

The transformation $[B_nW]$ represents the imposition of the boundary conditions on the right hand end-point of the n-th interval. Multiplying the transformation (VI.41) by $[B_nW]$, we obtain

$$[VA_1B_1A_2B_2\ldots A_n]\times[B_nW] = [VA_1B_1A_2\ldots A_nB_nW]. \qquad \text{(VI.44)}$$

The matrix of this transformation has two rows and two columns.

Thus we will have two homogeneous linear equations for the unknown quantities M_o and Q_o. The critical state is determined by the condition that the equations have a nontrivial solution. This condition is the vanishing of the detriment of the matrix of the transformation (VI.44):

$$|VA_1B_1A_2B_2\ldots A_nB_nW| = 0. \qquad \text{(VI.45)}$$

If one is required to determine the critical value of the radius for a given force, one should prescribe various values of R, compute the determinant in (VI.45), and then construct its graph. The points of intersection of the graph with the abscissa determines the values of R for which the determinant vanishes. In a similar way one can determine the critical temperature for a given radius.

In some cases the computations for CWR track should be carried out taking into account the displacement δ prior to buckling, since for large values of δ, large transverse displacements may endanger the safety of the moving train even if the track is stable (if there is no bifurcation from the state of equilibrium).

REFERENCES

(Titles of Russian publications translated)

Abbreviations:

IIT	Institut Inzhenerov Zheleznodorozhnogo Transporta (Institute of Railroad Transport Engineers)
DIIT	Dnepropetrovsk IIT
LIIT	Leningrad IIT
MIIT	Moscow IIT
TIIT	Tashkent IIT
NIT	Nauchno-issledovatel'skiĭ Institut Zheleznodorozhnogo Transporta (Scientific Institute of Railroad Transportation)
TsNIT	Tsentral'nyĭ NIT (Central NIT)
VNIT	Vsesoyuznyĭ NIT (All Union NIT)

1. Al'brecht, V. G., Concerning the longitudinal forces which arise at the interface between the foundation and the rail base due to the passage of rolling stock wheels (in Russian). Trudy MIIT, v. 80/1. Moscow, Transzheldorizdat, 1955.
2. Al'brecht, V. G., Concerning supplementary forces and the magnitude of the track creep due to brake friction on a slope (in Russian). Trudy MIIT, v. 80/1. Moscow, Transzheldorizdat, 1955.
3. Al'brecht, V. G., Contribution to the question concerning the resistance of the rail-tie grid to longitudinal displacement forces (in Russian). Tekhnika zheleznykh dorog , No. 12, 1951.
4. Andreevskii, M. G., Concerning the resistance of railroad track to longitudinal displacement (in Russian). Sbornik TIIT, v. 8, 1957.
5. Balakin, A. G., On the longitudinal displacement of the rail-tie grid and of the ballast layer under the action of rolling

5. (continued)
stock. (in Russian) Tekhnika zheleznykh dorog, No. 12, 1952.

6. Besicovich, A. S., Approximate Computations (in Russian). Moscow, Gostekhizdat, 1949.

7. Bochenkov, M. S., Longitudinal forces and deformations in CWR track with automatic thermal stress relaxation (in Russian). Vestnik VNIT, No. 7, 1957.

8. Wattmann, J., Längskräfte im Eisenbahngleis. Otto Elsner, Darmstadt, 1957.

9. Ventzel, E. S., Theory of Probability. Moscow, Fizmatgiz, 1958.

10. Verigo, M. F., Vertical forces acting on the track in the passage of rolling stock (in Russian). Trudy TsNIT, v. 97. Moscow, Transzheldorizdat, 1957.

11. Gantmakher, F. R., The Theory of Matrices (Transl). New York, Chelsea, 1959.

12. Dinnik, A. N., Stability of Arches (in Russian). Moscow, Gostekhizdat, 1946.

13. Dlin, A. M., Mathematical Statistics in Technology (in Russian). Moscow, Sovetskaya Nauka, 1958.

14. Ignyatich, D. V., Determination of the critical force deforming CWR track (in Russian). Vestnik Vsesoyuznogo nauchno-issledovatel'skogo instituta zheleznodorozhnogo transporta, No. 8, 1965.

15. Isakov, P. F., Investigation of the foundation resistance to transverse displacements of the rail-tie grid (in Russian). Trudy DIIT, v.27, 1958.

16. Kalkin, V. M., Advantages of installing long rails (in Russian). Zheleznodorozhnyĭ transport, No. 11, 1955.

17. Kogan, A. Ya., Contribution to the question of determining stability of railroad track in front of the moving train (in Russian). Sbornik studencheskikh nauchnykh rabot MIIT, No.2. Moscow, Transzheldorizdat, 1959.

18. Kogan, A. Ya., Graphical-analytical method of determining longitudinal forces and deformations in CWR track (in Russian). Vestnik VNIT, No. 3, 1961.

19. Korotkin, Ya. I. et al, Bending and Stability of Beams and Beam Systems (in Russian). Moscow, Mashgiz, 1953.

20. Cramer, H., Mathematical Methods in Statistics. Princeton, Princeton U. Press, 1946.

21. Krachkovskii, V. P., Effect of temperature on rails installed in track (in Russian). Trudy TsNIT, v. 7. Moscow, Gostransizdat, 1931.

22. Krivobodrov, A. A., Stability of thermally stressed railroad track (in Russian). Trudy LIIT, v. 144. Moscow-Leningrad, Transzheldorizdat, 1952.

23. Lanning, J. H. Jr., and Battin, R. H., Random Processes in Automatic Control. New York, McGraw-Hill, 1956.

24. Lyapunov, A. M., Probleme general de la Stabilite du Mouvement. Annals of Math. Studies 17, Princeton, Princeton U. Press, 1947.

25. Mishchenko, K. N., CWR Track (in Russian). Moscow, Transzheldorizd 1950.

26. Nikiforov, P. A., CWR track and its operation (in Russian). Zheleznodorozhnaya tekhnika, No. 4, 1937.

27. On the development of CWR track (in Russian). Bulletin tekhniko- ekonomicheskoĭ informatsii, No. 2, 1961.

28. Pershin, S. P., Method for stability analysis of railroad track (in Russian). Vestnik VNIT, No. 3, 1959.

29. Pershin, S. P., Matheods of Stability Analysis of CWR Track (in Russian). Trudy MIIT, v. 147. Moscow, Transzheldorizdat, 1962.

30. Pugachev, V. S., Theory of Random Functions and its Application to the Problems of Automatic Control (in Russian). Moscow, Gostekhizdat, 1957.

31. Rzhanitsin, A. P., Stability of Equilibrium of Elastic Systems (in Russian). Moscow, Gostekhizdat, 1955.

32. Rippenbein, Ya. M., Investigation of Beams on an Elastic Foundation, Subjected to Axial Forces (in Russian). In Issledovaniya po Teorii Sooruzheniĭ, v. 4. Moscow, Gostekhizdat, 1951.

33. Ryzhik, P. M., and Gradshtein, P. S., Tables of Integrals, Sums, Series and Products, 4th Ed (Transl). New York, Academic Press, 1965.

34. Sackmauer, L., Theoretical investigations of CWR track for different types of superstructures in railroad tracks in Checkoslovakia. Issledovatel' skii institut zheleznodorozhnogo trnasporta, Bratislava, 1958/9.

35. Smirnov, V.I., Course of Higher Mathematics (Transl), v. II, III, V. 1964 Pergamon Press, London.

36. Smirnov, A. F., Stability and Vibrations of Structures (in Russian). Moscow, Transzheldorizdat, 1958.

37. Snitko, N. K., Stability of Beam Structures Subjected to Axial Forces With and Without Bending Moments. Moscow, Gosstroĭizdat, 1956.

38. Chlenov, M. T., Long Rails (in Russian). Moscow, Transzheldorizdat, 1940.

39. Shakunyants, G. M., Analysis of long rails (in Russian). Teknika Zheleznykh Dorog, No. 1, 1948.

40. Shakunyants, G. M., Analysis of Track Superstructure (in Russian). Moscow, Transzheldorizdat, 1961.

41. Shakhunyants, G. M., Railroad Track (in Russian). Moscow, Transzheldorizdat, 1961.

42. Experimental investigation of stability of CWR track (in Russian). Zheleznodorozhniĭ Transport, No. 3, 1962.

43. Experiments on the Stability of Long-Welded Rails, British Transport Commission. London, 1961.

44. Temperatur and Längeänderung an der Schiene. Eisenbahntechn. Rundschau, No. 1, 1956.

45. Zimmerman, K., Wanderspannungen und andere Probleme des Lang-schienoberbanes. Deutche Eisenbahntechnik, No. 4, 1955.